An Investigation into the Free-Piston Engine Concept and its Potential for High Efficiency and Low Emissions Power Generation

Thesis by

Rikard Mikalsen

In Partial Fulfillment of the Requirements

for the Degree of

Doctor of Philosophy

Newcastle University

Newcastle upon Tyne

United Kingdom

July 2008

Abstract

An investigation into the feasibility of the free-piston engine concept and its potential for high efficiency and low emissions power generation has been conducted using computational modelling and simulation. A thorough background study and literature review was carried out covering previously reported experience with free-piston engines, particular features of this technology, and potential advantages and challenges associated with their design.

A single piston free-piston engine generator was proposed as a result of the background study and a design strategy for this engine configuration was formulated. Detailed simulation models for the free-piston engine were developed and extensive simulation studies conducted to investigate the performance and operating characteristics of such an engine. Engine performance indicators, such as fuel efficiency, power to weight ratio, and exhaust gas emissions formation, were studied along with engine operational control issues. The results were directly compared to those of equivalent conventional crankshaft engines in order to investigate potential differences in engine performance.

It was found that the free-piston engine has potential advantages over conventional technology in the areas of mechanical efficiency, exhaust gas emissions formation, and operational flexibility. The main challenge lies within the area of piston motion control and further research into engine control issues are required. A more detailed study of engine emissions formation is also recommended in order to fully understand the influence of the particular operating characteristics of the free-piston configuration on engine performance.

Acknowledgements

I would like to express my sincere gratitude to my supervisor, Professor Tony Roskilly, for his support throughout the work with this thesis. I also thank my co-supervisors, Dr Roger Moss and Dr Rose Norman, for their help and support.

Colleagues and other staff who deserve thanks include Ms Lynne Dixon, Mr Chris Mullen, Dr Sangram Nanda, Mr John Price, Mrs Lisa Smeaton, and Ms Michelle Wagner.

To my family and friends, who have supported and encouraged me during the work with this project: I shall thank you in person rather than in a thesis you will never read.

List of papers

I R. Mikalsen and A.P. Roskilly. A review of free-piston engine history and applications. *Applied Thermal Engineering*, 27:2339–2352, 2007.

II R. Mikalsen and A.P. Roskilly. The design and simulation of a two-stroke free-piston compression ignition engine for electrical power generation. *Applied Thermal Engineering*, 28:589–600, 2008.

III R. Mikalsen and A.P. Roskilly. Performance simulation of a spark ignited free-piston engine generator. In press: *Applied Thermal Engineering*, November 2007.

IV R. Mikalsen and A.P. Roskilly. Coupled dynamic–multidimensional modelling of free-piston engine combustion. In press: *Applied Energy*, June 2008.

V R. Mikalsen and A.P. Roskilly. A computational study of free-piston diesel engine combustion. Manuscript submitted to *Applied Energy*, March 2008.

VI R. Mikalsen and A.P. Roskilly. The control of a free-piston engine generator. Part 1: fundamental analyses. Manuscript submitted to *Mechatronics*, May 2008.

VII R. Mikalsen and A.P. Roskilly. The control of a free-piston engine generator. Part 2: engine dynamics and piston motion control. Manuscript submitted to *Mechatronics*, May 2008.

Contents

List of Figures

List of Tables

Nomenclature

α	heat transfer coefficient [W/m^{2}K]	C_R	compression ratio [1]
$\dot{Q}$	heat flow rate [J/s]	C_v	specific heat at constant volume [J/kgK]
η	efficiency [1]	E	energy [J]
γ	ratio of specific heats [1]	e	error
BDC	bottom dead centre	E_{comp}	compression energy [J]
bmep	brake mean effective pressure [Pa]	E_{mot}	motoring energy [J]
COV	coefficient of variation	F	force [N]
imep	indicated mean effective pressure [Pa]	F_{fr}	frictional forces [N]
PDF	pseudo-derivative feedback	F_{mag}	electric load force [N]
PID	proportional-integral-derivative	F_{mot}	motoring force [N]
PI	proportional-integral	F_b	bounce chamber gas force [N]
rpm	revolutions per minute	F_c	combustion cylinder gas force [N]
TDC	top dead centre	G	plant matrix
$\overline{v}_p$	mean piston speed [m/s]	K	gain matrix
ϕ	fuel-air equivalence ratio [1]	k_d	derivative gain [1]
A_p	piston area [m^2]	k_i	integral gain [1]
A_s	combustion chamber surface area [m^2]	k_p	proportional gain [1]
B	cylinder bore [m]	m	mass [kg]
C	controller matrix	N	operating frequency [1/s]
C_D	valve discharge coefficient [1]	P	engine power output [W]
C_p	specific heat at constant pressure [J/kgK]	p	pressure [Pa]

p_c	in-cylinder gas pressure [Pa]
Q	heat energy [J]
R	gas constant [J/kgK]
S	stroke length [m]
T	in-cylinder gas temperature [K]
t	time [s]
t_{id}	ignition delay [ms]
T_s	average in-cylinder surface area temperature [K]
U	internal energy [J]
V	cylinder volume [m^3]
V_{sw}	swept volume (displacement) [m^3]
W	work energy [J]
x	piston position [m]

Chapter 1

Introduction

Recent years have seen a significant increase in the awareness of environmental effects resulting from the use of fossil fuels as an energy source, within the scientific community, industry, government, and the general public. Extensive use of such fuels for transport (sea and land based) and power generation leads to significant amounts of carbon dioxide and other pollutants being produced, and much research is being undertaken within both academia and industry to develop more efficient and environmentally friendly energy chains. Much of this work is driven by the ever-tightening environmental legislation imposed by governments worldwide, requiring among others car manufacturers to comply with stringent emissions targets. Both 'local' pollutants which pose health risks to humans, such as carbon monoxide and particulates, and carbon dioxide, which is widely accepted to influence global climate, are increasingly being regulated.

1.1 Alternative power generation systems

To comply with tightening emissions regulations and to improve engine efficiency there is a growing interest in alternative power generation systems, unconventional engine technology, and the use of alternative fuels. Technology which was previously not commercially viable may have advantages in a marketplace with heavier taxation on fuel consumption and emissions generation.

1.1.1 Stationary power generation

A substantial part of the electric power generation is in most industrialised countries based on fossil fuels utilised in large scale power stations. In such power plants, significant amounts of waste heat are produced which can not be easily utilised, and much research is therefore being undertaken in the area of small scale combined heat and power systems. By generating electric power locally, the waste heat can more easily be used for heating purposes and the utilisation of the fuel energy is improved, giving an increased total efficiency. A requisite for such a system to

be feasible is, however, the availability of an efficient combustion engine suitable for small scale power generation.

1.1.2 Propulsion systems

In the automotive industry, technologies offering near-zero emissions, such as electric vehicles and hydrogen-based fuel cell vehicles, are under continuous development by a number of manufacturers. The implementation barrier for such a radical technology change is, however, large. The hybrid electric vehicle has shown to be able to realise large emissions reductions within a shorter timescale, and such technology is becoming commercially available from an increasing number of manufacturers. A similar concept with the same motivations and potential advantages, currently being explored within the marine industry, is the all-electric ship concept.

Both hybrid electric vehicles and the all-electric ship employ an efficient electric distribution network with energy storage devices and electric end drives, which partly or fully separates the combustion engine from the mechanical drive chain. This reduces the load variations on the engine and allows it to work closer to its optimum operating conditions, resulting in improved fuel efficiency and reduced emissions. Vessel or vehicle "braking" energy can be recuperated, further reducing fuel consumption. Moreover, eliminating the need for a wide load and speed range may allow a more optimised engine design or the implementation of alternative technologies such as fuel cells or other types of internal or external combustion engines.

1.1.3 Alternative fuels

Alternative fuels used in power generation or vehicle propulsion include fuels which can be generated from renewable sources. Examples include biodiesel, vegetable oils, alcohols such as methanol and ethanol, as well as gaseous fuels such as hydrogen and synthetic gas ('syngas') resulting from the gasification of biomass or other waste material. Economic incentives have been introduced by several governments to increase the use of alternative fuels, and blends of fossil and renewable fuels are commercially available in many countries.

Alternative fuels may have characteristics different to those of conventional, fossil fuels, in areas critical for engine operation such as energy content, combustion properties, and lubricating properties, and modifications or conversions may be required prior to the use of such fuels in existing combustion engines. The ability to operate on a variety of fuels is therefore of high importance in modern engines, and unconventional engine configurations may offer better performance than conventional technology in this area.

1.2 Internal combustion engines

The internal combustion engine has, since its first development (in the form that we know it today) in the late 19th century, played a key role in industrialisation and technological development in the modern world. It is arguably among, if not *the*, most successful and widely used piece of machinery the world has seen. Although significant improvements in engine performance have been made, mainly through the use of advanced materials and modern engine technology, the basic operating principle of modern engines is identical with those used more than 100 years ago.

The focus for engine developers has, however, changed, due to changes in customer demand and governmental regulation. While the main focus half a century ago was engine power output (i.e. achieving a high power to weight ratio), today's engine manufacturers face customer demands for high fuel efficiency, due to high fuel oil prices, and stringent emissions legislation imposed by governments. Continuous improvements in engine performance are being made through the use of advanced computational models in the engine design process and the development of modern engine technology such as microprocessor-based control, high-pressure injection systems, knock sensors, and effective catalysts and filters.

1.3 The free-piston engine

Free-piston engines are linear, 'crankless' internal combustion engines, in which the piston motion is not driven by a crankshaft but by an interaction of forces acting on the piston. This allows a significantly simpler engine structure, making the engine more compact and with lower frictional losses, but also requiring more complicated engine control.

Free-piston engines were first proposed around 1920, and enjoyed some degree of success in the mid-20th century as air compressors and gas generators in large scale powerplants. In recent years, the free-piston engine concept has again attracted attention from researchers and engine developers seeking to reducing engine emissions and improving fuel efficiency.

The main attractions with the free-piston engine concept are its potential for optimised engine operation and low frictional losses. In conventional engines, the energy delivered by the combustion gases on the linearly moving piston is converted into a rotating power output by the crankshaft, before it is converted into electric or hydraulic power through a generator or pump. In the free-piston engine the linear energy from the moving piston is utilised directly through a linear load device, eliminating the complicated crank mechanism and associated losses.

Furthermore, the absence of the crankshaft means that the compression ratio in the free-piston engine is not fixed, but can be varied in order to optimise engine operation (provided that an appropriate control system can be realised). This may allow the possibility of optimising engine

operation for e.g. different load levels, alternative fuels or given emissions targets.

1.4 Contribution to existing research

A large number of patents and research reports describing free-piston machinery exist, and a number of different free-piston engine configurations have been proposed. However, only very few authors have presented detailed studies of the performance of modern free-piston engines, and there is no general agreement on what is the best configuration. Some reports have indicated potential advantages over conventional technology, but little is known about the details of free-piston engine operating characteristics and performance.

This thesis presents a number of contributions to existing research in the form of a detailed investigation into the performance and operational characteristics of a single piston free-piston engine. Advanced computational simulation models have been used to investigate the general operational characteristics of the engine, controllability, the combustion process and exhaust gas emissions formation. A direct comparison to equivalent conventional engines is presented, allowing an evaluation of potential advantages of the free-piston engine concept on a fundamental level.

The structure of the thesis is as follows.

- Chapter 2 presents a detailed background study, thoroughly evaluating the particular features of the free-piston engine and reviewing reported free-piston engine applications and their performance.

- Based on the background study, Chapter 3 proposes a design for a free-piston engine generator, intended for electric power generation in medium to large size applications. Justification for the chosen single piston configuration is presented, and a design strategy for the engine is outlined.

- Chapter 4 presents a full-cycle simulation model for the proposed engine. Simulation results are presented, showing the operational characteristics of the free-piston engine, along with the influence of the main engine design and operational variables.

- Chapter 5 investigates the in-cylinder processes in free-piston engines in greater detail, using a multidimensional simulation model. In-cylinder gas motion, combustion and emissions formation are studied and directly compared to results predicted for conventional engines in order to identify potential advantages of the free-piston engine.

- In Chapter 6, engine control issues are studied using the full-cycle simulation model. The transient response of the engine resulting from changes in the input variables is studied, and control strategies investigated.

- Finally, in Chapter 7 the results are summarised and evaluated, and further work is suggested.

The free-piston engine is evaluated in relation to the need for modern engine technology to provide efficient energy conversion with low exhaust gas emissions, to allow operation on alternative and multiple fuels, and to satisfy the requirement of a compact and flexible engine configuration in modern vessel and vehicle designs.

Chapter 2

Review of free-piston engine features and reported applications

Due to the breadth of the free-piston term, many engine configurations will fall under this category. This introductory chapter presents the basic features of free-piston engines and establishes the terminology for the rest of the text. Proposed advantages and disadvantages associated with the free-piston engine concept are reviewed and reported free-piston engines and experience with free-piston engine operation are presented.

Parts of the work presented in this chapter were presented by Mikalsen and Roskilly [73].

2.1 Basic features of the free-piston engine

The free-piston term is most commonly used to distinguish a linear engine from a conventional crankshaft engine. The piston is 'free' because its motion is not restricted by the position of a rotating crankshaft, as known from conventional engines, but is decided by the interaction between the gas and load forces acting upon it. This gives the free-piston engine some distinct characteristics, the most important being (a) variable stroke length and (b) the need for active control of piston motion. Another important feature of the free-piston engine is the potential reduction in friction losses due to the simplicity of the concept. In addition to fewer moving parts the purely linear connecting rod motion gives very low side forces on the piston, further reducing frictional losses.

A number of configurations fitting the description above have been proposed. The following sections give an overview of the most common types of free-piston engine configurations, their design and operating characteristics.

2.1.1 The original concept

The invention of the free-piston engine concept is usually credited to Raul Pateras Pescara, based on his patent from 1928 [82]. It should, however, be noted that other vendors, among others the Ger-

man company Junkers, were also working on free-piston machinery at this time and other patents describing free-piston machinery had also been published [37].[1]

Pescara was an Argentinian born inventor and lawyer who lived most of his life in Europe, where he worked on numerous inventions including helicopters, seaplanes, automotive vehicles and engines. Pescara started his work on free-piston engines around 1922 and developed prototypes with both spark ignition (1925) and compression ignition combustion (1928). The latter ultimately led to the development of the Pescara free-piston air compressor described in Section 2.2.1.

The original Pescara patent describes a spark ignited air compressor, but the patent seeks to protect a large number of applications utilising the free-piston principle. The machine illustrated in the patent consists of a single piston moving in a bouncing manner between the ends of a two-end cylinder, in which one end consists of a combustion cylinder and the other of an air compressor. The cylinder is allowed to slide within a frame, with a motion in opposite phase to that of the piston in order to cancel out vibrations. The sliding of the cylinder also controls the opening and closing of a number of ports in the cylinder liner.

Pescara continued his work on free-piston machinery for several years and also patented a multi-stage free-piston air compressor engine in 1941 [83].

2.1.2 Piston configuration

Free-piston engines are usually divided into four categories based on the piston and cylinder configuration and operational characteristics. Three of these, the single piston, dual piston and opposed pistons configurations, are related to the number of pistons and cylinders and their arrangement. The fourth, the free-piston gas generator, describes engines in which the power output is taken from an exhaust turbine.

2.1.2.1 Single piston configuration

An illustration of a single piston free-piston engine is shown in Figure 2.1. The load may be an electrical machine, an air compressor, a hydraulic pump or in theory any linear-acting force. Many of the recent approaches in free-piston engine developments are of the single piston type, mainly due to the simple design and high degree of controllability.

The working principle of the engine is more or less self-explanatory: the combustion cylinder works on a two-stroke cycle, with combustion when the piston is near top dead centre (TDC)[2] in the cylinder and scavenging in the lower part of the cylinder. The rebound device, here shown as a

[1] For a comprehensive timeline of free-piston engine developments, see Aichlmayr [3].

[2] Top dead centre and bottom dead centre are defined as the positions where the piston velocity changes direction (as such, the piston velocity at those points is equal to zero). It should be noted that in the free-piston engine, this is not a fixed value as in conventional engines but will vary according to engine operating conditions.

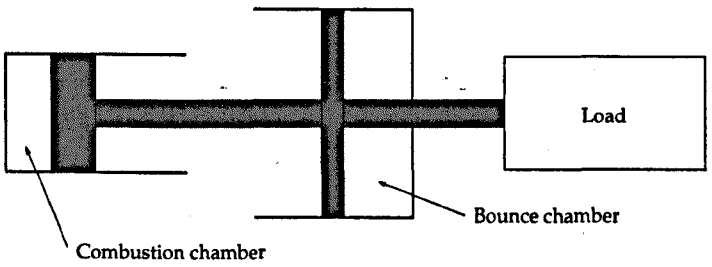

Figure 2.1: Single piston free-piston engine configuration [3].

bounce chamber, works as an energy storage device, storing energy from the combustion process to drive the compression process for the next cycle. Since the combustion process produces net work over the cycle, energy can be extracted from a load coupled to the system.

Controllability is regarded to be the main strength of the single piston design compared to the other free-piston engine configurations. The rebound device may accurately control the amount of energy put into the compression process and thereby regulate the compression ratio and stroke length. Such control can for instance be achieved by using a variable pressure, gas filled bounce chamber, an electric machine or a hydraulic actuator as rebound devices.

The single piston free-piston engine is in its basic configuration not balanced, and vibrations must be taken into account in the design and mounting of the engine. An important control aspect if the engine is to be synchronised with other engines, or if it faces other vibration limitations, is therefore the possibility to apply frequency control. For an engine with a gas-filled bounce chamber, the system will resemble a spring-mass system and the bouncing frequency will be determined by the moving mass and the stiffness of the springs. The stiffness of the combustion chamber 'gas spring' can be controlled by the mass of fuel injected. If the amount of gas in the bounce chamber can also be varied, the bounce chamber spring stiffness can be varied and some degree of controllability can possibly be achieved.

Another approach, intended for providing flow control in hydraulic free-piston engines, has been applied among others by the Dutch engineering company Innas BV [2]. They apply 'pulse pause modulation' frequency control which pauses the piston motion at BDC using a controllable hydraulic cylinder as a rebound device. At BDC the piston velocity is zero and the upwards motion will only begin when the rebound device releases the stored energy. The frequency can therefore be controlled by applying a pause between the time at which the piston reaches BDC and the release of compression energy for the next stroke. The frequency can in theory be varied down to zero, unlike in conventional engines where the idle speed represents the minimum operating frequency. This is possible because the piston motion is not frequency-dependent since it will be the same regardless of operating frequency. Another consequence of this is that the frequency will have very low in-

fluence on the efficiency of the engine, giving the potential of very good part-load performance in such engines. Such frequency control also allows frequency changes to take place instantaneously and step wise. Somhorst and Achten [90] reported an idle speed for the Innas Free-Piston Engine of 1 Hz (60 rpm). An illustration of the principle for an engine with a 20 Hz maximum frequency is shown in Figure 2.2. Note that the piston trajectory is similar regardless of operating frequency.

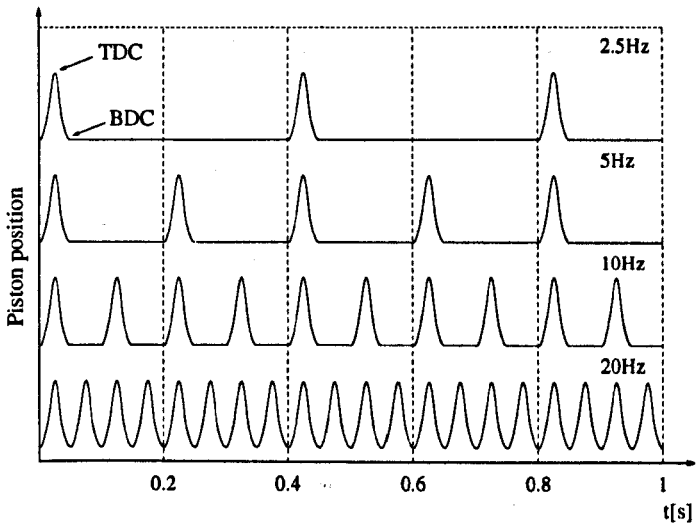

Figure 2.2: The principle of pulse pause modulation frequency control.

The single piston configuration with a hydraulic load device has been the most successful of recent free-piston engine applications. Some mainly theoretical studies have proposed the use of single piston engines for electric generators and air compressors, but only a limited number of successful prototypes have been reported. In a review of different free-piston concepts, Achten [1] claimed that the single piston engine is the only free-piston configuration for which control problems have been successfully resolved and highly accurate control achieved for emission reductions and optimal efficiency operation.

2.1.2.2 Dual piston configuration

The dual piston (or dual combustion chamber) configuration, illustrated in Figure 2.3, has been a topic for much of the recent research in free-piston engine generator technology. A number of dual piston designs have been proposed and a few prototypes have emerged, both with hydraulic and electric power output. The main advantage of the dual piston configuration is that it eliminates the need for a rebound device, since the working piston (at any time) provides the work to drive the compression process in the other cylinder. This allows a more compact device with higher power to weight ratio.

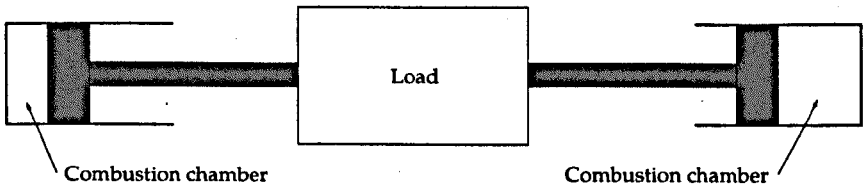

Figure 2.3: Dual piston free-piston engine configuration.

There are, however, some significant challenges with the dual piston design. The engine, like the single piston engine, is not balanced in its basic configuration. A more serious problem is the potential difficulty in achieving effective piston frequency and stroke length control, two influential factors in engine performance and operation. Since the compression work is provided by the power expansion in the other cylinder, variations in the combustion process will influence the next compression and combustion part of the cycle. This is a great control challenge if the combustion process is to be accurately controlled to optimise emissions and/or efficiency [1,3]. Reports on experimental work with dual piston engines have reported high sensitivity to load nuances and high cycle-to-cycle variations [31,96].

Efficient load control can also represent a problem because the operating frequency of the engine can only be varied within limits, since the bouncing frequency is restricted by the resonant frequency of the system. Flow control of a hydraulic load by frequency regulation can only be achieved within these limits and other solutions may have to be introduced. One example of this is to use multiple hydraulic pump plungers, as suggested by Achten [1]. For linear alternators, a higher degree of load control can be obtained using power electronics and the limited speed range may not represent a problem.

Despite large development efforts, the dual piston free-piston engine has not yet found widespread application and reported engines are mostly concept developments within academia.

2.1.2.3 Opposed piston configuration

An opposed piston free-piston engine configuration is illustrated in Figure 2.4 and essentially consists of two opposing single piston engines with a common combustion chamber. A mechanical linkage usually connects the two pistons to ensure symmetric motion, this is not shown in the illustration. Variations on the illustrated design, such as a single bounce chamber, are possible but the opposed piston design is necessarily larger and more complex than the free-piston configurations described above.

The main advantage of the opposed piston configuration is the perfectly balanced and vibration-free original design which can be achieved if the two piston assemblies have equal mass. This is not shared by any of the other free-piston configurations. Furthermore, it can be controlled the same

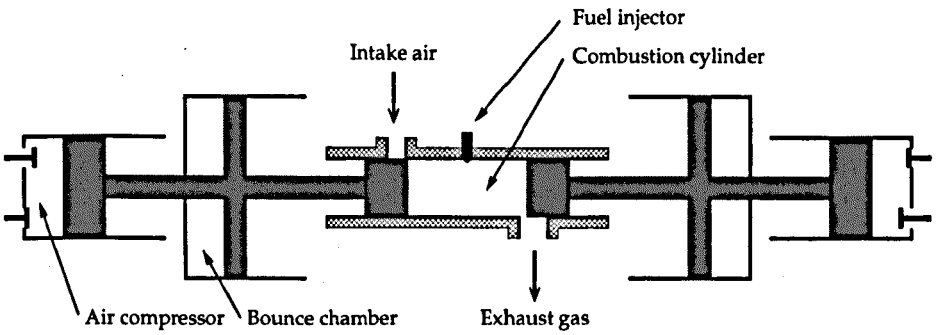

Figure 2.4: Illustration of an opposed piston configuration. Note that the piston synchronisation mechanism is not shown.

way as the single piston engine, both regarding frequency, compression ratio and stroke control if the rebound devices allow this. The opposed piston configuration also eliminates heat transfer losses to the cylinder head, improving engine fuel efficiency.

The opposed piston design has, however, some fundamental design challenges which give it disadvantages compared to the other configurations, with the need for a piston synchronisation mechanism being the most important. This has traditionally been solved with a mechanical linkage between the pistons, creating a heavier and more complex design with increased frictional losses. Other means of piston synchronisation have been proposed but the feasibility of these has not yet been well documented. A further possible disadvantage with the opposed piston design is that the fuel injector in a compression ignition engine, or the spark plug in a spark ignited engine, is located on the cylinder wall. This potentially hinders fuel air mixing, the combustion process, and cylinder lubrication and may require design changes in the injection system.

The opposed piston configuration has been the basis for several compressor, gas generator and hydraulic pump designs since the first developments of the free-piston engine concept. Practically all of the free-piston engines developed in the period between 1930 and 1960 were of the opposed piston type, which include the limited number of free-piston engine applications that have seen commercial success.

Only a few modern opposed piston free-piston engines can be found, some of which attempt to avoid the complicated mechanical synchronisation mechanism known from the mid-20th century engines and use electronic control of the rebound device to synchronise the pistons. Achten [1] thoroughly reviewed the opposed piston engine and rejected this configuration, whereas Hibi and Ito [52] used it and reported promising results.

2.1.2.4 Free-piston gas generators

Free-piston gas generators (or gasifiers[3]) can have any of the configurations described above, however the vast majority of reported free-piston gas generators were opposed piston engines during the period 1940–1960. An example of an opposed piston free-piston gas generator is shown in Figure 2.5. The particularity of the gas generator is that the work output is taken entirely from a power turbine. The only work done by the engine pistons is in the supercharging of the intake air. Compared to a conventional gas turbine, the free-piston gas generator differs in the way that the work needed to compress the intake air is already extracted from the gas when supplied to the power turbine. Consequently, the gas holds a lower temperature which reduces the materials requirement for the turbine and allows the turbine to be placed farther away from the combustor without extensive heat transfer losses.

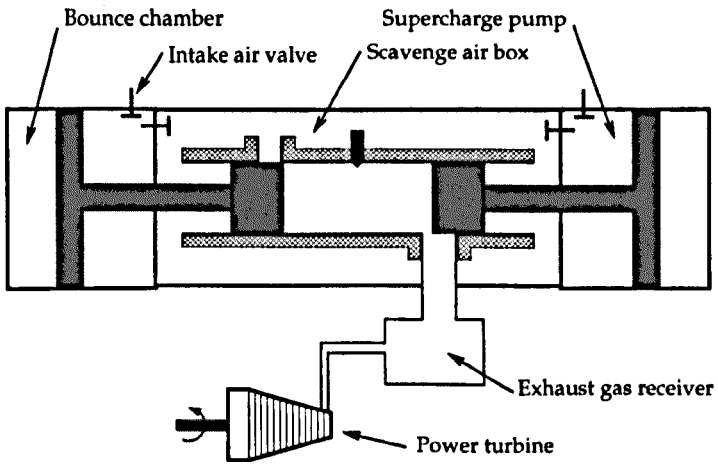

Figure 2.5: Illustration of a free-piston gas generator. Note the similarity to Figure 2.4

Two types of free-piston gas generators have been reported, the inward compressing type and the outward compressing type. Figure 2.6 shows the principal construction of these. The inward compressing type, shown on the left-hand side of the figure, is compact but requires the compression energy for the supercharging to be intermediately stored in the bounce chamber, thus increasing the size of this part. In addition, larger pumping losses result from the need for intermediate storage of scavenging air in the air box [101]. For the outward compressing unit, shown on the right-hand side, a smaller bounce chamber can be used since it only needs to store the amount of energy needed to compress the cylinder charge. The placement of the bounce chambers and the need for additional air pipes will, however, lead to an increase in engine size [101].

The operational characteristics of the gas generator do not differ much from those of another free-piston engine of the same configuration. The absence of a load force does not change the fact

[3]The term gasifier is sometimes used for the free-piston gas generator.

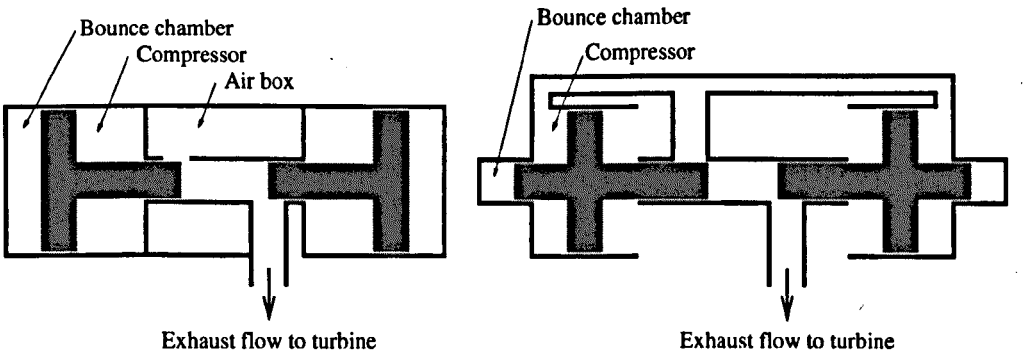

Figure 2.6: Illustration of the inward compressing (left) and outward compressing (right) types free-piston gas generator [3].

that a piston control mechanism must be established but possibly eases this task since disturbances in the form of load changes do not directly influence the piston dynamics.

The opposed piston free-piston gas generator was a topic of much research in the mid-20th century, providing some advantages over present-time conventional engines and gas turbines. Most notable were higher fuel efficiency and lower fuel quality requirements than conventional gas turbines and higher power density than conventional engines. As gas turbine and conventional engine technology advanced, the advantages of the gas generator vanished and the concept was abandoned in the early 1960's. Only very few modern attempts to build free-piston gas generators have been reported. A more detailed presentation of free-piston gas generator history can be found in Section 2.2.2.

2.1.3 Free-piston engine unique features

The free-piston engine has a number of unique features when compared to conventional internal combustion engines, some of which potentially give the free-piston engine advantages over conventional technology. However, there are a number of challenges with the free-piston concept that must be addressed if it is to become an alternative to conventional technology. This section will discuss the main unique features of the free-piston engine and their effects on engine operation and performance.

2.1.3.1 Piston dynamics and control

In a conventional engine, the crankshaft and flywheel serve as both piston motion control and energy storage. The piston motion control ensures sufficient compression at one end of the stroke and sufficient time for scavenging at the other, while the energy storage provides compression energy and ensures that the engine does not immediately stall if the load changes rapidly or there

are fluctuations in combustion performance. In the free-piston engine the piston motion is not restricted by a crankshaft but determined by the sum of the forces acting upon the piston assembly at any point in the cycle. Hence, the interaction of these forces must be arranged in a way that controls the piston motion for all types of operation if the concept is to be feasible.

To better understand the dynamics of the piston and the influence of the different forces acting upon it, one can formulate the piston motion mathematically using a free-body diagram, as shown in Figure 2.7. The figure shows combustion chamber pressure force F_C, bounce chamber (rebound) force F_R, load force F_L and the piston assembly with mass m_p. x denotes piston position, TDC_N and BDC_N are nominal top dead centre and bottom dead centre positions and ML denotes the mechanical limits of the piston motion.

Applying Newtons 2nd law to the moving mass in Figure 2.7, the piston position can be expressed as

$$\sum_i F_i = m_p \frac{\mathrm{d}^2 x}{\mathrm{d}t^2}. \tag{2.1}$$

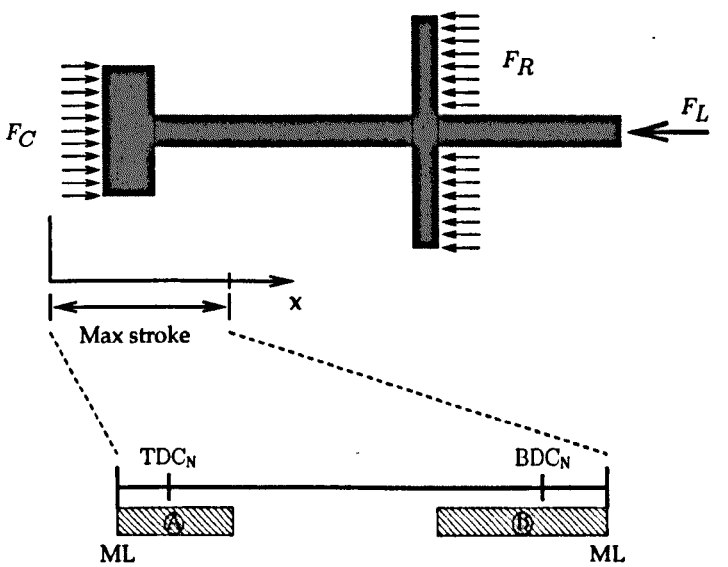

Figure 2.7: Free body diagram of the piston assembly in the free-piston engine illustrated in Figure 2.1.

Knowing that the combustion cylinder and the bounce chamber will have characteristics similar to those of a gas spring, it becomes clear that they will produce a oscillating-type piston motion. When adding a load force, this must be subordinate to the other two forces in order to ensure the reciprocating motion of the piston needed to produce work in the combustion cylinder. If a rebound device with other characteristics than those of a spring is used, such as a hydraulic cylinder, the operating characteristics will be slightly different but the same principles will apply.

Figure 2.7 also shows the different parts of the engine stroke. Area Ⓐ shows the piston position range where the compression ratio of the engine is sufficient for fuel autoignition. For the engine to run, one outer point of the piston reciprocating motion clearly needs to be within this area. Area Ⓑ shows the piston position range where the scavenging ports are open and the burnt gases can be replaced with fresh charge. For the scavenging to be effective, the piston needs to spend a sufficient amount of time in this area in each cycle.

These requirements are absolute and for the engine to be practical, an engine control system needs to be able to meet these requirements for all types of engine operation.

2.1.3.2 Frequency control

For an engine with a gas filled bounce chamber or a dual piston engine, the spring-mass nature of the system means that the frequency and stroke length are closely related. The system will operate at its natural frequency, and the pressure in the gas springs (i.e. spring stiffness) can only be varied over a limited range. The stroke length is strictly limited by the need for sufficient compression and scavenging, hence the speed control possibilities of the engine are likely to be limited. This may also limit the power output range of such free-piston engines, an issue that has been noted by a number of authors as a problem with the free-piston concept.

Engines using rebound devices with higher degrees of controllability can, however, have very effective frequency control schemes. An example is the pulse pause modulation control described in Section 2.1.2.1.

2.1.3.3 Starting

The free-piston engine cannot be cranked over several revolutions for starting like conventional engines and other methods for starting must therefore be implemented. Starting can be achieved by impulsing the piston to give it sufficient energy to reach sufficient compression for fuel ignition and combustion, or by driving the piston back and forth until sufficient compression is reached. The latter can be achieved if the load device can be run as a motor, for example with an electric machine or a hydraulic cylinder. If the impulse strategy is used, it is crucial that the engine starts on the first stroke and that the engine control system is able to keep the engine running after this.

Most of the gas generators reported in the mid 20th century used compressed air to aid starting, by rapidly introducing it into the bounce chamber. Achieving combustion on the first stroke was not reported as a problem, because high compression ratios were achievable with this method. More challenging was to be able to immediately control the amount of air in the bounce chamber to achieve sufficient scavenging for stroke number two, since the bounce chamber at this point was full of high pressure starting air. Although some reports indicate that starting was a challenge for the free-piston engines, this is never mentioned as a crucial problem.

Recent free-piston engine developments use stored electric or hydraulic energy to aid starting, by using the load device in motoring mode. For single piston and opposed piston hydraulic free-piston engines, the rebound devices are hydraulic cylinders and the first stroke is not different from any other stroke and starting does not represent a problem.

2.1.3.4 Misfiring

Another potential control related problem is misfiring. If the piston fails to build up sufficient compression or if other factors influence the injection or ignition and the combustion process in one stroke, the engine may stop. The same result may follow from a mistiming in the fuel injection or ignition timing [13]. In a conventional engine the inertia of the flywheel and crank system ensures sufficient compression energy to drive the engine for several revolutions if the fuel fails to ignite, however the free-piston engine has no such energy storage device.

Although this is often considered a potential problem in theoretical surveys on free-piston engine feasibility, such problems are not mentioned by any of the reviewed reports on experimental work with free-piston engines.

2.1.3.5 Free-piston loads

The free-piston engine requires a linear load, and for the overall system to be efficient the load must provide efficient energy conversion. Rotating power sources, such as internal combustion engines and turbines, have been the de facto standard for many years within electric power generation but also rotating hydraulic and pneumatic machinery are highly developed technologies. A challenge for free-piston engine developers is to find linear equivalents to those machines with comparable performance.

In addition, mechanical requirements for free-piston engine load devices may be high since the load is coupled directly to the moving piston. The load device will be subjected to high acceleration forces, and secondary effects from the high acceleration, such as cavitation in hydraulic cylinders, and must also be considered. Furthermore, the load device may be subjected to heat transfer from the engine combustion cylinders.

Reported free-piston engine loads include electric generators, hydraulic pumps and air compressors. The dynamic properties of these differ widely. Important features when determining the feasibility of a linear load for a free-piston engine are: moving mass, physical size, efficiency and load force profile. The following characteristics are typical for the mentioned load devices:

- Hydraulic pumps typically work against a high discharge pressure. Combined with incompressible working fluid, this allows a small unit with very low moving mass. The efficiency

of such units is generally high and high operational flexibility has been demonstrated using electronically controlled hydraulic control systems with fast-acting valves in free-piston engines. The load force of a hydraulic pump is approximately constant due to the constant discharge pressure over the stroke length.

- Electric generators can be relatively compact in size but usually have a high moving mass due to magnets or back iron in the translator, which is required to supply or direct the power generating magnetic flux within the machine. The efficiency of electric machinery is, however, generally very high. The load force of a permanent magnet electric machine coupled to a purely resistive load will be proportional to the translator speed, however with other designs or the implementation of power electronics, a different relationship may be designed.

- Air compressors were the original free-piston load devices but are not necessarily better suited for this purpose than the other two. The variable stroke of the free-piston engine may lead to poor volumetric efficiency of the air compressor when operating at varying load levels. If operating with atmospheric inlet pressure, a large compressor cylinder is needed and results in a large and heavy construction. One advantage is that a stepped compressor piston can be applied, giving a compact multi-stage compressor. The load profile of an air compressor is like that of a gas filled bounce chamber in the compression phase and with an approximately constant load force when the discharge valves are open towards the end of the stroke.

The typical load characteristics of free-piston engine loads are illustrated in Figure 2.8.

2.1.3.6 Simplicity of the concept

The simplicity of the free-piston engine compared to conventional technology is one of the driving forces behind many of the recent free-piston engine developments. The elimination of the crank mechanism reduces the number of parts and the complexity of a free-piston engine significantly and this potentially gives a number of advantages.

- Low frictional losses. Fewer moving parts in the free-piston engine give reduced frictional losses. The absence of a crankshaft eliminates losses due to bearings in the crank system, and the purely linear motion leads to very low side loads on the piston. This also reduces the cylinder lubrication requirements. Figure 2.9 illustrates the sources of frictional losses in a conventional engine which will not be present in the free-piston engine.

- Reduced manufacturing costs. The reduced number of complex load bearing parts in the free-piston engine results in lower manufacturing costs.

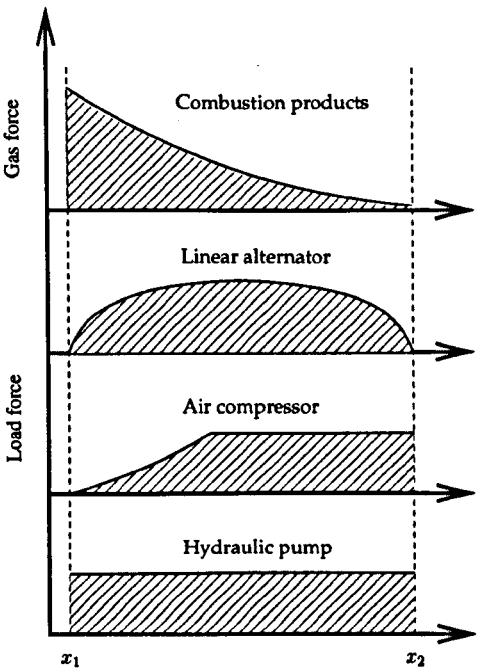

Figure 2.8: Characteristics of free-piston engine load devices [3].

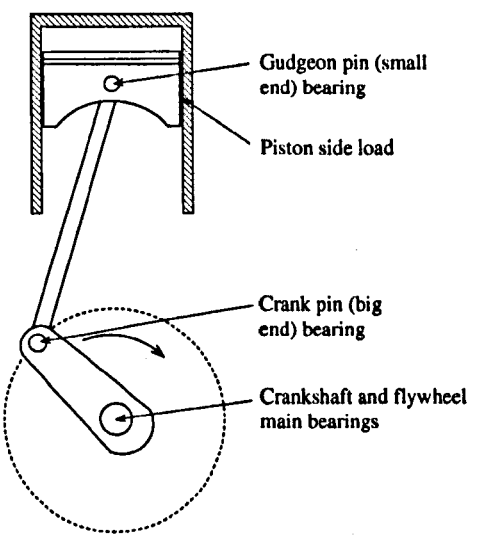

Figure 2.9: Sources of frictional losses in conventional internal combustion engines.

- Compactness. With a reduced number of parts, the size and weight of the free-piston engine compared to an equivalent conventional engine can be reduced, giving a more compact unit.
- Low maintenance costs and increased lifetime. The reduced number of load bearing and heavily stressed parts and the lower frictional losses reduce the maintenance costs of the free-piston engine.

- Engine design. The construction of the engine and the piston layout in a multi-cylinder engine are not constrained by a need for mechanical connection of the pistons to a crankshaft. The cylinders can be arranged in any configuration appropriate for a given purpose.

2.1.3.7 The combustion process

Some reports have indicated that the combustion in free-piston engines benefits from the high piston speed around TDC. This leads to higher air velocity and turbulence level in the cylinder, which benefit air-fuel mixing and increase the reaction rate and flame speed. The high piston acceleration just after TDC leads to a rapid expansion, and time-dependent chemical reactions, such as NO_x formation, are potentially reduced.

Achten et al. [2] presented experimental results showing significantly faster combustion in the Innas Free-Piston Engine compared to conventional engines. Values for ignition delay were found to be comparable to those found in conventional engines. Tikkanen et al. [96] presented similar experimental results, and both groups indicated that combustion takes place predominantly in the premixed phase. Fleming and Bayer [39] also reported faster combustion and described how theoretical thermodynamic analysis of the engine processes had to be changed to achieve good agreement with experimental data, however this was partly due to long ignition delays. Baruah [13] reported significant advantages in emissions for a spark ignited free-piston engine over crankshaft engines, particularly for nitrogen oxides.

As a result of the particular operating characteristics, the in-cylinder heat transfer will also differ between the free-piston engine and conventional engines. The rapid power stroke expansion gives less time available for heat transfer from the hot gases to the cylinder wall, but increased in-cylinder gas motion may have the opposite effect and increase the heat transfer rate. However, Uludogan et al. [100] investigated the effects of increased engine speed on the combustion in a DI diesel engine and found that the advantages of increased fuel-air mixing far outweigh the disadvantages associated with increased heat transfer. R. Huber, an authority on free-piston engine development in the mid-20th century, stated in the discussion section of McMullen and Payne [71] that the heat losses from the cylinder to the cooling water and piston cooling oil are only 18 % of the fuel heating value in the SIGMA GS-34 free-piston engine, compared to 25 % in conventional diesel engines. Huber relates this to two factors: the reduced cylinder area in an opposed piston free-piston engine compared to a conventional engine and the high acceleration of the pistons reducing the time the cylinder walls are exposed to the hot gases.

A particular feature of the free-piston engine is the ability of the combustion process to influence the speed of the expansion, due to the direct coupling of the combustion cylinder to the low-inertia moving member. A rapid combustion process and pressure rise may lead to a faster expansion and vice versa. In a conventional engine, the inertia of the crank system and flywheel ensures that the

speed of the engine stays constant in the time frame of the combustion process. This intricate coupling between thermodynamics and mechanics makes detailed modelling of the free-piston engine complex, and models developed for conventional engines are therefore not necessarily suitable for modelling free-piston engine processes.

Combustion optimisation and multi-fuel operation The variable compression ratio in the free-piston engine may allow an optimisation of the combustion process not achievable in conventional engines. Given that a sufficiently accurate piston motion control system can be realised, the compression ratio can be regulated during operation to achieve best possible performance for all operating conditions. Tikkanen and Vilenius [97] described the varying of the compression ratio at different loads, with nominal compression ratio varying from 15:1 at full load to 30:1 at lower loads. Free-piston engines with compression ratios as high as 50:1 were reported in the mid-20th century [6].

The design of the free-piston engine makes it well suited for multi-fuel operation. The variable compression ratio combined with modern engine technology, such as variable fuel injection and valve timing, enable the free-piston engine to run satisfactorily on a wide range of fuels. Flynn [61] reported the successful operation of a free-piston engine on a range of different fuels, including gasoline, diesel fuel and crude oil, and stated that "It seems that these engines do not care whether they get fuel with octane or cetane numbers". He further stated that the engine runs satisfactorily on vegetable and animal oils, with the only noticeable effect being the engine power output varying according to the heat content of the fuel. The same conclusion has also been reached by other authors [79].

Homogeneous charge compression ignition Homogeneous charge compression ignition (HCCI) engines compress a premixed charge until it self-ignites, resulting in very rapid combustion but with poor control of ignition timing. The HCCI concept is under widespread investigation due to its potential to lower engine emissions and increase efficiency. The free-piston engine is well suited for HCCI operation since the requirements for accurate ignition timing control are lower than in conventional engines. Potential advantages of HCCI include high efficiencies due to close to constant volume combustion and the possibility to burn lean mixtures to reduce gas temperatures and thereby some types of emissions. HCCI operation of free-piston engines has been studied experimentally by among others Aichlmayr [3] and van Blarigan [17].

A quasi-HCCI approach was mentioned by Hibi and Ito [52]. In the engine described, diesel fuel is injected very early in the compression process but after the intake and exhaust ports have closed. The fuel does not ignite at injection because the temperature and pressure are too low, but distributes more or less evenly within the cylinder and self-ignites when the pressure and

temperature reach higher values. Ignition occurs at multiple points around the cylinder and the burning fuel spray with high local temperatures is avoided. Computational investigations into the same concept were presented by Kleemann [64] and Fredriksson [40].

2.1.3.8 Balancing

The inherent vibration-free design was an often reported advantage of the early opposed piston air compressors and gas generators. These engines, from the earliest air compressor designs in the 1930s to the gas generators developed during 1945-1960, all had mechanical linkages synchronising piston motion. In the first presentation of the Junkers free-piston air compressor at the Leipzig fair in 1936, the excellent dynamic characteristics of the engines were demonstrated by suspending the compressors from the ceiling in a single steel cable and balancing pencils on the engine housing while running [3]. Underwood [101] stated that the smoothness of the General Motors GMR 4-4 'Hyprex' gas generator was "frequently demonstrated by balancing a nickel on a horizontal machine surface".

The excellent dynamic properties of the opposed piston free-piston engine are well documented, and give a significant amount of freedom in the mounting of the engine. This also lowers the requirements of engine auxiliaries to withstand vibrations and may also allow a weaker structure to be used, reducing engine weight.

For the single piston and dual piston engine, however, balancing issues need to be addressed when mounting the engine. Vibrations may be cancelled out by running two or more engines in parallel, but this requires accurate control of engine speed. Another possibility is to apply counterweights, as demonstrated by Braun [22]. Disadvantages of counterweights are a more complex design, increased engine size and weight and additional friction losses. Achten [1] stated that for the 17 kW hydraulic free-piston engine considered in his paper, vibrations can be isolated by suitable mounting of the engine and that the acceleration forces will have about the same magnitude as in conventional engines.

2.1.3.9 Mechanical requirements

The mechanical requirements for the free-piston engine may be high, particularly if operating at high compression ratios and high pressures. High pressure gradients, resulting from high fuel burn rate, lead to high forces and accelerations and increased material stress in the free-piston engine. Although crankshaft bearing loads, as known from conventional engines, are eliminated in the free-piston engine, such high pressure gradients may set high requirements on the material properties of the piston and piston rings. High accelerations may also increase the demands on the load and rebound devices.

Flynn [61] described the testing of a free-piston engine, and reported that the major problems are mechanical wear and damage, mainly due to high temperatures and pressures. Flynn further described how many repairs and replacement parts were needed during engine testing. Toth-Nagy [98] reported very high failure rates in a diesel free-piston engine prototype. High pressure forces caused failures in components including pistons and load shafts, whereas engine vibration caused failures in injectors, fuel lines, position sensor etc.

Due to the variable stroke of the free-piston engine, high peak pressures may be also be experienced during transient operation or from operation of the engine at too high compression ratios.

2.2 Reported free-piston engine applications

Since the free-piston engine was first presented circa 1930 a number of different designs have been proposed using the free-piston concept. Although the majority of these have not seen commercial success, the current increase in research effort in the field of free-piston engines suggest that it may be a promising candidate for applications where rotating power output is not strictly necessary, such as electric power generators and hydraulic pumps.

This section gives an overview of reported free-piston engine developments, with an emphasis on engines where experimental results or operational performance data have been reported. It should be noted that in addition to these, a high number of patents describing free-piston machinery exist, where the actual development of the engines has not been reported.

2.2.1 Free-piston air compressors

The original free-piston configuration proposed by Pescara was an air compressor, and free-piston air compressors proved to possess some very attractive features. Despite the large research efforts on the free-piston gas generator concept in the period 1940–1960, the air compressor is by many considered to be the only really successful free-piston engine application. The free-piston air compressor concept saw some degree of commercial success, and the excellent performance of these machines was a strong contributor to the later significant research efforts put into the free-piston gas generator.

These early free-piston engines had perfect dynamic balance, a feature that was frequently demonstrated, due to the opposed piston configuration with mechanical piston synchronisation. A further unique feature of the opposed piston air compressors was the nearly constant operating speed, independent of load. Speed variations of 1 Hz for the Pescara-Muntz engine [37] and 0.4 Hz for the Junkers engine [67] were reported. London and Oppenheim [67] attribute this to the mass-spring behaviour of the system.

The most significant advantage of the air compressor was, however, what is now considered one of the main challenges with the free-piston concept, namely piston motion control. The earliest free-piston air compressors were reported to have been essentially self-regulating in terms of compression ratio and TDC control. The reason for this is the interaction between the bounce chamber and the compressor cylinders. Considering a free-piston air compressor such as the one shown in Figure 2.10.

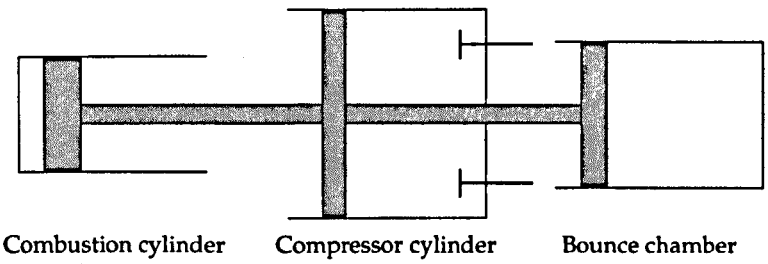

Figure 2.10: Free-piston air compressor.

As the combustion cylinder piston moves towards BDC, compression energy for the next cycle will be stored in the bounce chamber, and the amount of energy stored will vary with the stroke length. However, the compressed air left in the compressor cylinder clearance volume after discharge will also contribute to the returning of the piston, and as the stroke varies the amount of air left in the compressor varies. These two sources of compression energy will have different characteristics: an increase in stroke length will store more energy in the bounce chamber due to higher compression, but less in the compressor cylinders due to more air being discharged, and vice versa. This is illustrated in Figure 2.11.

Farmer [37] described how the amount of compression energy can be made practically constant and independent of stroke length by matching the design of the bounce chamber to the characteristics of the compressor.

The piston motion of the free-piston air compressor differs significantly to that of conventional engines. Since the load force from the air compressor is very low at the beginning of the power expansion stroke, the piston acceleration just after TDC is very high. Farmer [37] stated that this reduces the time available for the hot gases to lose heat to the cylinder walls. Farmer also described how the piston speed in the compression stroke is lower than in the expansion stroke. The compression stroke for the combustion cylinder is the intake stroke for the air compressor and the lower speed leads to increased volumetric efficiency of the compressor intake. Farmer further showed that the piston speed in the compression stroke in a free-piston engine is significantly lower than that of a comparable crankshaft engine.

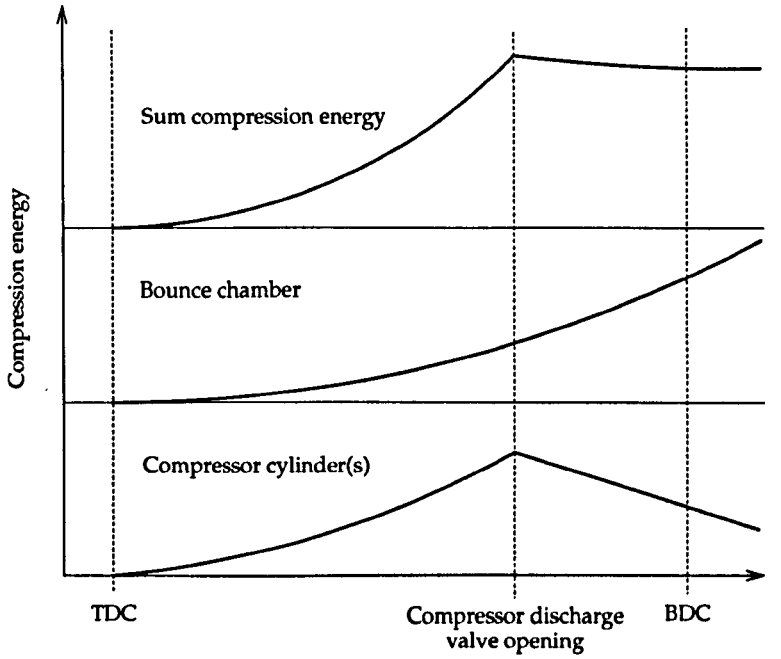

Figure 2.11: The available compression energy in a free-piston air compressor.

The question of why the free-piston air compressor did not gain more widespread success is a difficult one. No reports of serious deficiency or flaws in the concept have been found, except that the free-piston air compressor had a narrow output range. Most reports are, however, of the opposite opinion, such as McMullen and Payne [71] who state that the free-piston air compressor has proved "reliable and efficient under all conditions of service".

Beachley and Fronczak [14] evaluated the same question and presented some possible factors, including that (a) stationary installations tended to use cheaper electric motors to drive compressors, (b) demands for varying power output disfavoured the free-piston air compressor for portable applications, and (c) low fuel prices and a limited market for such applications discouraged the development of such an unconventional design.

2.2.1.1 Junkers

The Junkers free-piston air compressor was one of the earliest successful free-piston engine applications and Junkers had already started development work when Pescara presented his earliest work. The Junkers air compressor was first exhibited in 1936 and was used by the German Navy during World War 2 to provide compressed air for launching torpedoes. After the war, US company Worthington continued development on the Junkers model with only minor design changes [99].

The Worthington-Junkers air compressor was a four-stage, opposed piston engine, illustrated in Figure 2.12. It should be noted that air passages, air-coolers between stages and piston synchro-

nisation mechanism are not shown, and that the third and fourth stage compressors were nested within the first and second stage ones to make the engine more compact than the figure indicates. The main engine design data are listed in Table 2.1. The engine had no rebound device, as the compressed air left in the clearance volumes in the compressor cylinders provided the work to drive the next compression. This was possible because the compressor had close to constant delivery and the fuel pump was set to deliver a fixed amount of fuel. When the delivery pressure reached the required level, the fuel pump would trip and the engine stop [37].

A mechanical synchronisation mechanism ensured vibration-free operation, and the engine imbalance was reported to be small enough to allow the use of a lightweight and low-friction mechanism. Starting was carried out using compressed air, by manually moving the pistons to its outer positions, pressurising the compressor cylinders and then releasing the pistons. London and Oppenheim [67] reported that a compression ratio of 40:1 was achieved with this method, virtually ensuring combustion and unproblematic starting.

Toutant [99] reported that the unit occupied about 50 % of the space required by a conventional electrically driven compressor and that this, together with low fuel consumption, gave the unit great advantages in submarine installations.

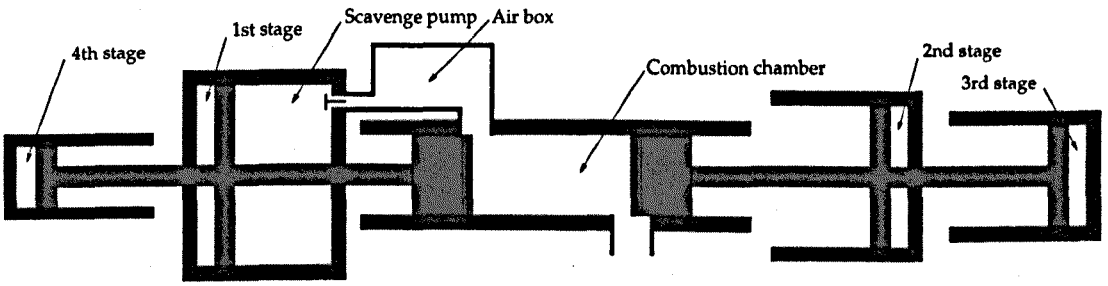

Figure 2.12: Principle configuration of the Junkers free-piston air compressor [99].

Capacity (atmospheric air)	0.0333 m^3/s
Discharge pressure	20.3 MPa
Operating frequency	880 rpm
Indicated engine power	65 hp (48 kW)
Cylinder bore	0.115 m
Stroke (full load/light load)	0.217 m/0.198 m
No. of compressor stages	4
Pressure ratio per stage	3.75
Mass of each piston	29.7 kg
Unit shipping weight	567 kg

Table 2.1: Junkers air compressor specifications [67].

2.2.1.2 Pescara

Farmer [37] described an opposed piston, single-stage air compressor based on Pescara's work. Unlike the contemporary Junkers engine it had variable output, ranging from 1.04 to 3.46 kg/min at a delivery pressure of 690 kPa, with an indicated full-load power output of 37.2 hp (28 kW). Farmer stated that the fuel consumption of the unit was comparable to conventional technology. A speed range from no load to full load of 1000 to 940 cycles per minute was reported, and the variable output was achieved through changes in the stroke length. Although the variable stroke length led to a reduction in compressor volumetric efficiency, Farmer noted that this did not have a significant influence on overall engine fuel efficiency.

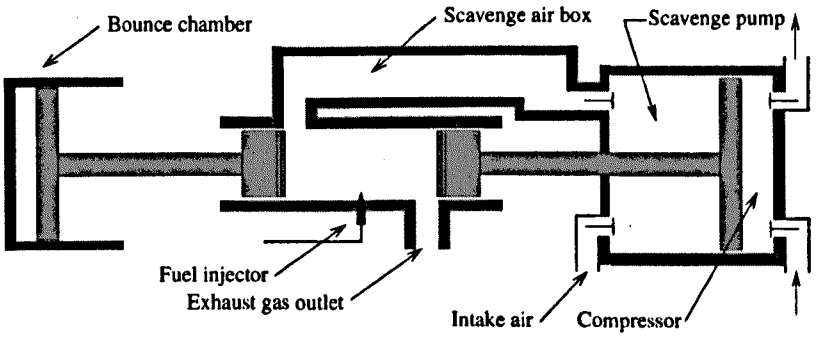

Figure 2.13: Principle configuration of the Pescara free-piston air compressor [37]. (Note that the piston synchronisation mechanism is not shown.)

Figure 2.13 shows the principal configuration of the Pescara free-piston air compressor. It can be seen that the engine was asymmetric, having the bounce chamber coupled to one piston and a combined compressor piston and scavenge pump coupled to the other. A mechanical linkage (not shown in the figure) was used to synchronise the pistons, and engine accessories, such as fuel injection pump and lubrication oil pump, were driven by shafts connected to the synchronisation mechanism.

This free-piston air compressor design was the basis for the later Pescara-Muntz P-42 air compressor [3]. Pescara also proposed a three stage free-piston engine air compressor with design similarities to the Pescara-Muntz engine [83].

2.2.1.3 Braun linear engine

Braun and Schweitzer [22] presented a single piston free-piston engine, patented by Braun [21]. The load device in the engine was an air compressor but the authors state that any suitable linear load may be applied. The engine operates on a crankcase-scavenged spark ignited cycle and counterweights are applied to make the engine completely balanced. Reported engine design and

performance data are listed in Table 2.2. A compression ignition version of the engine was reported to have been operated successfully.

Extensive engine testing with favourable results was reported, among this 15,000 hours of operation without breakdown and 40,000 consecutive starts without failure. The authors stated that superior fuel economy was possible due to the on/off control of the compressor, where conventional engine-compressor sets would run idle. A comparison with other air compressors, including the Pescara-Muntz free-piston air compressor, was also presented, showing significant space and weight benefits for the Braun engine.

Nominal stroke	0.127 m
Bore	0.114 m
Operating frequency	1350 rpm
Compressor cylinder bore	0.191 m
Power output	22 hp (16 kW)
Corresponding mep	552 kPa
Delivery (atmospheric air)	2.41 m^3/min
Discharge pressure (gauge)	689 kPa
Fuel consumption (gasoline)	5.0 kg/h

Table 2.2: Braun linear engine specifications [22].

2.2.2 Free-piston gas generators

During the period 1945–1960, much attention was given to the free-piston gas generator as an alternative for power generation in a number of applications. Both General Motors and Ford Motor Company had working prototypes aimed for vehicle propulsion and larger free-piston gas generators were installed in a number of stationary and marine powerplants. Much experience of free-piston operation and performance was reported over this period.

These free-piston gas generators were based on the free-piston compressors which at this time had proved favourable performance. They were all opposed piston, diesel powered engines with mechanical synchronisation of the two pistons. The synchronisation mechanism would, in addition to making the engines vibration-free, also drive the accessories such as fuel injection pump, oil pump and water pump. The starting of the engines was carried out in a similar way to the free-piston air compressors with a rapid introduction of compressed air into the bounce chamber.

The free-piston gas generators showed some attractive features compared to present-time conventional crankshaft engines and gas turbines. Most important features were the ability to burn low-quality fuel, operate free of vibration and have good dynamic response. London and Oppenheim [67] stated that the fuel economy of the free-piston gas generator was competitive with conventional diesel engines and 80–100 % better than conventional gas turbine plants for the size

investigated. The power density of the units was poorer than the high power to weight ratio of the gas turbine but better than the low power to weight ratio of the conventional diesel engine.

McMullen and Ramsey [72] claimed that the efficiency advantages of the free-piston gas generators compared to conventional gas turbines were due to the higher compression pressures. They stated that free-piston engines could achieve an end-of-compression pressure of 100 times the atmospheric pressure, whereas in the simple type gas turbine this value was limited to around 6. However, it was noted that as material quality increased, complex gas turbine plants with intercooling, regeneration and multiple stages would approach the performance of the free-piston gas generator.

Despite being highly supercharged, these engines had no cooling of the intake air. McMullen and Payne [71] pointed at the possibility of improved performance with intercooling or a higher level of supercharging and stated that higher pressures can be allowed in the free-piston engine due to the absence of bearings. It is, however, evident from a number of reports that the limiting factor was the engine material properties in components such as piston and piston ring, and the gas generators were already running with higher pressures than those allowed in conventional diesel engines. London and Oppenheim [67] stated that the indicated mean effective pressure in the SIGMA GS-34 would be difficult to achieve in a conventional engine. In addition, the gas generator engines commonly ran with high excess air ratios and the advantages with cooling of the inlet air would therefore be limited.

Due to the high excess air ratio, the possibility of applying afterburning in these machines was discussed by several authors, including Huber [55]. Theoretical analyses revealed that a considerable power increase could be achieved but no reports describe afterburning being applied in practice.

A particular feature of the free-piston gas generators that gave these engines a further advantage over conventional gas turbines, was the reduced temperature of the gas supplied to the power turbine. This was a result of the work required to compress the inlet air already being extracted from the gas when fed to the turbine. This allowed the free-piston unit to be placed further away from the power turbine without extensive heat transfer losses from the gas, a feature that was particularly attractive in automotive applications.

McMullen and Payne [71] noted the wide range of applications in which the free-piston gas generator could be applied, including electric power plants, pumping stations, locomotives, marine installations and truck engines. However, despite some well documented advantages against conventional technology, the free-piston gas generator never gained the necessary advantages to be-

come a real competitor neither to the conventional diesel engine nor to the gas turbine. Some reasons for this were:

- Higher levels of development effort were put in to both conventional diesel engines and gas turbine technology, giving rapid performance improvements.
- Matching a pulsating-flow compressor with a narrow operating range to a continuous-flow turbine proved problematic, reducing part-load efficiency and limiting the gas generator to constant power applications.
- High failure rates and low lifetime and availability are reported in some of the reported performance tests, related to high pressure and temperature operation.
- The engines did not provide large advantages in weight or fuel economy over conventional engines and could not compete with the power to weight ratio of the gas turbine.

With the maturing of conventional gas turbine technology, development of the free-piston gas generator was largely abandoned in the early 1960's [3,6,61].

2.2.2.1 SIGMA

Together with the Junkers air compressor, the model GS-34 free-piston gas generator manufactured by Société Industrielle Générale de Mécanique Appliquée (SIGMA) in France is widely regarded as one of the most successful free-piston engine ever made. SIGMA built a free-piston gas generator prototype in 1938 and finished the development of the SIGMA GS-34 gas generator in 1944. The GS-34, illustrated in Figure 2.14, was based on Pescara's patents, which he at that point had sold, and Huber, the former leader of Pescara's technical staff, was heavily involved in the development of the SIGMA [3].

The GS-34 was aimed for large scale applications and had an output power of around 1000 kW. Table 2.3 shows design and performance data for the engine. Some plants used more engines in parallel supplying a single turbine, and Huber [55] reported that in October 1957, 90 gas generators with a total running time of about 250 000 hours were in commercial use and more units were on order. The engines were used in various installations such as stationary plants, the largest one being the Cherbourg power plant consisting of 8 gas generators feeding one turbine and giving 6000 kW electric power output. Huber also reported that a similar powerplant six times the size of the Cherbourg plant was on order at the time of writing. As marine powerplants, free-piston gas generators were installed in 21 minesweepers of the French Navy. Huber reported favourable results with excellent vessel manoeuvrability with gas generator compared to conventional diesel engine propulsion. Other marine installations are also mentioned, in addition to other applications such as locomotives and the powering of pumps and compressors.

Flynn [61] described some experiences from testing of the GS-34 engine. The perfect dynamic balance was noted, along with the fact that the free-piston gas generators were efficient machines. However, many problems during the performance test runs were reported, including cylinder wear, piston ring wear and breakage, high oil consumption, oil leakage and airbox (intake manifold) fires due to the oil leakage. When General Motors later developed the GM-14 gas generator based on the GS-34, Flynn reported that "Several hundred engineering changes were incorporated [...]".

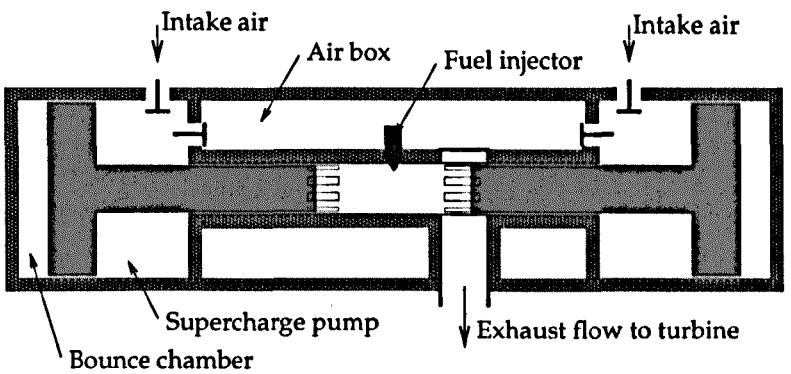

Figure 2.14: Simplified illustration of the SIGMA GS-34 free-piston gas generator [67].

Power output	1138 hp (849 kW)
Weight (approx.)	8000 kg
Speed	613 rpm
Cylinder bore	0.34 m
Bounce chamber bore	0.90 m
Stroke	0.44 m
Compressor pressure ratio	5.42
Engine compression ratio	8.5
Piston mass	503 kg
Overall thermal efficiency	34.6 %

Table 2.3: SIGMA GS-34 design and performance [67].

2.2.2.2 General Motors

General Motors (GM) gained interest in the free-piston engine concept after testing a number of free-piston engines including the SIGMA GS-34 gas generator in the mid-1950's. This ultimately led to the development of two free-piston engines, the GM-14 and the GMR 4-4 'Hyprex'.

The GM-14 was based on the SIGMA GS-34 and Flynn [61] reported that significant design improvements were made in the new engine, based on extensive testing of the SIGMA engine which at this time had reached some degree of commercial success in Europe. (London and Oppenheim [67] reported in 1952 that SIGMA 'has reached a state of commercial exploitation'.)

A marine powerplant based on six GM-14 units was installed in GTS William Patterson, a United States Maritime Administration vessel, in the late 1950's but with disappointing results. Specht [91] evaluated the powerplant and reported a number of problems during the test period but also explains how some of them were addressed. Reported problems included air pulsation and noise in the machinery room, piston ring breakage, difficulties in matching the gas generators with the turbines and higher maintenance costs. Reported advantages of the powerplant included allowing high manoeuvrability of the vessel, the possibility of rapid changes in the power level, easy maintenance of the units with low impact on vessel operation, and high operational flexibility with 6 gas generators and 2 turbines. The fuel economy was reported to have been comparable to that of conventional technology. Specht concluded that the gas generator plant was unsuitable for scaling up due to the necessary increase in number of units, increasing labour costs for maintenance and operation, compared with existing gas turbine plants.

The GMR 4-4 'Hyprex' was a dual ('siamesed') opposed piston, diesel powered free-piston engine aimed for automotive applications, with a power output of around 185 kW at 2400 rpm. Underwood [101] listed the reasons for the chosen siamesed design, among others a more compact unit and reduced pressure oscillations at the turbine inlet. The engine was installed in a car, the XP-500, for testing, making this the first car in the world to be powered by a free-piston engine. Despite optimistic reports from the GM engineers, the Hyprex did not provide manufacture and operational benefits following improvements in conventional engine technology and was therefore abandoned [6].

Flynn [61] observed that the part load efficiency of the earliest free-piston gas generators was poor, due to problems matching the free-piston engine with a conventional turbine over the full operating range. This led to the need for a bypass valve to dump gas at low loads, with obvious heavy penalties in the fuel efficiency. GM solved this problem by introducing a bypass valve between the intake manifold and the air inlet. Using this, the engine could run on lower speeds and compression ratios at part-load and the gas output matched the turbine requirements for the full load range. Amann [6] reported that by using this method the idle fuel consumption dropped from 25 % of the full-load fuel flow rate, down to 8 %.

2.2.2.3 Ford

Like General Motors, Ford saw a potential for the free-piston gas generator in automotive applications in the mid-1950's. Frey et al. [42] described the potential advantage of mounting the gas generator in the front of the vehicle and the power turbine in the rear, thereby eliminating the drive tunnel and achieving better weight distribution. (The same was mentioned by Underwood of General Motors [101].)

Frey et al. [42] also developed analytical models in the design of a free-piston gas generator and they described the development of a 150 hp (112 kW), 2400 rpm unit. They reported initial development difficulties regarding starting, piston rings breakage, injection pump failures and poor combustion, but described how most of these were addressed by improvements in the design. The authors further described that since the fuel pump was driven by the piston assembly, a delay had to be implemented in the fuel injection system. This was due to the low piston kinetic energy around TDC, making it unsuitable to drive the fuel pump by the piston. (The problems associated with fuel injection in free-piston engines were discussed by a number of other authors, including General Motors researchers [39]).

Noren and Erwin [79] described the development of the Ford model 519 free-piston powerplant and its implementation in a farm tractor. The authors stated that for this application the free-piston powerplant was more compact, has lower weight and provides more freedom in the mounting of the engine than a comparable conventional diesel engine. Based on results from the test vehicle they reported superior torque characteristics for the free-piston gas generator unit, illustrated in Figure 2.15. As the conventional engine torque will decrease as the speed is reduced and the engine finally stalls or a gear shift has to be made, the torque from the free-piston unit increases at lower speeds. Further reported advantages of the free-piston unit include vibration free operation and low noise.

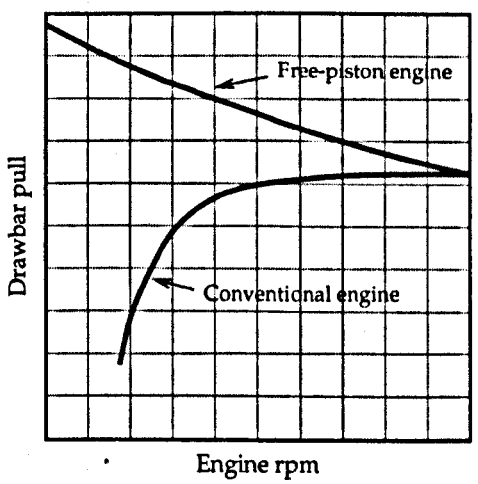

Figure 2.15: Torque characteristics of the free-piston powerplant compared to those of a conventional engine [79].

2.2.2.4 Kværner

In a more recent approach, the Norwegian company Kværner ASA and the Norwegian University of Science and Technology (NTNU) designed an 8-cylinder, 8 MW free-piston gas generator [59]. The engine was a single-piston gas generator, illustrated in Figure 2.16 and with design data as

listed in Table 2.4. Experimental results from a one-cylinder test engine were reported. The intake air was highly supercharged through a turbocharger, an intercooler and a charge air compression chamber, and power output was taken entirely from an exhaust turbine. A thermal efficiency of around 50 % was reported.

The developers derived a control strategy for piston motion control, controlling TDC, BDC and synchronisation of the cylinders, along with supervisory control objectives of load and combustion optimisation, through the varying of the fuel mass flow and the amount of air in the bounce chamber. Simulation results were presented showing the feasibility of the control approach [60].

This engine is the only reported modern attempt of building a free-piston gas generator. However, through personal communication with the developers, the author has learnt that the project was terminated before the engine was fully developed, and further information on the operation and performance of the engine is therefore not available [58]. The reasons for this are not known.

Power output	1000 kW
Speed	1800 rpm
Cylinder bore	0.180 m
Bounce chamber bore	0.180 m
Stroke	0.189 m
Piston mass	100 kg
Overall thermal efficiency	50 %

Table 2.4: Numerical values for Kværner KLC test engine [59].

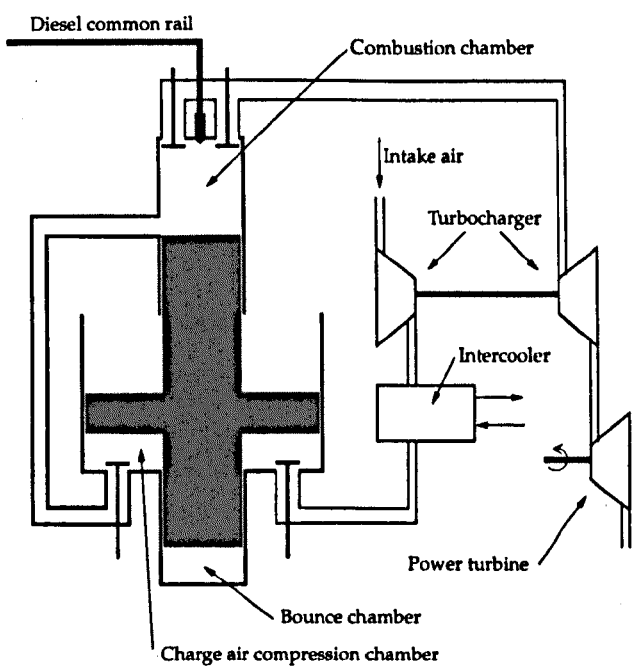

Figure 2.16: Kværner KLC free-piston gas generator [59].

2.2.2.5 Other reports

Baldwin-Lima-Hamilton In 1943, Baldwin-Lima-Hamilton (BLH) started the development of a large-scale free-piston gas generator for the United States Navy, aimed for marine propulsion [3]. Requirements for the unit were high specific output, low weight, high efficiency and high reliability. A model was also designed for use in locomotives and performance superior to that of the SIGMA GS-34 was reported [71].

The BLH unit consisted of two outward compressing gas generators feeding one turbine with a reduction gear. The operation of the two gas generators was synchronised to reduce pressure pulsations and the unit could operate with only one gas generator if the load requirements were low. McMullen and Payne [71] stated that the BLH unit was intended to work under "extreme temperature and pressure conditions" to maximise engine performance.

Cooper-Bessemer McMullen and Ramsey [72] presented results from a free-piston gas generator test engine developed by Cooper-Bessemer, but state that most of the engine information and findings are of confidential nature. The test engine was reported to have developed 1750 hp (1305 kW) running at 555 rpm with an achieved thermal efficiency of 45 per cent. Very simple and fast starting of the machine was reported, using a simple push-button to achieve running conditions almost instantly.

McMullen and Ramsey further reviewed the feasibility of the free-piston gas generator in a number of different applications, including stationary electric power plants, pipeline pumping units and marine propulsion powerplants. A number of potential advantages using free-piston gas generators in such applications were listed, including low costs, high reliability, high flexibility in both the mounting and the operation of the machinery, high thermal efficiency and vibration-free operation. McMullen and Ramsey also suggested the use of free-piston gas generators in pumping stations, claiming that the gas generator turbine is well suited for this purpose because it adapts well to centrifugal machinery.

2.2.3 Hydraulic free-piston engines

Many of the modern approaches in free-piston engine technology are hydraulic engines, in which the combustion piston is directly coupled to a hydraulic pump cylinder. A number of development projects are ongoing, both within academia and in industry. Most of these units are aimed at off-highway vehicles such as forklift trucks and earth-moving machinery and, consequently, most developments are of small size (typically 30-50 kW). Such vehicles typically have high hydraulic loads from vehicle accessories and propulsion, and they are commonly powered by a conventional diesel engine coupled to a hydraulic pump.

Hydraulic free-piston engines may apply a hydraulically driven rebound device, using part of the produced hydraulic energy to return the piston, or a bounce chamber. A number of prototypes have been developed in recent years and experimental results from these are currently being reported. The reports show generally good fuel economy and very good performance at part load.

2.2.3.1 Toyohashi University

Researchers at Toyohashi University of Technology in Japan have been doing research in the field of hydraulic free-piston engines for more than 20 years. They have reported experimental results from both single piston [53] and opposed piston [52] diesel powered free-piston engines.

The latter is the latest published work, with reported engine hydraulic thermal efficiency of 31 %[4]. The authors stated that this value stays practically constant even with very low hydraulic power output. The fuel injection is hydraulically actuated and the fuel is injected very early in the compression process to achieve a combustion process similar to that of a homogeneous charge compression ignition engine.

Hibi and Ito [52] further presented an alternative piston synchronisation method for the opposed piston engine, eliminating the traditional mechanical linkage. The pistons in the hydraulic free-piston engine are synchronised by using a combination of the electronically controlled hydraulic rebound device and a mechanical spring. A small synchronisation error is reported, but this is not sufficiently large to affect the performance of the engine.

2.2.3.2 Technische Universität Dresden

The German university Technische Universität Dresden, Bosch Rexroth AG and Brefa GmbH have developed a hydraulic free-piston engine with a patented hydraulic control system [23, 24], illustrated in Figure 2.17. The unit is a single piston engine coupled to a hydraulic cylinder, where the hydraulic system acts as both load device and rebound device, along with providing engine control. The engine is controlled with simple on/off control and relies on energy storage units in the hydraulic system to smooth engine operation. The developers present the implementation of the engine in a hydraulic circuit and report a hydraulic efficiency of above 30 %.

2.2.3.3 Innas

The Dutch company Innas BV is among the research leaders within free-piston engine technology today, and has developed a single piston, diesel powered, hydraulic free-piston engine, shown in Figure 2.18 [2]. The unit is intended as an alternative to conventional engine and hydraulic pump systems in off-highway vehicles and the implementation of the engine in a fork lift truck was

[4]For comparison, consider a conventional diesel engine with fuel efficiency of 40 % coupled to a hydraulic pump with efficiency 85 %. The total ('hydraulic thermal') efficiency for this system would be 34 %.

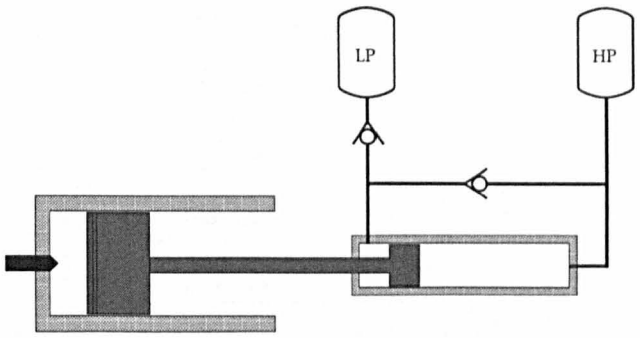

Figure 2.17: Illustration of the hydraulic free-piston engine developed at TU Dresden. Note that the hydraulic circuit is simplified.

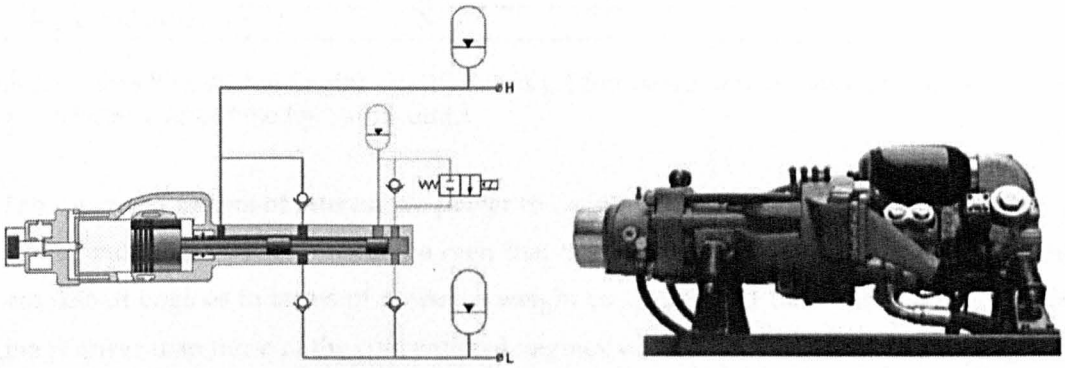

(a) The working principle of the Innas Free-Piston Engine.

(b) Photograph of the engine.

Figure 2.18: The Innas Free-Piston Engine. (Reprinted with the permission of Innas BV.)

described [102]. The developers claim that reduced exhaust emissions and lower fuel consumption can be achieved due to a mechanically less complex design and high operational flexibility. An electronic control system is implemented and the engine uses pulse pause modulation frequency control.

The engine has a nominal speed of 42 Hz and a 17 kW power output, and indicated efficiencies of around 50 % are reported [90]. The working principle of the engine is shown in Figure 2.18a. Fuel consumption is reported to be around 20 % lower than a conventional engine-pump unit and at low loads even 50 % lower [2].

As documentation of engine design and performance exists for the Innas Free-Piston Engine, a comparison with conventional engines can be made. Table 2.5 lists the reported specifications of the Innas Free-Piston Engine and those of two conventional diesel engines in the same power range, the John Deere model 3009D [33] and the Perkins 403C-07 [69]. It should be noted that listed specifications for the two conventional engines are for the combustion engines only, without a hydraulic pump, whereas for the Innas Free-Piston Engine they are for the complete engine-pump unit.

	Innas Free-Piston Engine	John Deere 3009D	Perkins 403C-07
Power output	17 kW	14.2 kW	15.3 kW
Engine height	0.35 m	0.71 m	0.56 m
Engine length	0.82 m	0.64 m	0.44 m
Engine width	0.30 m	0.53 m	0.35 m
Dry weight	90 kg	120 kg	76 kg
Aspiration	Natural	Natural	Natural
No. of cylinders	1	3	3
Operation	2-stroke	4-stroke	4-stroke
Bore	110 mm	72 mm	67 mm
Nominal stroke	120–125 mm	72 mm	72 mm
Displacement	1.188 dm^3	0.879 dm^3	0.762 dm^3
Operating frequency	42 Hz	50 Hz	60 Hz
Mean piston speed	10.5 m/s	7.2 m/s	8.6 m/s
NO_x emissions	6 g/kWh	–	–
Indicated efficiency	51 %	–	–

Table 2.5: Innas Free-Piston Engine specifications [2] compared to two conventional diesel engines. (The two latter without the hydraulic unit.)

The two main factors of interest are power to weight ratio (and to some extent the volume of the units) and fuel efficiency. It can be seen that the free-piston engine compares favourably to the crankshaft engines in terms of power to weight ratio, and that the volume of the free-piston engine is lower than those of the conventional engines without a hydraulic pump. Typical values for indicated efficiency in diesel engines of this size lie between 40 and 45, %, as such, the free-piston engine appears to have a significant fuel efficiency advantage. The differences in indicated efficiency will be further enhanced by the lower frictional losses in the free-piston engine.

The reported values of NO_x emissions in the Innas Free-Piston Engine are comparable to what one would expect from conventional engines of the same size.

2.2.3.4 Tampere University

Tikkanen et al. [96] described the performance of a dual piston hydraulic free-piston engine prototype developed at Tampere University of Technology, Finland. A version of the engine with around 20 kW power output was implemented in a mobile machine platform [94]. This group of researchers have also published work on engine design, including parametric studies of the effects of various engine parameters on engine operation [95], and engine control [97].

The engine, illustrated in Figure 2.19, is diesel powered, utilising a common rail injection system with electronic control. Starting is achieved using stored hydraulic energy, by driving the piston with the hydraulic cylinder until sufficient compression for fuel injection is achieved.

Test results from a test engine were described by Tikkanen et al. [96], and showed a piston motion profile different to that of conventional engines and piston acceleration peak values of more than double those of comparable crankshaft engines. In comparison to conventional engine piston

motion, it was observed that the maximum piston velocity was lower for the free-piston engine. The authors further stated that the piston velocity is nearly constant for long periods of the stroke with fast speed reversals around the dead centres, benefitting the hydraulic pump circuit. The engine was reported to run asymmetrically due to the fuel injectors not delivering exactly equal amounts of fuel and to asymmetric hydraulic loads. The cycle-to-cycle variation in stroke length was reported to be ±1 %, giving a variation in compression pressure of around ±15 %. Variations in the combustion pressure of 77-88 bar were reported.

The developers stated that the results from the initial tests were satisfactory as proof-of-concept for the hydraulic dual piston engine but that the control issues should be addressed. Total efficiency of 20 % was reported for the test engine.

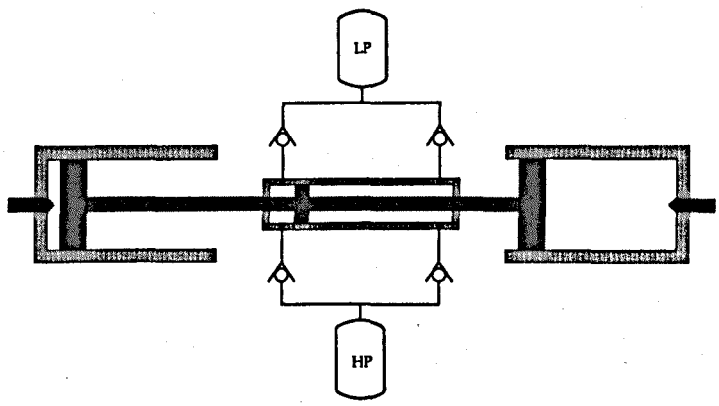

Figure 2.19: Illustration of the hydraulic free-piston engine developed at Tampere University of Technology [95].

2.2.3.5 Others

Heintz [49] proposed a dual piston free-piston engine hydraulic pump and outlined the design strategy of such a unit through generalised equations. Other free-piston engine configurations were also briefly reviewed. Allowing the unit to move freely was suggested in order to cancel out vibrations and Heintz pointed out that this would not have been possible with a mechanically driven power output. It was stated that control of such a unit can be carried out in a "simple and efficient manner" and that starting represents the most challenging control issue. Heintz was also granted two patents on dual piston hydraulic engine solutions similar to that described in the paper [47,48].

Baruah [13] proposed a spark ignited hydraulic free-piston engine of the single piston type, aimed for vehicle propulsion. Detailed modelling of the engine was presented, along with simulation results showing clear advantages for the free-piston engine over conventional engines regarding nitrogen oxide emissions formation. No thermodynamic advantages were found and the

author listed a number of limitations for the free-piston concept, including a narrow speed range and operational control challenges. On these grounds, the feasibility of the hydraulic free-piston engine for use in vehicle propulsion was questioned.

Beachley and Fronczak [14] presented the design of an opposed piston free-piston engine pump. The proposed design shares many features with that proposed by Hibi and Ito [52], including the frequency control system. A piston control system to secure operation if the engine misfires and to aid starting was also described, and the authors proposed future work to investigate the feasibility of the hydraulic free-piston engine.

Galitello [62] presented a dual piston free-piston hydraulic pump. The proposed engine has two double-acting pumping pistons attached to the moving member, and a timing module was also described to allow computer control of various aspects of engine operation.

Rittmaster and Booth [87] presented a dual piston hydraulic free-piston engine for powering a hydraulic motor. The hydraulic system included a flywheel to dampen pulsations from the engine. The back sides of the combustion pistons were proposed as the hydraulic pumping pistons, and the design included a blower to provide scavenging air for the spark ignited engine.

Bock [18] presented a dual piston hydraulic free-piston engine in which the pump cylinder is situated in the centre of the engine between the two combustion cylinders, and a pump piston fixed on the reciprocating rod between the combustion pistons divides the pump cylinder into a pair of pump cylinder chambers.

2.2.4 Free-piston engine generators

Another application of the free-piston concept that has received considerable attention in recent years is the free-piston engine generator, in which a free-piston engine is coupled to a linear electric machine. Such technology is currently explored by a number of research groups worldwide and some prototype engines have been reported. The high flexibility and controllability of electric power systems and the high efficiencies of electrical machinery make this an interesting concept.

A driving force behind the interest in free-piston engine generators is the automotive industry's recent research and development efforts within hybrid-electric vehicle (HEV) technology. Such technology is becoming commercially available from an increasing number of manufacturers and provides significant fuel consumption and vehicle emissions benefits.

HEV's employ electric machinery and energy storage devices, which partly or fully separate the combustion engine from the mechanical drive chain. This reduces the load variations on the engine which allows it to work closer to its optimum operating conditions, resulting in increased fuel efficiency and reduced emissions. Eliminating the need for a wide load and speed range may allow greater optimisation of the engine design, further enhancing engine performance.

In the marine industry, the all-electric ship concept is based on many of the same principles as the hybrid electric vehicle, namely optimised engine operation and an efficient electric power distribution system and end drives. In a ship, such a system consists of a number of generator sets for power generation, and the propulsion and utilities, such as thrusters, pumps, ventilation and air conditioning, would be electrically driven.

2.2.4.1 West Virginia University

Researchers at University of West Virginia reported the development of a spark ignited dual piston engine-generator prototype, illustrated in Figure 2.20, and later also attempted to develop a similar compression ignition engine. This group of researchers have thoroughly documented their work and findings in a number of publications, concerning linear alternator design, design and operation of the combustion engine and analysis of the combined system [29–32, 36]. The prototype gasoline engine is reported to have achieved 316 W electric power output at 23.1 Hz, with 36.5 mm bore and 50 mm maximum stroke [36]. High cycle-to-cycle variations are reported, in particular at low loads [31].

A 75 mm bore and 71 mm maximum stroke compression ignition engine was built but was reported to have problems running [98]. Toth-Nagy [98] related the problems to two factors: (a) the engine was built from gasoline engine components which were not dimensioned for the diesel engine application and (b) the engine vibration caused excessive fatigue load on the components. Together, these factors are reported to have caused catastrophic failure to a number of engine components.

This group of researchers is the most successful within academia regarding free-piston engine generator research. It is one of very few that have reported the successful development of a running prototype.

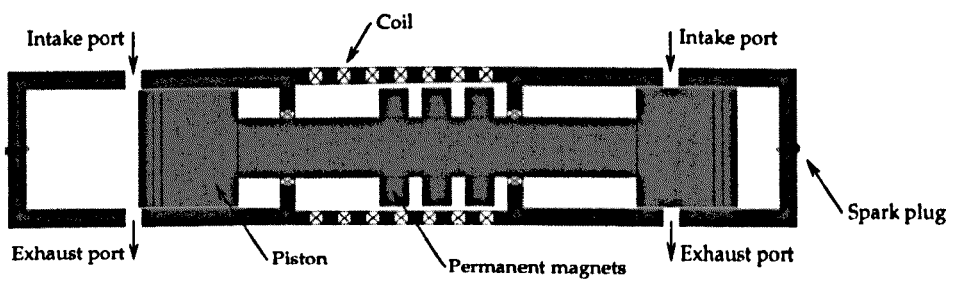

Figure 2.20: Illustration of the free-piston engine generator prototype developed at University of West Virginia [36].

2.2.4.2 Sandia National Laboratories

Van Blarigan et al. [17] presented the design of a patented [16] dual piston free-piston engine generator. The engine employs homogeneous charge compression ignition (HCCI) and is aimed at operating on a variety of fuels. Applying HCCI operation gives faster combustion than that in SI or conventional CI engines, and allows the use of lean mixtures at high compression ratios, thereby reducing NO_x emissions formation. Test results from a compression-expansion machine were presented, showing close to constant volume combustion with high thermal efficiencies at fuel-air equivalence ratios of around 0.3.

A numerical simulation model of the engine was presented by Goldsborough and Van Blarigan [43] and the same authors described detailed modelling of engine scavenging [44], investigating various port and valve configurations. It was found that achieving good scavenging together with the very low short-circuiting of the charge air that is required in pre-mixed engines is a challenge.

2.2.4.3 Others

University of Regina Researchers from University of Regina described the modelling and simulation of a patented hybrid engine solution [35, 65, 106]. Simulation results for both a single piston and a dual piston configuration were presented, both units employing two electrical machines which can be run as either motor or generator. In motoring mode, the electric machines will provide the work needed for the compression process, and a computer control system was proposed to control various aspects of engine operation. The theoretical study was based on very simplified combustion modelling and predicts power outputs in the area of 700 W at around 50 Hz for the dual combustion chamber engine, with a bore of 30.5 mm and a stroke of 26.7 mm. The development of an engine prototype has not been reported.

Pempek Systems Carter and Wechner [25] presented the design of a "Free Piston Power Pack", a unit consisting of four dual piston free-piston engines, intended for powering hybrid electric vehicles. Total power output was 100 kW, and proposed advantages of the engine are high power density, long life, dynamic balance and multi-fuel capability.

Aerodyne Research Annen et al. [7] described a miniature internal combustion engine developed by Aerodyne Research, Inc. The unit is a single-cylinder free-piston engine with a linear alternator, giving an output power of 10 W. It uses a mechanical spring to return the piston and runs on glow-plug ignited propane. Other reported engine data are: 390 Hz operational speed, diameter 15 mm, length 45 mm, weight 15 g (data are for the complete unit). It was reported to work with only solid film lubrication, due to the low frictional losses.

University of Minnesota Aichlmayr [3] and Aichlmayr et al. [4,5] studied the feasibility of miniature homogeneous charge compression ignition (HCCI) free-piston engines. Design aspects for such engines were presented, along with a parametric study investigating the effects of various engine parameters on engine performance and the effects of the small scale. Aichlmayr [3] presented modelling of small-scale HCCI combustion, along with some experimental work.

Engines in the size range of 10 W to 0.1 W were investigated and it was found that heat transfer becomes increasingly significant in small scales and sets a practical limitation to the minimum size of a small-scale engine. Chemical kinetics will also impose limitations in small, high-frequency engines.

Patented applications

Iliev et al. [56] presented a spark ignited dual piston free-piston engine generator. A lightweight electric machine translator was applied and the engine was intended to operate on low compression ratios and with high reciprocating speeds.

Vallon [103] described a single piston free-piston engine generator. The proposed unit consists of a vertical cylinder in which the piston slides and a combustion chamber is situated in the bottom of the cylinder. Return of the piston is done by gravity and part of the piston consist of magnetic material generating electric current in coils situated on the cylinder wall.

Deng and Deng [34] described a double-acting opposed piston free-piston engine, aimed for hybrid-electric vehicles. The engine resembles an opposed piston configuration, with the exception that the bounce chambers are replaced by firing cylinders, giving three combustion cylinders in total. Linear electric alternators are fixed on the connecting rods of the two moving pistons.

Sagov [88] presented a free-piston pump, based on the same principles as free-piston engine generators but with reverse energy flow. The unit consists of a pumping piston coupled to a linear electric machine and a fixed mechanical spring. Energy is supplied to the electric machine, creating a reciprocating (bouncing) motion of the piston assembly. Pumping work can be extracted from the cylinder, like a conventional piston pump.

2.3 Summary

On evaluating the feasibility of the free-piston engine concept, Beachley and Fronczak [14] stated that "...there is little doubt that the free-piston engine is a viable concept. Numerous free-piston engines have demonstrated reliable, efficient, long-life service".

Still, a number of questions arise. Most importantly, can the free-piston engine provide advantages over modern conventional engines? Conventional internal combustion engine technology is highly developed and such engines have been in widespread use and continuously improved over

decades. Efficient mass production lines exist, meaning that such engines can be produces at a low cost. Although much of modern engine technology can be applied to the free-piston engine concept, there are areas that need addressing, such as finding linear load devices with a performance comparable to that of rotating ones.

Furthermore, can an engine control system be realised to ensure steady operation and to optimise free-piston engine performance? It should be noted that the control systems implemented in the mid-20th century engines, although satisfactory for their purpose, merely had the objective of keeping the engines running. Modern engines have significantly higher control requirements for emissions and efficiency optimisation.

On a more positive note, many of the challenges reported with the mid-20th century engines should be possible to address using modern engine technology and improved materials (in fact, many of the reported problems were partly or fully solved before the free-piston engine concept was abandoned).

Recently proposed free-piston engines range from 10 W [7] to 8 MW [59] in size, suggesting that the free-piston concept is suitable for a wide size range. Hydraulic free-piston engines appear to be the most promising variant at the moment due to their superb controllability, with some developments having reported favourable results compared to conventional technology. Free-piston engine generators are under investigation by a number of research groups worldwide, indicating their potential. The flexibility and controllability of electric machinery, along with increasing interest in technologies such as hybrid-electric vehicles and the all-electric ship concept, are incentives driving the development of free-piston engine generator technology, and the performance of such engines is expected to improve significantly in the future.

Chapter 3

Engine design

Along with the modest number of free-piston engine designs that have resulted in working prototypes, a high number of theoretical studies have been published on the subject. Varying opinions exist regarding the feasibility of the different free-piston engine designs.

This chapter proposes a design for a free-piston engine generator based on the background study presented in the previous chapter. The main design issues are discussed and a design strategy for the engine is suggested.

3.1 Basic configuration

An engine as shown in Figure 3.1 is proposed. The engine will consist of a combustion cylinder, a gas filled bounce chamber and a linear electric machine. The pistons of the combustion cylinder and the bounce chamber cylinder are rigidly connected and the translator of the electric machine is fixed on this connection, forming the single major moving part of the engine. The piston assembly is not connected to any external crank mechanism and its motion is therefore only influenced by gas forces from the cylinders, engine friction forces and the force from the electric machine.

The engine will operate on a turbocharged, two-stroke direct injection cycle with electronically controlled fuel injection, utilising modern common rail technology. Scavenging is provided through scavenging ports in the cylinder liner and electronically controlled exhaust poppet valves in the cylinder head, utilising uniflow scavenging for high scavenging efficiency.

The bounce chamber will be a closed cylinder with pressure control valves to regulate the amount of gas trapped within it, and thereby the gas pressure force on the piston. Pressurised air will be provided from the turbocharger or an external source for this purpose, and the bounce chamber pressure control system will be able to vary the bounce chamber pressure from the available supply pressure down to atmospheric pressure.

The linear electrical machine is initially assumed to be of the moving magnet, permanent magnet type. The design of the electric machine will be discussed in further detail below.

The free-piston engine generator is intended to be modular in the way that a number of such units can be operated in parallel to achieve power outputs required in large-scale applications. Operation of a number of cylinders with a common turbocharger would be possible, and a computer control system is to optimise the operation of each unit and synchronise the motion of the pistons in each unit to reduce or cancel out vibrations.

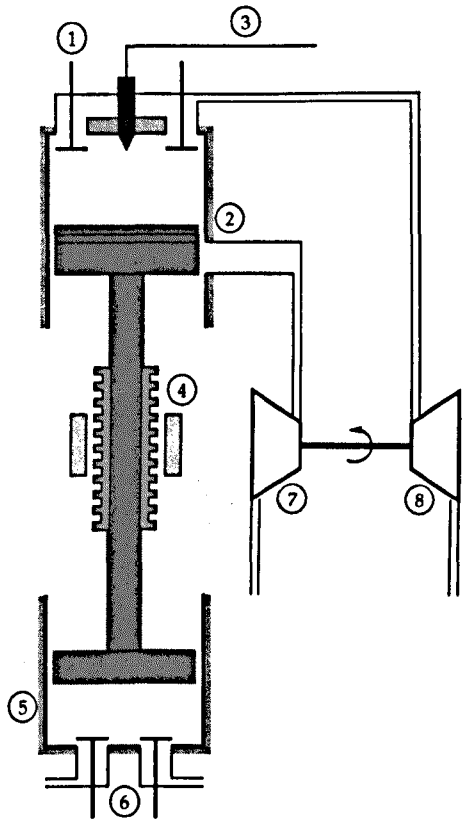

Figure 3.1: Single piston free-piston engine generator.

Figure 3.1 shows the principle engine design, with

① Exhaust poppet valves

② Scavenging ports

③ Common rail fuel supply

④ Linear alternator

⑤ Bounce chamber

⑥ Bounce chamber pressure control inlet and exhaust valves

⑦ Turbocharger compressor

⑧ Turbocharger turbine

3.1.1 Justification

Based on the discussion in Chapter 2, the design presented above was chosen as the most suitable for the free-piston engine generator. The single piston configuration was chosen due to its simplicity and advantages with regards to the control of the engine. With the controllable pressure in the bounce chamber, this design possesses an additional control variable compared to the dual piston design. While the dual piston design benefits from higher power to weight ratio and reduced frictional losses, there is some uncertainty regarding the controllability of such engines. Achten [1] stated that high efficiency and low emissions can only be realised if the compression energy and injection timing can be accurately controlled, and further that the single piston engine is the only free-piston engine configuration for which control issues have been fully solved.

If the performance of the proposed single piston engine and its controllability can be proved satisfactory, investigations into the replacement of the bounce chamber with a firing cylinder would be a natural extension of this work. The third alternative free-piston engine configuration, the opposed piston design, is complex but has clear advantages regarding vibration, since the engine can be perfectly balanced by design. However, there is some uncertainty with this design, including the possibility of piston synchronisation without a mechanical linkage, fuel injection from the cylinder liner and the fixed scavenging ports timing.

3.2 Design methodology

Although the free-piston engine in its basic form is a simple machine, designing such an engine can be a complicated task. The fact that the engine stroke length is variable, and that it depends both on other design variables and on engine operational variables, complicates the design process significantly.

This section presents the main areas that need addressing in the design process of a free-piston engine such as the one illustrated in Figure 3.1, and the discussion forms the outline of a design strategy for such an engine. For any real design case, some of the variables will be fixed, for example in a laboratory where existing engine parts are to be used or if operation at a given frequency is required. The design methodology will therefore have to be adapted accordingly, and general design guidelines for all types of application is therefore not possible to obtain.

The approach presented here will be suitable for a wide range of engine sizes. Some assumptions that can be made for engine design and operational variables will be discussed and numerical values will be presented to provide a design example for an engine such as the one presented above. The chosen engine size for the design examples is based on data from a Volvo TAD1260 six-cylinder diesel engine. This engine has a bore of 0.131 m, stroke length 0.150 m, and a nominal operating speed (piston frequency) of 25Hz. The modelling presented in the chapters below was validated

against experimental data from this engine.

3.2.1 Combustion cylinder

The first question that arises in an engine design process is obviously that of engine size. For a two-stroke engine, the power output will be related to the brake mean effective pressure, swept volume and engine speed with

$$P = \text{bmep} \times V_{sw} \times N. \tag{3.1}$$

The swept volume of the engine is a function of stroke length and cylinder bore, and can be expressed as $V_{sw} = \pi \times B^2/4 \times S$, where B is bore [m] and S is stroke length [m].

Furthermore, the engine speed can be expressed in terms of the stroke length and the mean piston speed. Mean piston speed is defined as $\overline{v}_p = 2SN$, and is usually of much higher importance in the engine design than the engine speed itself. Modern internal combustion engines face limitations on mean piston engine speed of between 8 m/s and 15 m/s due to inertia stress of critical engine components and resistance to gas flow within the engine [51]. Large, low-speed engines usually operate at the lower end of this range, while high-speed engines, such as those found in automotive applications, operate at the higher range. The Volvo TAD1260 diesel engine achieves a mean piston speed of 7.5–9.0 m/s at nominal operating conditions.

Typical values for brake mean effective pressures in turbocharged diesel engines lie between 1000 kPa and 2000 kPa, with large, low-speed engines operating at the higher end of this range. Experimental data shows that the brake mean effective pressure for the Volvo TAD1260 engine is within this range, at above 1500 kPa at high loads.

Combined with the expressions for swept volume and mean piston speed, Equation 3.1 can be written as

$$P = \text{bmep} \times \pi \frac{B^2}{4} S \times \frac{\overline{v}_p}{2S}. \tag{3.2}$$

Hence, the power output in terms of cylinder bore is given by

$$P = \frac{\pi}{8} \times \text{bmep} \times B^2 \times \overline{v}_p. \tag{3.3}$$

The ratio of stroke length to cylinder bore, $(\text{S/B})_r = S/B$, is an important design variable in internal combustion engines, and is effectively a measure of the relationship between engine efficiency and power density. A high stroke to bore ratio gives a compact combustion chamber with low surface

area, which reduces heat transfer losses, whereas a low stroke to bore ratio allows higher engine speeds, increasing engine power output.

The stroke to bore ratio typically ranges from around 0.8 to 3.5, depending on the engine size and application. Small, high-speed engines, such as those found in automotive applications, have stroke to bore ratios of around 1, and the highest values of stroke to bore ratio are found in large, marine diesel engines. The mentioned Volvo engine has a stroke to bore ratio of 1.15.

Knowing the relation between cylinder bore and stroke length, Equation 3.3 can be rewritten to express power as a function of stroke length:

$$P = \frac{\pi}{8} \times \frac{1}{(\mathrm{S/B})_r^2} \times \mathrm{bmep} \times \bar{v}_p \times S^2. \tag{3.4}$$

Figure 3.2 shows the required stroke and bore to achieve a given engine power with the assumptions discussed above, along with the corresponding engine operating speed. It can be seen that as the cylinder bore and engine stroke length increase for increasing power outputs, the operating speed is reduced to maintain a constant mean piston speed.

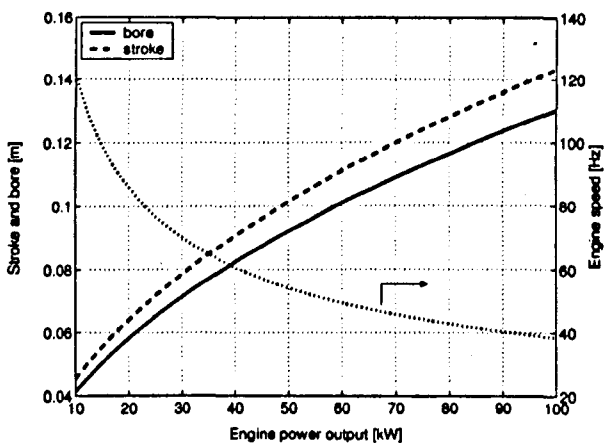

Figure 3.2: Stroke and bore required for an engine with $\bar{v}_p = 10\,\mathrm{m/s}$, bmep $= 1500\,\mathrm{kPa}$ and $(\mathrm{S/B})_r = 1.1$ for different loads.

Figures 3.3, 3.4 and 3.5 show the effects of variations in mean piston speed, brake mean effective pressure and stroke to bore ratio on the required cylinder bore. It can be seen that increasing the mean piston speed or brake mean effective pressure improves engine power density, due to a reduction in the engine bore requirement. Similarly, reducing engine stroke to bore ratio will significantly increase engine operating speed (for a constant mean piston speed), and therefore reduce the required engine bore and increase power density.

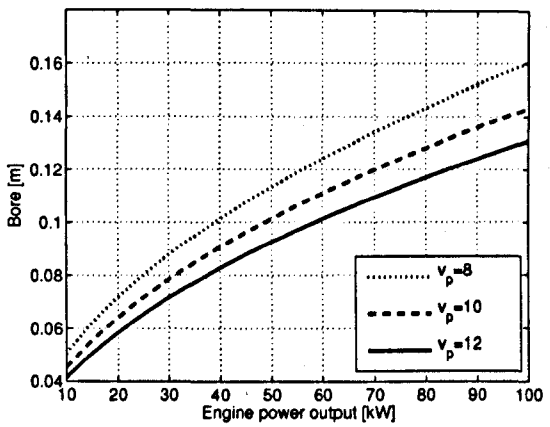

Figure 3.3: Effects of varying mean piston speed, $\overline{v}_p$, on engine design predictions with bmep = 1500 kPa and $(S/B)_r = 1.1$.

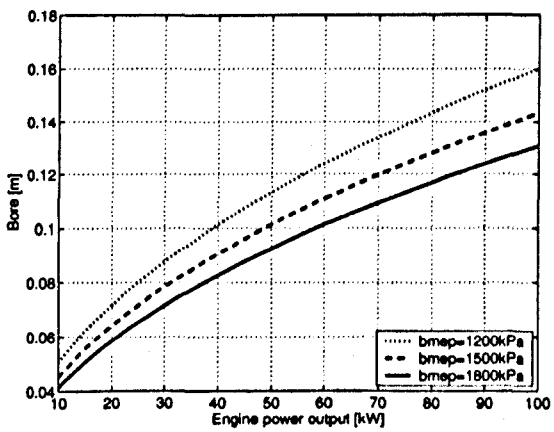

Figure 3.4: Effects of varying brake mean effective pressure on engine design predictions ($\overline{v}_p$ = 10 m/s and $(S/B)_r = 1.1$).

3.2.2 Bounce chamber

The basic design of the bounce chamber is straight-forward using an energy balance. For no-load (idle) operation, the bounce chamber needs to store sufficient energy to compress the cylinder charge to the desired compression ratio. Hence, ignoring frictional losses and assuming equal start-of-compression pressures of the bounce chamber and combustion cylinder, the bounce chamber cylinder could be identical to the combustion cylinder. However, that ignores the fact that scavenging ports are not necessary in the bounce chamber and the full stroke can be utilised for storing compression energy, as can be seen in Figure 3.1.

For normal operation, the load force generating electricity will extract energy not only during the power expansion stroke but also during the compression stroke, and the bounce chamber there-

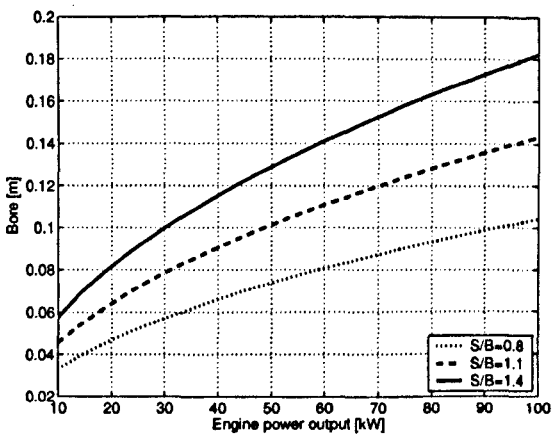

Figure 3.5: Effects of varying stroke to bore ratio on engine design predictions ($\overline{v}_p = 10\,\mathrm{m/s}$ and bmep $= 1500\,\mathrm{kPa}$).

fore needs to intermediately store approximately half of the electric energy extracted in each cycle. If the engine runs with constant stroke length, i.e. constant compression ratios in both combustion cylinder and bounce chamber, storage of additional energy can be achieved by increasing the start-of-compression pressure in the bounce chamber. It is clear that this pressure will always be larger in a loaded case than when running idle, and the basic requirements of the bounce chamber will therefore be decided by the no-load case.

Figure 3.6 illustrates this, showing the energy stored in the engine combustion chamber and bounce chamber, along with the energy dissipated in the load device, over one engine cycle. At TDC the energy content in the combustion cylinder increases through the heat input from the fuel, from the compression energy E_{comp} to a peak combustion energy E_{comb}. The bounce chamber provides a reversible compression of the trapped gas, storing an amount of energy at BDC equal to E_{BC}. The load energy is assumed to be extracted evenly over the full cycle, and E_{load} represents the load energy extracted in one cycle.

If frictional losses are ignored and steady state engine operation is assumed, the energy stored in the bounce chamber when the combustion cylinder is at BDC, E_{BC}, must equal $E_{\mathrm{comp}} + E_{\mathrm{load}}/2$. As the load is reduced towards zero, E_{BC} will tend towards E_{comp}, and E_{comb} will at the same time tend towards E_{comp} since the required energy input from the fuel is reduced.

In practice, the bounce chamber needs to store slightly more energy than that found from theoretical calculations to allow for frictional and thermodynamic losses. When designing the bounce chamber, one would seek the configuration giving the least total losses. A small, high-compression bounce chamber cylinder may give less frictional losses but thermal losses and blow-by will be higher due to the higher gas pressures and temperatures. A larger bounce chamber cylinder allows

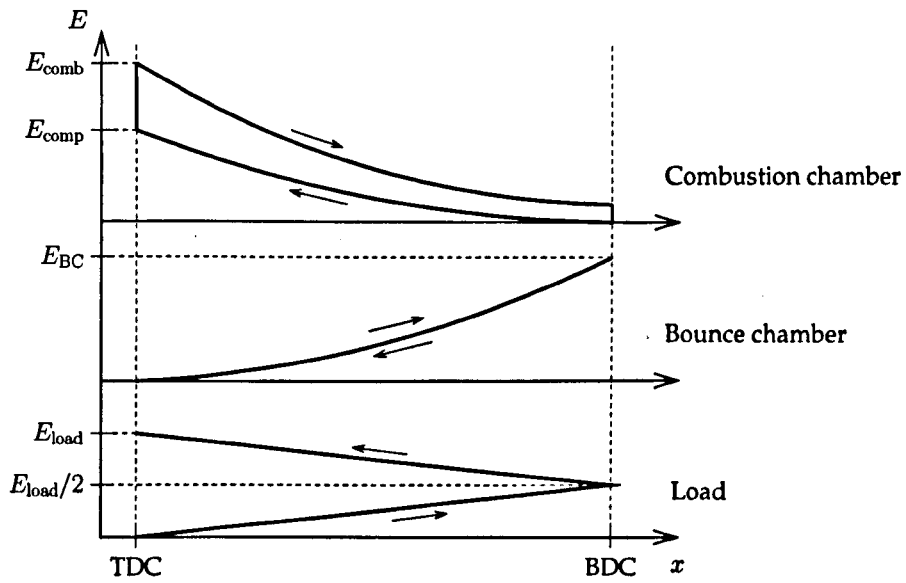

Figure 3.6: Illustration of energy flow over one engine cycle. (Note that the graphs are not drawn to scale.)

a more modest compression ratio to be used but may have larger frictional losses and increases the mass of the piston assembly. A general conclusion on what is the most favourable configuration therefore depends on the specific application and cannot be made without further analyses.

Bounce chamber design methodology

Assuming that a combustion cylinder of stroke S, bore B and compression ratio of C_R has been decided upon, the energy needed to compress the fresh charge for the combustion is given by

$$E_{comp} = \int_{x_1}^{x_2} A_p p_c \, dx = \int_{V_1}^{V_2} p_c \, dV. \tag{3.5}$$

For a polytropic process with constant ratio of specific heats, γ, the instantaneous gas pressure can be expressed as a function of cylinder volume:

$$p_c = p_0 V_1^{\gamma} \frac{1}{V^{\gamma}} \tag{3.6}$$

where p_0 is the gas pressure at the start of compression.

Substituting for p_c in Equation 3.5 and solving the integral gives:

$$E_{comp} = \frac{p_0 V_1^{\gamma}}{\gamma - 1} \left(V_1^{(1-\gamma)} - V_2^{(1-\gamma)} \right), \gamma \neq 1. \tag{3.7}$$

For a polytropic process, the ratio of specific heats is always greater than unity. Knowing that

the compression ratio is the ratio of BDC and TDC volumes, $C_R = V_1/V_2$, and that the difference between BDC and TDC volumes equals the swept volume, $V_1 - V_2 = \pi(B^2/4)\,S$, Equation 3.7 can be rearranged to give

$$E_{comp} = \frac{p_0}{\gamma - 1}\left(\frac{C_R\left(\pi\frac{B^2}{4}S\right)}{(C_R - 1)}\right)^{\gamma}\left(\left(\frac{C_R\left(\pi\frac{B^2}{4}S\right)}{(C_R - 1)}\right)^{(1-\gamma)} - \left(\frac{\pi\frac{B^2}{4}S}{(C_R - 1)}\right)^{(1-\gamma)}\right). \tag{3.8}$$

Simplifying and rearranging gives

$$E_{comp} = \frac{p_0\,\pi\,(C_R - C_R^{\gamma})}{4\,(\gamma - 1)\,(C_R - 1)}\,B^2\,S. \tag{3.9}$$

thus providing an expression for the required compression energy as a function of start-of-compression pressure, compression ratio and cylinder dimensions.

Having found the energy required for compression of the combustion cylinder charge, a similar approach can be used to derive an expression for the bounce chamber dimensions needed to store this amount of energy. Frictional and thermodynamic losses in the engine can also be taken into account at this stage by designing the bounce chamber to store slightly more energy than that required for compression. The bounce chamber stroke equals the engine stroke, so information on compression ratio, ratio of specific heats and start-of-compression pressure for the bounce chamber is needed to derive an expression for bounce chamber bore from Equation 3.9.

Rearranging Equation 3.9 gives

$$B_{BC} = \left(\frac{4\,(\gamma - 1)\,(C_{R,BC} - 1)}{p_{0,BC}\,\pi\left(C_{R,BC} - C_{R,BC}^{\gamma}\right)}\,\frac{E_{comp}}{S}\right)^{(1/2)} \tag{3.10}$$

with $C_{R,BC}$ and $p_{0,BC}$ being the specifications for the bounce chamber.

Figures 3.7 and 3.8 show the bounce chamber bore required to store sufficient compression energy for the combustion cylinder, as a function of combustion cylinder bore. The combustion cylinder is assumed to have a start-of-compression pressure of 150 kPa, compression ratio of 16 and stroke to bore ratio of 1.1 for all cases. It can be seen that for a given energy storage requirement, the bounce chamber design will depend on the compression ratio and start-of-compression pressure design variables. As discussed above, in the design process one would seek the combination of bounce chamber bore, compression ratio, and start-of-compression pressure that minimises thermodynamic and frictional losses while providing sufficient compression and load energy storage capacity.

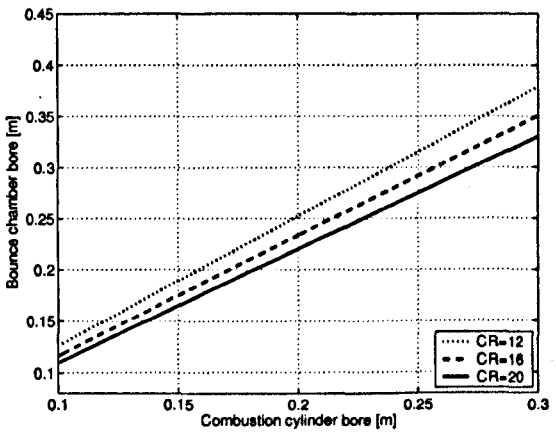

Figure 3.7: Required bounce chamber bore for varying bounce chamber compression ratios with a start-of-compression pressure of 1100 kPa.

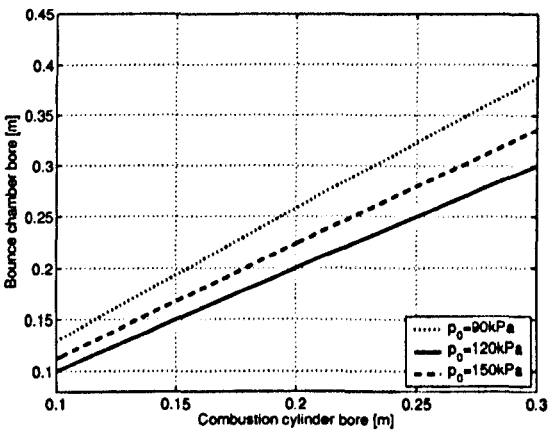

Figure 3.8: Required bounce chamber bore for varying start-of-compression bounce chamber pressures with a bounce chamber compression ratio of 16.

Load energy storage in the bounce chamber

As the pressure in the bounce chamber must be increased to store a part of the load energy, it is of interest to know the start-of-compression pressures required to store this energy. This information is needed to design the pressurised air supply, since an external air compressor may be required to control this pressure. However, if the maximum required start-of-compression pressure is lower than the boost pressure, pressurised air can be bled off from the turbocharger outlet. This will clearly be a desired solution.

The bounce chamber is required to store approximately half of the the load energy per cycle in addition to the compression energy. Typically, the net output work from a combustion engine cycle is in the order of 3 times the compression work when operating at full load. Equation 3.9 shows that for a constant stroke length, the energy storage is proportional to the start-of-compression

pressure. Hence, in order to store a sufficient amount of energy at all operating conditions, the bounce chamber start-of-compression pressure may have to be increased to 2.5–3 times that of the no-load design conditions.

If using a no-load start-of-compression pressure equal to atmospheric pressure (100 kPa), the required supply pressure to the bounce chamber at high loads would be slightly higher than the turbocharger delivery pressure commonly found in modern diesel engines (commonly around 200 kPa). However, as the highest required supply pressure is not significantly higher than the pressure that is likely to be available from the turbocharger, additional energy storage in the bounce chamber can be solved by adjustments in the design. This can be done in at least two ways: (a) To design the bounce chamber to operate with a start-of-compression pressure of below atmospheric at idle operation and thereby increase the range in which the start-of-compression pressure can be varied. This can readily be achieved by controlling the opening and closing of the pressure control valves. (b) To allow the bounce chamber to operate with a higher compression ratio at high loads by varying the BDC setpoint to increase the stroke length.

3.3 Linear electric machine design

The linear electric machine will have a high influence on the operational characteristics and performance of the free-piston engine generator. The interaction between both the design and operational variables of the electric machine and the combustion engine part of the unit will be higher in the free-piston engine than in conventional engines due to the direct coupling of the combustion piston to the electric machine. It is clear that if an electric machine with suitable specifications cannot be found, the free-piston engine generator concept will not be feasible.

Of highest importance is the weight of the translator in the electric machine, as this will directly influence the piston motion and bouncing frequency since it forms part of the moving mass. If a translator of sufficiently low weight cannot be realised, the speed of the engine will be low, leading to a poor power to weight ratio. Furthermore, the operational characteristics of the electric machine (load force profile) may also influence piston motion, and thereby the engine performance. Finally, in addition to posessing the required dynamic properties, the electric machine must provide efficient energy conversion in order for the free-piston engine generator to be a realistic alternative to conventional technology.

3.3.1 Linear electric generators

The amount of published research on the design of linear electric generators for free-piston engines is limited. Some reports discussing the use of linear electric generators with free-piston Stirling

engines exist, but the operational differences between such engines and internal combustion free-piston engines will be significant [26]. Linear electric motors are, however, widely used in industrial automation applications such as robots, machine tools and positioning systems. Linear electric machine technology is therefore well established and a high number of commercial available units exist.

Reported work

Redlich [86] presented an overview of different types of linear electric machines aimed at use with Stirling engines, including moving coil, moving iron and moving magnet configurations. Only the moving magnet alternator was found to give satisfactory performance and cost for the purpose. Redlich further described a patented moving magnet machine used by Sunpower, Inc. along with simple design guidelines for machines of this design with a power range from a few watts to 10 kW.

Cawthorne et al. [27] suggested the use of a permanent magnet linear alternator for a free-piston engine generator and presented a design procedure for such a machine. The claimed key advantages of this machine are high power density, high field strength, high efficiency and the fact that no brushes, slip rings or other connections to the translator are necessary. Modelling and experimental results were presented, and the authors concluded that with optimisation of the design and matching to the combustion engine, such an electric machine is a suitable choice for a free-piston engine generator.

A research group from the Royal Institute of Technology (KTH) in Stockholm, Sweden has published a number of reports evaluating different electrical machine possibilities for a free-piston engine generator [9–11]. It was stated that finding an electric machine fulfilling the requirements for the free-piston engine is a challenging task but that the permanent magnet, transverse-flux machine is the most promising candidate. The transverse flux machine has the benefits of low translator mass compared to other permanent magnet configurations but suffer from a low power factor and high manufacturing costs. The authors stated that all the evaluated machines have satisfactory efficiency, and that the main challenge is to achieve the specific power requirements.

Van Blarigan [17] presented the design of a free-piston engine generator with an electrical power output of 40 kW and electric machine efficiency of 96 %. The electric machine was based on conventional brushless, permanent magnet, direct current technology. The author stated that such a linear machine will be around 30 % heavier than its rotary counterpart but will have comparable efficiency. Basic electric machine design was presented and a modelling approach was briefly discussed.

Hew [50] presented results from the fabrication and testing of a permanent magnet linear generator for a free-piston engine. Electric power output from the engine was in the order of 1–5 kW, and both short stator and short translator designs were investigated. It was concluded that the con-

cept is feasible and that such machines can be realised using commonly available manufacturing techniques and materials, and that the cost of the machines therefore will be 'reasonable'.

Boldea and Nasar [19] presented a design procedure to achieve the main geometrical dimensions and basic performance of a permanent magnet, tubular linear electric generator. The approach was aimed at the design of electric machines for use with Stirling engines but the design methodology has been used by other researchers to achieve a preliminary design of an electric machine for internal combustion free-piston engines. The same authors have described in detail the design and operation of various types of linear electric motors and generators [20].

3.3.2 Electric machine design

A number of electric machine designs have been proposed for use with free-piston engine generators, including permanent magnet, moving coil and moving iron machines. It is clear that all machine types can achieve satisfactory efficiencies (above 90 per cent), and most designs should therefore be able to provide efficient energy conversion in the free-piston engine. The moving mass of the machines, a key design parameter for the free-piston engine, does however differ widely between the different designs.

The mass of the translator will depend heavily on the required continuous load force, and the power output from the generator will be a function of this load force and the reciprocating speed of the engine. As an example of the required load force, consider an engine with an electric power output $P = 50\,\text{kW}$, 0.150 m stroke length and a nominal operating speed $N = 30\,\text{Hz}$ (giving a mean piston speed $\overline{v}_p = 9\,\text{m/s}$). Assuming a machine efficiency of $\eta = 0.95$, the required electromagnetic thrust force to produce this power is

$$F_{\text{xr}} = \frac{P}{\overline{v}_p \cdot \eta} = \frac{50 \cdot 10^3\,\text{W}}{9\,\text{m/s} \cdot 0.95} = \underline{5848\,\text{N}}.$$

This assumes a constant electric load force over the full stroke, however the load force is likely to be dependent on the instantaneous speed of the translator. (An electric load force proportional to the velocity of the translator is commonly assumed.) A slightly higher design load force than the one calculated with this method is therefore required.

In a design study for a free-piston engine generator similar in size to the one investigated here, Arshad et al. [11] stated that a machine with a power output of 61.7 kW, a continuous load force of 10.3 kN and a moving mass of 12 kg can be realised using a permanent magnet, longitudinal flux machine. For transverse flux machines a translator mass of the order 6 kg can be achieved, however such engines have significantly poorer power factor. Wang et al. [104] and Chen et al. [28] presented similar results.

The power to weight ratio of electric machines is commonly measured in specific power, kW/kg, either based on the total mass of the machine or the mass of the translator. For this application, using a measure of 'specific force', which relates the maximum continuous load force to the mass of the translator, will be more useful, since the mean piston speed of the engine is not known.

Reported values of specific force for permanent magnet, longitudinal flux machines are in the range of 0.7 kN/kg [77] to 0.9 kN/kg [9,11,104]. For transverse flux, permanent magnet machines, values of specific force of approximately 2 kN/kg is achievable [9–11].

It will be shown in Section 4.3.2 that with the reported values of specific power and specific force quoted above, an electric machine with sufficiently low weight can be designed for the free-piston engine generator. Penalties in engine power output or performance due to the weight of the translator are therefore not expected. It will be shown that the weight of the piston assembly is not as critical in the turbocharged, diesel-powered free-piston engine as in naturally aspirated free-piston engines, due to the higher pressure levels giving higher bouncing frequencies.

Hence, for the purpose of this study it can be assumed that a linear electric machine with acceptable performance can be realised. Using reported values for specific force, a qualified estimation can be made on the moving mass of the electric machine with a given power output without the need to go into a detailed design process.

3.4 Estimating engine speed

Unlike in the design of conventional engines, no knowledge exists on whether the assumption made above for the reciprocating speed of the free-piston engine is realistic. The operating frequency will be decided by the engine dimensions, including the mass of the piston assembly, and the in-cylinder processes in the two cylinders, whose characteristics will be decided by a number of factors, particularly in the case of the combustion cylinder. While the overall dimensions are set by the designer, detailed knowledge of the combustion cylinder sub-processes and their effects on the gas pressure does not exist at such an early design stage. It is clear that if a sufficiently high reciprocating speed, comparable to that of conventional engines, cannot be obtained, the free-piston engine concept may not be practical for all applications. The engine speed is therefore of high interest, and an estimation can be made using a simplified model of the system.

The system resembles a spring-mass system with gas springs, and a simplified dynamic model of such a system can be derived. Assume that a mass, m, is connected between two opposing gas-filled cylinders, as illustrated in Figure 3.9. The cylinders are assumed to be identical for simplicity. The mass bounces between two endpoints with a stroke length of S, only influenced by the forces

from the gas springs. Friction and irreversibility are ignored.

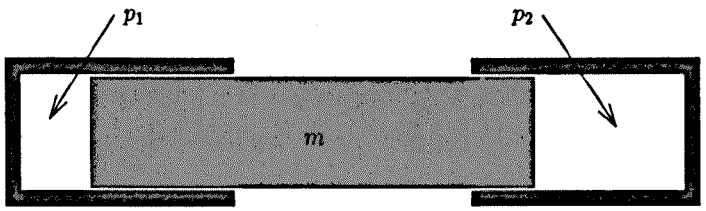

Figure 3.9: Illustration of mass bouncing between two gas springs.

The mass motion can be described using Newton's second law:

$$F_1 - F_2 = m\ddot{x} \tag{3.11}$$

where F_1 and F_2 are gas forces from cylinder 1 and 2 respectively and x is the position of the mass.

The forces acting on the mass can be expressed by the instantaneous in-cylinder pressure and the piston area, $F = pA_p$. Knowing the start-of-compression pressure and cylinder volume, pressure at any point can be estimated using polytropic state changes:

$$p = p_0 V_0^{\gamma} \frac{1}{V^{\gamma}} \tag{3.12}$$

where the subscript 0 refers to any reference condition. Cylinder volumes can be related to piston position by

$$V_1 = V_{\mathrm{cl}} + A_p x \tag{3.13}$$

$$V_2 = V_{\mathrm{tot}} - A_p x \tag{3.14}$$

where

V_{cl} is cylinder clearance volume [m^3]

V_{tot} is total cylinder volume (clearance volume + swept volume) [m^3]

and $x = 0$ when $V_1 = V_{\mathrm{cl}}$.

Therefore, Equation 3.11 can be rewritten as

$$p_0 V_0^{\gamma} A_p \left(\frac{1}{(V_{\mathrm{cl}} + A_p x)^{\gamma}} - \frac{1}{(V_{\mathrm{tot}} - A_p x))^{\gamma}} \right) = m\ddot{x}. \tag{3.15}$$

Similarly, knowing the piston bore, stroke length and compression ratio, the total volume and

the clearance volume can be found using $C_R = V_{tot}/V_{cl}$ and $V_{tot} - V_{cl} = \pi(B^2/4)S$.

An analytical solution of Equation 3.15 is not possible with standard techniques. Solving the equation numerically is trivial, and a simple numerical solver was written to find the mean piston speed for different values of cylinder dimensions, start-of-compression pressures and moving masses.

Figures 3.10 and 3.11 show the predicted mean piston speed of the bouncing spring-mass system with a constant stroke length. It can be seen that acceptable values of mean piston speed can be achieved, comparable to those in conventional engines, even with the relatively modest pressure levels assumed here. (For comparison: the Volvo TAD1260 diesel engine has a bore of 0.131 m and a nominal mean piston speed of 7.5 m/s). The bouncing frequency can be seen to depend heavily on cylinder bore, due to the gas pressure force being proportional to the piston surface area.

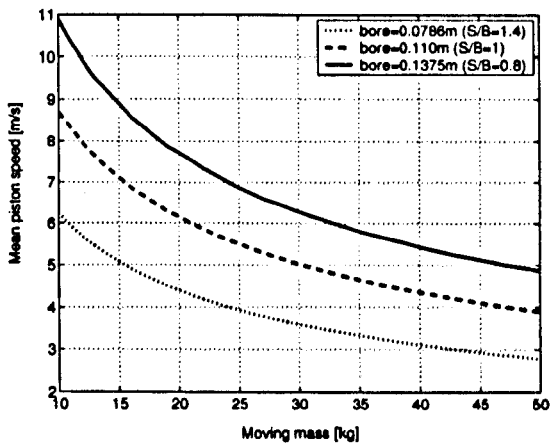

Figure 3.10: Mean piston speed of a spring-mass system for varying moving mass and piston bore. $S = 0.110\,\text{m}$, $C_R = 16$ and $p_0 = 150\,\text{kPa}$.

Figure 3.11 shows that increasing pressure levels in the cylinders, equivalent to a higher level of turbocharging, will increase the bouncing frequency, as one would expect. In a real engine, the combustion process will also lead to increased pressure levels compared to the ones investigated here, and therefore give higher mean piston speeds than those found in this analysis. Knowing that the free-piston engine is likely to have a simpler construction than that of crankshaft engines, one would expect this type of engine to be able to provide engine power densities similar to, or better than, those of conventional engines.

3.5 Starting

The energy needed to start modern free-piston engines is commonly provided by running the load device in motoring mode. This can be achieved with an appropriate control system and the use

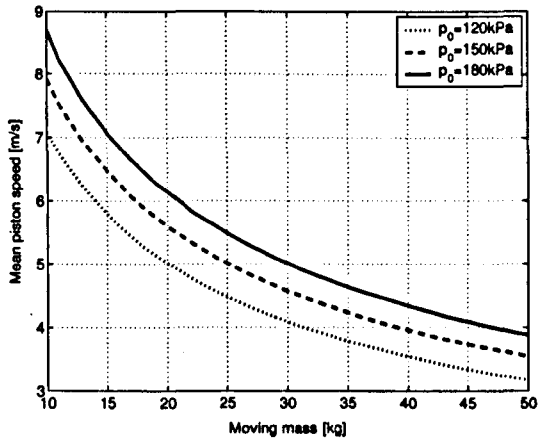

Figure 3.11: Mean piston speed of a spring-mass system for varying moving mass and start-of-compression pressure. $S = 0.110\,\mathrm{m}$, $C_\mathrm{R} = 16$ and $B = 0.100\,\mathrm{m}$.

of stored hydraulic or electric energy to drive the piston assembly. In the present design, rapidly introducing compressed air into the bounce chamber could present an alternative starting method, but the former is probably the preferred solution in most applications.

The energy needed to compress the charge in the combustion cylinder can be found using the method described in Section 3.2.2. It should be noted that the compression ratio needed for starting is lower than for normal operation, since the charge is only required to reach a point at which the fuel autoignites to ensure start-up.

The energy that can be supplied by the linear electric machine for one half-cycle can be found with

$$E_\mathrm{mot} = F_\mathrm{mot} \times S. \tag{3.16}$$

The maximum motoring force will be decided by electric machine design and will be in the same range as the maximum load force, which in turn is set by the power output requirements of the electric machine. If the electric motoring force is sufficiently high, the compression energy may be provided over one stroke only, i.e. from BDC to TDC, and the electric machine can thereafter immediately be switched over to generating mode. This may, however, not be feasible as it would require the combustion engine to start and retain operation following the first stroke, in addition to requiring a high electric motoring force from an electric machine that is mainly designed to operate as a generator. A better solution may be to drive the piston assembly back and forth until sufficient compression has been achieved and the engine runs smoothly, although this would require a slightly more sophisticated control system. Using this method, the engine can be 'cranked' for several cycles to secure problem-free start-up, similar to conventional engines.

A numerical example will be shown in order to obtain insight into the magnitude of the motoring force required for engine start-up. Assuming that an engine of 0.100 m bore and 0.110 m stroke has been designed to produce an electric power output of 50 kW with a mean piston speed of 10 m/s. Start-of-compression pressure is taken to be 100 kPa (atmospheric pressure).

If the electric load force is constant over the full stroke, the load force required to produce 50 kW power is

$$F_{\text{load}} = \frac{P}{2SN} = \frac{50000\,\text{W}}{10\,\text{m/s}} = \underline{5000\,\text{N}}. \tag{3.17}$$

This force can, in theory, be used as a motoring force.

In Section 3.2.2 a method of calculating the energy needed to compress the charge in an engine cylinder to a given compression ratio was derived. If assuming that a compression ratio of 10 is sufficient for starting, the constant motoring force needed to supply this energy in one half-cycle is

$$F_{\text{req}} = \frac{E_{\text{comp}}}{S} = \frac{6000\,\text{J}}{0.110\,\text{m}} = \underline{53\,\text{kN}}. \tag{3.18}$$

It can be seen that the force required to achieve a compression ratio sufficient for fuel autoignition is one order of magnitude higher than the motoring force that can be expected to be achieved from the electric machine. It is therefore likely that the method of driving the piston assembly back and forth to build up sufficient compression, as described above, will be the only realistic option for starting.

Using such 'cranking' of the engine, the electric machine must only overcome the frictional losses in the engine to be able to increase the piston assembly bouncing energy. Frictional losses in internal combustion engines are commonly measured by the friction mean effective pressure, fmep, and a typical value of fmep for conventional engines at normal operation is around 100 kPa.

With the engine dimensions listed above, a friction mean effective pressure of 100 kPa is equivalent to a constant friction force of approximately 400 N. The lower frictional losses in the free-piston engine and the low piston speeds and gas pressures during starting makes this a conservative estimate. It can be seen that the available motoring force of the electric machine is significantly higher than the frictional forces, and as such, the bouncing energy and the compression ratio can be built up using stored electric energy and an appropriate control system.

3.6 Summary

The main design variables in the free-piston engine generator have been discussed. The design of such an engine is more complex than that of a comparable conventional engine due to the higher level of interaction between the different design variables. The challenges associated with the de-

sign of free-piston engines are mainly attributed to the variable stroke and the limited speed range of the engine.

The design of such an engine requires an iterative approach, and some degree of knowledge or prediction of engine performance is crucial. This can, for example, be achieved through a simulation model. Typical basic requirements in a design process are engine output power and engine speed. An iterative strategy to design an engine of a given power output could look like:

1. Set engine power requirements.
2. Set the desired stroke to bore ratio.
3. Estimate the required cylinder bore and calculate the corresponding stroke length.
4. Design an electric machine to give an estimation of the mass of the piston assembly.
5. Simulate engine operation to find actual power output, engine speed and other performance parameters.
6. Update bore and stroke estimate and return to point 4.

The simulation can be based on the equations presented above, however a more detailed simulation model will give more reliable results.

Chapter 4

Full-cycle modelling and simulation

A full-cycle simulation model for the engine illustrated in Figure 3.1 was developed and simulations were performed to investigate a number of issues regarding free-piston engine operation and performance. Having a full-cycle engine model, the interaction between engine operational variables can be investigated in detail, which is of high interest for the free-piston engine due to the limited amount of operational experience reported for this type of engine. While simplified engine models are capable of predicting the main effects of design variables such as the mass of the piston assembly or cylinder dimensions, accurate simulation of engine operation requires a more sophisticated model.

The full-cycle model also accounts for secondary effects such as the influence of poor scavenging on the following cycle or prolonged ignition delay, which allows the simulation of engine transient operation. This is particularly useful for investigations into engine control, a known challenge with the free-piston engine concept, and a study of free-piston engine control issues is presented in Chapter 6.

This chapter describes the engine simulation model and its submodels in detail, along with presenting extensive simulation results giving insight into the performance and operating characteristics of the free-piston engine. Potential advantages over conventional technology are also investigated. Parts of the work presented in this chapter were presented by Mikalsen and Roskilly [75].

4.1 Modelling free-piston engines

Basic modelling of the free-piston engine piston dynamics is straight-forward, since the piston motion is determined by the force balance on the piston assembly. Simplified models of the bounce chamber and electric machine can readily be derived, however the combustion cylinder sub-processes require significantly more advanced models, as they depend on a complex interaction between fluid flow, combustion, chemical kinetics and heat transfer. The formulation of simplified models to describe engine combustion processes has been studied extensively for decades, but many as-

pects of engine development, such as emissions reduction measures, still rely on computationally intensive, multidimensional models or experimental studies.

A particular feature of the free-piston engine is the ability of the combustion process to influence the speed of expansion, due to the direct coupling of the combustion piston to the low-inertia piston assembly. This means that a fast combustion process and pressure rise will lead to a faster power stroke expansion, and vice versa. In comparison, in a crankshaft engine the inertia of the crank system and flywheel ensure that the speed of the engine is effectively constant in the timescale of the combustion process and the piston motion is pre-determined. This intricate coupling between thermodynamics and mechanics gives the free-piston engine particular characteristics that must be taken into account when modelling the engine.

4.1.1 Free-piston engine combustion

The particular piston motion profile of the free-piston engine may influence in-cylinder gas motion and the combustion process, and some reports on experimental work with free-piston engines have indicated differences in the combustion process between free-piston and conventional engines.

Somhorst and Achten [90] investigated the combustion process in a hydraulic free-piston engine. It was found that most of the fuel in the free-piston engine was burned in the pre-mixed phase, resulting in a very high rate of heat release, and a pressure gradient two to five times the value of a comparable conventional engine was reported. It was suggested that this is due to the high piston velocities around TDC, increasing in-cylinder gas motion and turbulence levels [2, 90]. Tikkanen et al. [96] reported the same behaviour in a dual piston free-piston engine and stated that combustion takes place mainly in a single, pre-mixed phase.

After testing some of the mid-20th century free-piston engines, Fleming and Bayer [39] reported abnormal combustion and stated that thermodynamic models had to be modified to fit free-piston engine data due to high heat release rates. It was further stated that when recreating the conditions under which the free-piston engine showed this performance in a conventional engine, the conventional engine would not run.

The engine processes in the free-piston and conventional engines are similar and existing conventional engine models may predict the general performance of free-piston engines with sufficient accuracy. However, reports such as those mentioned above suggest that models developed for and calibrated against conventional engines may not be directly applicable to investigate free-piston engine operation in detail, and the use of such models should be treated with some caution. Free-piston combustion will be investigated in detail in Chapter 5.

4.1.2 Reported work

The force balance on the piston inevitably leads to a differential equation, and with the use of complex submodels this equation may be highly nonlinear. Consequently, before computers were available modelling of free-piston engines relied on simplified models, that could be solved analytically, or the use of charts and tables. Some approaches were presented by Farmer [37], Frey et al. [42] and London and Oppenheim [67]. They typically employ an energy balance to the piston and solve simplified equations for subprocesses such as compression and expansion, friction, valve flow etc. Some recent approaches, including Heintz [49] and Zhang et al. [106], are also based on very simplified modelling, and the earliest free-piston engine developments have shown that the accuracy of such models is sufficient for basic engine design.

Most modern work is based on the same principle of solving the equation for the force balance on the piston assembly, but more sophisticated models for sub-processes, such as the combustion process and in-cylinder heat transfer, are usually employed. Perfect scavenging is commonly assumed, restricting the models to simulate steady-state engine performance. The submodels used in modern free-piston engine simulation models are based on the vast amount of research done on conventional engine modelling, although some modifications to existing models have been reported. Experimental work investigating the combustion process in the free-piston engine and comparing this to engine models is scarce.

Heintz [49] presented the modelling of a free-piston engine pump based on very simplified piston motion equations. The author employed an energy balance to the moving pistons and predicted the influence of engine design variables on engine performance and operation characteristics.

Baruah [13] presented more advanced modelling of a spark ignited free-piston engine, combining the solving of the piston dynamics with single-zone models of the in-cylinder processes. Models for engine emissions were implemented, and the simulation results for the free-piston engine were compared to simulations of conventional engines.

Larmi et al. [66] presented the modelling of free-piston engine performance through zero-dimensional and one-dimensional modelling frameworks. Well-known crankshaft engine models for the subprocesses were used, such as Wiebe functions for heat release and the Woschni heat transfer correlation. The models were fitted to experimental data from a free-piston engine, a process that is reported to have been 'laborious'. The tuned models were shown to give satisfactory predictions of engine performance.

Tikkanen et al. [95] simulated the performance of a dual piston diesel free-piston engine. The authors neglected the diffusion-based combustion phase and modelled the combustion as a completely pre-mixed reaction, partly based on results reported by Somhorst and Achten [90]. Experi-

mental results showing the validity of this approach were presented by Tikkanen et al. [96].

Atkinson et al. [32] presented the modelling and simulation of a dual piston, spark ignited free-piston engine. Standard polytropic compression and expansion relations were used, along with idealised scavenging models and a Wiebe heat release model. The simulation model was fitted to experimental results of a prototype engine and the authors stated that this was an 'extremely complicated' task.

Fredriksson and Denbratt [41] simulated the performance of a free-piston engine for a variety of fuels, including hydrogen and natural gas. A combination of simplified submodels known from conventional engine modelling and detailed chemical kinetics models were used. The authors stated that some inaccuracy may be present due to the use of empirical submodels developed for conventional engines.

Multidimensional, computational fluid dynamics (CFD) modelling of free-piston engines has recently been presented by some authors, including Fredriksson [40], Golovitchev et al. [45] and Kleemann et al. [64]. These models typically employ a piston motion profile obtained from a zero-dimensional dynamic model, and as such, they require a simplified model to be developed to predict the engine dynamics. CFD modelling of free-piston engines is discussed in detail in Chapter 5.

4.2 Full-cycle simulation model

A full-cycle simulation model was derived in order to investigate the performance of the proposed free-piston engine and the influence of the main design variables. The modelling of the engine was based on existing research on the modelling of conventional engines, as the amount of research specifically addressing the modelling of free-piston engines is limited. The following sections describe the details of the simulation model.

4.2.1 Engine dynamics

Figure 4.1 shows the free body diagram of the piston assembly in the free-piston engine generator illustrated in Figure 3.1. The piston motion can be described by Newton's 2nd law:

$$F_c - F_{mag} - F_{fr} - F_b = m\frac{d^2x}{dt^2}. \tag{4.1}$$

4.2.2 Simulation algorithm

A simulation program was written using the numerical computation toolbox Matlab by The Mathworks, Inc. [93]. The simulation code solves Equation 4.1 numerically to give piston speed and

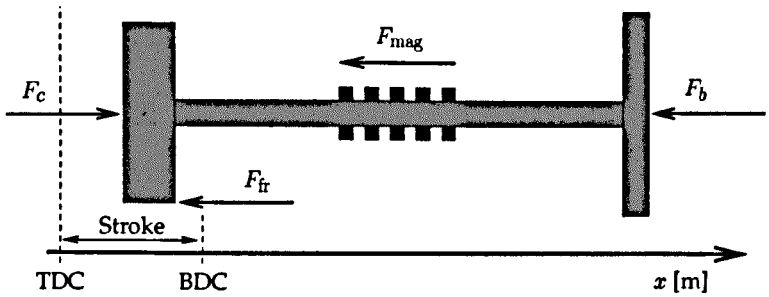

Figure 4.1: Free body diagram of the piston assembly in the free-piston engine generator illustrated in Figure 3.1.

position. The instantaneous combustion cylinder and bounce chamber pressures are calculated at each simulation step to find gas pressure forces, using the submodels presented below. The force from the electric machine and the frictional forces are calculated similarly. All the forces are functions of one or more of the factors time, piston position, piston speed, input operating variables and ambient conditions.

The simulation model was written using standard forward Euler numerical integration to solve Equation 4.1 due to its simplicity in implementation. When testing the code it was found that the solution converged satisfactorily with decreasing timestep length, without extensive penalties in computation time. The implementation of a more accurate numerical scheme, such as the midpoint method or a Runge-Kutta method, was therefore not found necessary. Figure 4.2 shows a simplified flowchart of the simulation code.

The simulation model takes the following inputs:

- cylinder bore;
- moving mass;
- nominal stroke length and compression ratio;
- ambient air temperature and pressure;
- turbocharger isentropic efficiencies and exhaust back pressure;
- number of exhaust valves, dimensions and valve timing;
- scavenging ports height and width;
- fuel calorific value, mass of fuel per injection and injection timing;
- linear alternator force function;
- bounce chamber bore and nominal compression ratio.

The model calculates the following performance parameters:

- speed;
- stroke;

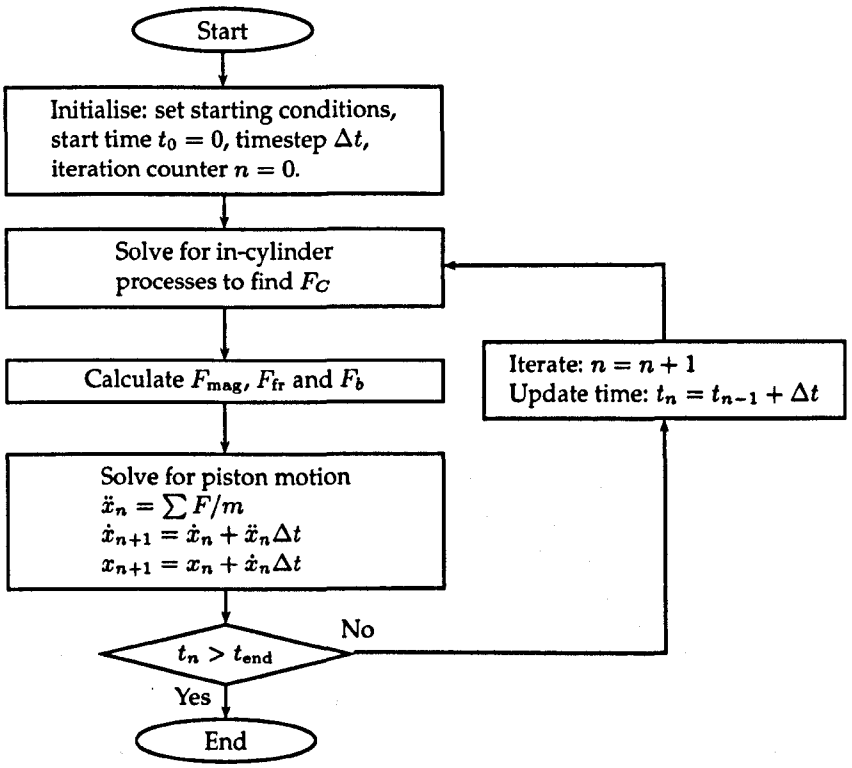

Figure 4.2: Flowchart for Euler integration of piston motion equations.

- generator power output;
- cylinder temperature and pressure history;
- boost pressure, boost temperature and exhaust gas temperature;
- fuel/air equivalence ratio;
- scavenging efficiency;
- predicted ignition delay and fuel burn rate;
- in-cylinder heat transfer rate;
- engine efficiency.

The start of the simulation is performed by assuming that the piston is at TDC, that the in-cylinder air is compressed to the given compression ratio and that all the fuel is injected and burnt instantaneously at time $t = 0$. The simulation is subsequently run until the engine operation stabilises, i.e. until two consecutive cycles are identical. Engine transient response is investigated by first letting the engine stabilise at the desired operating conditions and then imposing a change in one or more of the input variables. A number of engine operational variables are logged on a time basis,

including piston motion, cylinder charge composition and gas pressures and temperatures.

4.2.3 Submodels

4.2.3.1 Ignition delay

Ignition delay is defined as the time between start of fuel injection and start of combustion. In practise, determining the actual point of ignition is a matter of definition, and a 'noticeable' pressure rise due to the combustion must be identified.

Somhorst and Achten [90] stated that values for ignition delay in the Innas Free-Piston Engine do not differ much from values predicted by a model based on crankshaft engine experimental data. The ignition delay depends mainly on the physical properties of the fuel and the conditions under which it is burnt, and not necessarily on the combustor design. It is therefore believed that correlations developed for conventional engines will be able to predict ignition delay in the free-piston engine with sufficient accuracy.

Correlations for ignition delay based on the Arrhenius equation for reaction rate are widely used in internal combustion engine modelling and a correlation of this type, described by Stone [92], has been used. The ignition delay is defined as a function of in-cylinder gas pressure and temperature:

$$t_{\mathrm{id}} = \frac{3.52\ \exp(2100/T)}{(p/10^5)^{1.022}}. \tag{4.2}$$

The variables p and T are the mean values of pressure and temperature during the ignition delay and to account for the changing conditions in the ignition delay period the following correlation must be satisfied [51]:

$$\int_{t_{\mathrm{si}}}^{t_{\mathrm{si}}+t_{\mathrm{id}}} \left(\frac{1}{\tau}\right) \mathrm{d}t = 1 \tag{4.3}$$

where t_{si} is the time at the start of injection and τ is the ignition delay at time t.s

4.2.3.2 Combustion

The modelling of the heat release in the free-piston engine is one of the factors with the highest degree of uncertainty in the simulation model. Very little research exists on the combustion process in free-piston engines compared to the vast amount available for conventional engines. Although the research on conventional engines may provide a starting point for the modelling, care should be taken if using models developed for and validated against conventional engines as discussed above.

Numerous correlations have been proposed for predicting diesel engine combustion. Single-zone models, which treat the cylinder charge as uniform in composition and temperature and

merely add heat to this charge according to the fuel burn rate, are commonly used for basic engine modelling. Calibrated against experimental data, single-zone models have been shown to give good predictions of general engine performance when investigating effects that do not highly influence the combustion process, such as changes in compression ratio and injection– or valve timing [63].

A single-zone combustion model described by Heywood [51] has been used in this study, in which the mass fraction burned is defined as

$$m_b(t) = \beta f_1(t) + (1 - \beta) f_2(t) \tag{4.4}$$

where m_b is the mass fraction burned [1], t is time, non-dimensionalised by total time for combustion [1], and β is the fraction of fuel burned in the pre-mixed phase [1].

The function f_1 is the pre-mixed burning function, given as

$$f_1 = 1 - (1 - t^{K_1})^{K_2} \tag{4.5}$$

and f_2 is the diffusion burning function

$$f_2 = 1 - \exp(-K_3 t^{K_4}). \tag{4.6}$$

The fraction of fuel burned in the pre-mixed phase, β, is a function including the ignition delay:

$$\beta = 1 - a\,\phi^b / {t_{id}}^c \tag{4.7}$$

K_1, K_2, K_3, K_4, a, b and c are empirical coefficients. Values of these based on experimental data from a truck engine are presented by Heywood [51], and these have been adjusted to fit experimental data and implemented in the model. The total time allowed for combustion was set to 5 ms based on experimental data. (For details on the validation of the model, see Section 4.2.4.)

4.2.3.3 Scavenging

Predicting the scavenging performance is a difficult task in a preliminary engine design, as it heavily depends on engine design details. Perfect scavenging models, in which predictions of exhaust blowdown and the gas exchange are ignored and a constant pressure is assumed while the scavenging ports are open, are commonly implemented in engine models at an early stage. In order to simulate engine transient operation, a scavenging model that predicts the effects of variations in engine operation on the scavenging process is required. This is particularly important in the free-piston engine due to the variable stroke length and potential variations in BDC position. Al-

though not validated against experimental data, such a scavenging model will be able to take into account the effects of poor scavenging on the next combustion process, and to predict the effects on scavenging when other engine variables are changed.

Exhaust blowdown is modelled in the parts of the cycle where exhaust valves are open but the scavenging ports have not yet been uncovered. The process is modelled as a polytropic expansion down to the exhaust back pressure, with mass flow through the exhaust valves modelled as flow through nozzles, given by [51]

$$\dot{m} = \frac{C_D\, A_C\, p}{(RT)^{1/2}} \left(\frac{p_{exh}}{p}\right)^{1/\gamma} \left(\frac{2\gamma}{\gamma - 1}\left[1 - \left(\frac{p_{exh}}{p}\right)^{(\gamma-1)/\gamma}\right]\right)^{1/2}. \tag{4.8}$$

For choked flow (i.e. if $p_{exh}/p \leq [2/(\gamma+1)]^{\gamma/(\gamma-1)}$), the mass flow is given by

$$\dot{m} = \frac{C_D\, A_C\, p}{(RT)^{1/2}} \gamma^{1/2} \left(\frac{2}{\gamma+1}\right)^{(\gamma+1)/2(\gamma-1)}. \tag{4.9}$$

In Equations 4.8 and 4.9, $\dot{m}$ is the mass flow through the valve, C_D is the valve discharge coefficient, A_C is the flow area, taken as valve curtain area, p is the in-cylinder gas pressure, R is the gas constant, T is the in-cylinder gas temperature, p_{exh} is the exhaust back pressure and γ is the ratio of specific heats. Appropriate valve discharge coefficients, as suggested by Heywood [51], were implemented.

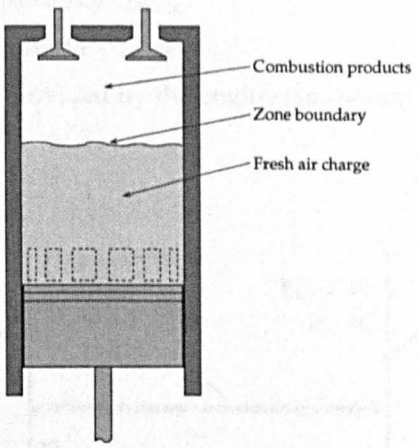

Figure 4.3: Illustration of the scavenging model.

During the parts of the cycle when both exhaust valves and inlet ports are open the gas flow rate through the valves and ports was calculated as above, whereas the gas exchange in the cylinder was modelled with a perfect displacement model. During scavenging the cylinder was assumed to comprise two zones: one zone consisting of fresh air which displaces zone two which consists

of combustion products, as illustrated in Figure 4.3. The zones do not exchange mass or heat, and only when all the combustion products have been fully displaced will fresh air flow out through the exhaust ports. Gas temperatures are calculated as the instantaneous mass-weighted average of fresh air and combustion products in the cylinder, and the two zones mix instantaneously at the point where both exhaust valves and inlet ports are closed.

Using such an approach, the thermodynamic consequences of poor scavenging on the next cycle are taken into account. The scavenging efficiency, defined as the fraction of the cylinder charge that consist of fresh air at the start of compression, is calculated and given as one of the model outputs.

4.2.3.4 Turbocharger model

The performance of the turbocharger varies with engine operating conditions due to changes in the flow rate and energy content of the exhaust gas. The turbocharger model calculates the boost pressure and temperature based on the exhaust temperature, exhaust back pressure and turbocharger properties.

Figure 4.4 illustrates the turbocharger with the mass flows through the compressor and the turbine. The turbocharger model requires the following inputs:

- ambient air pressure and temperature, p_{atm} and T_{atm};
- exhaust back pressure, p_{exh};
- turbine and compressor isentropic efficiencies, η_t and η_c;
- turbocharger mechanical efficiency, η_{mech};
- exhaust gas temperature from the engine, T_{exh}.

The exhaust gas temperature is provided by the engine simulation model, all other parameters are set by the user.

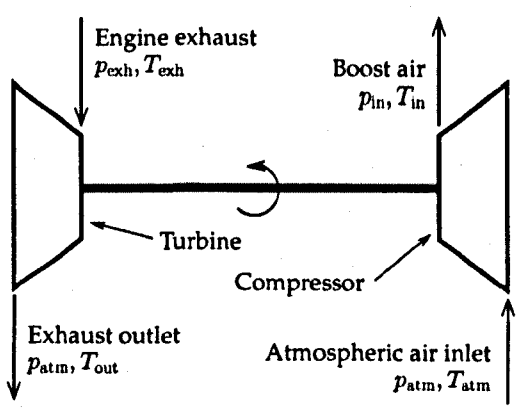

Figure 4.4: Turbocharger model parameters.

Standard equations for ideal processes, assuming constant specific heat for the gases but allowing for efficiency losses in the turbocharger, were used in the calculations. The calculation procedure can be found in numerous combustion engine and turbomachinery textbooks, including Stone [92] and Heywood [51]. The temperature of the exhaust gas after an isentropic expansion from p_{exh} down to p_{atm} is $T_{out\,s}$ and can be found by using

$$T_{out\,s} = T_{exh}\left(\frac{p_{atm}}{p_{exh}}\right)^{\left(\frac{\gamma-1}{\gamma}\right)}. \tag{4.10}$$

The actual gas temperature, T_{out}, after the expansion can be found using the turbine isentropic efficiency:

$$\eta_t = \frac{T_{out} - T_{exh}}{T_{out\,s} - T_{exh}}. \tag{4.11}$$

The work done by the turbine, W_t, depends on the mass flow of exhaust gas, $\dot{m}_{exh}$, the specific heat of the gas, $C_{p\,exh}$, and the actual temperature change:

$$W_t = \dot{m}_{exh}\, C_{p\,exh}\,(T_{exh} - T_{out}). \tag{4.12}$$

The only work done by the turbine is to drive the compressor and overcome friction. Hence, the compressor work can be determined using

$$W_c = \eta_{mech}\, W_t. \tag{4.13}$$

Having determined the compressor work, the same method can be used to find the pressure rise in the compressor. The mass flow of exhaust can be found using the engine model, however, this differs only slightly from the mass flow of air (the difference between the two is typically less than 5 per cent). It has been assumed that these two mass flows are equal, which simplifies the implementation of the model and does not introduce any significant error. The actual temperature rise of the intake air is

$$T_{in} = T_{atm} + \frac{W_c}{\dot{m}_{air}\, c_{p\,air}} \tag{4.14}$$

where W_c is found from Equation 4.13.

Knowing the isentropic efficiency of the compressor, the isentropic temperature rise is found similarly as above with

$$T_{in\,s} = T_{atm} + \eta_c(T_{in} - T_{atm}). \tag{4.15}$$

The boost air pressure, p_{in} can now be found with

$$p_{in} = p_{atm}\left(\frac{T_{in\,s}}{T_{atm}}\right)^{\left(\frac{\gamma}{\gamma-1}\right)}. \tag{4.16}$$

Efficiency values for the turbocharger compressor and turbine were chosen as $\eta_c = 0.70$, $\eta_t = 0.80$, as suggested by [92]. The mechanical efficiency, η_{mech}, is higher than those of the compressor and turbine, and η_{mech} is commonly included in η_t. For simplicity, a value of $\eta_{\text{mech}} = 1$ was therefore used.

The dynamics of the turbocharger, i.e. its transient response to changes in engine operation, is not modelled. This is achieved by averaging the calculated values over a number of cycles.

4.2.3.5 Heat transfer

As the in-cylinder gas temperature varies during the processes of compression, combustion and expansion, heat will be transferred between the gases to the cylinder walls and piston surface. Stone [92] stated that typically 20–30 per cent of the fuel energy in a conventional engine passes to the coolant and around half of the heat flow to the coolant comes from in-cylinder heat transfer. The heat transfer will depend on a number of factors, including the exposed in-cylinder surface area, the temperature of the trapped gases and the gas motion within the cylinder.

In-cylinder heat transfer was modelled using Newton's law of thermal convection, giving the heat transfer rate as

$$\dot{Q} = \alpha A_s (T - T_s) \tag{4.17}$$

The heat transfer coefficient, α, was found using the correlation presented by Hohenberg [54]:

$$\alpha = 130 V^{-0.06} \left(\frac{p}{10^5}\right)^{0.8} T^{-0.4} (\overline{v}_p + 1.4)^{0.8}. \tag{4.18}$$

Stone [92] suggests an average in-cylinder surface temperature, T_s, of 350 K, and this value was used in the simulations. The surface area exposed to the combustion gases is calculated with the assumption that the combustion chamber geometry is that of a perfect cylinder.

The heat transfer was calculated in the closed-cylinder parts of the operating cycle only, i.e. when scavenging ports are not uncovered and exhaust valves are closed. This includes the compression, combustion and power stroke expansion, which are the parts of the cycle where the highest temperature gradients, and thereby highest heat transfer, occurs. This approach is supported by Heywood [51], who stated that the heat transfer during combustion can reach significant values and that the heat transfer during the rest of the cycle is essentially zero.

4.2.3.6 Gas properties

Having calculated the instantaneous heat transfer rate to or from the in-cylinder gases (heat release from combustion minus heat transfer losses to the combustion chamber walls), new values for

cylinder pressure and temperature were calculated at each simulation step. The rates of pressure and temperature change were found by applying the 1st law of thermodynamics on the cylinder charge:

$$\frac{dU}{dt} = \frac{dQ}{dt} - \frac{dW}{dt}. \tag{4.19}$$

Assuming that the cylinder charge will behave as a ideal gas (a common simplification in this type of analysis), the internal energy is a function of temperature only:

$$U - U_0 = mC_v(T - T_0). \tag{4.20}$$

The gas will follow the ideal gas law:

$$pV = mRT. \tag{4.21}$$

Assuming that the mass, specific heat, C_v and gas constant, R, are constant, and letting $R/C_v = (\gamma - 1)$, one can derive expressions for the change in gas temperature and pressure as a function of heat and work energy transfer to the gas. Differentiating Equation 4.20 with respect to time and subsituting for $\frac{dU}{dt}$ in Equation 4.19, one gets an expression for the gas temperature change. Knowing that the work is a function of gas pressure and volume change, $\frac{dW}{dt} = p\frac{dV}{dt}$, the gas temperature can be found as

$$\frac{dT}{dt} = \frac{1}{mC_v}\left(\frac{dQ}{dt} - p\frac{dV}{dt}\right). \tag{4.22}$$

The pressure change can be found from the ideal gas law directly, or by differentiating Equation 4.21 and substituting for $\frac{dT}{dt}$ in Equation 4.22. The pressure change is given by

$$\frac{dp}{dt} = \frac{1}{V}\left((\gamma - 1)\frac{dQ}{dt} - \gamma p\frac{dV}{dt}\right). \tag{4.23}$$

Combustion chamber volume can be derived from piston position and the rate of change of volume change rate was found from the instantaneous piston speed.

4.2.3.7 Friction

Frictional losses in the free-piston engine are expected to be lower than those in conventional engines, which, as discussed in Section 2.1.3, is one of the main advantages of the free-piston concept. In the single piston design, however, it should be noted that the additional frictional losses in the bounce chamber must be taken into account, and these advantages will therefore be lower than in dual piston free-piston engines.

A breakdown of engine friction mechanisms in four stroke spark ignition and diesel engines was presented by Heywood [51]. This was used as the basis to estimate the frictional losses in the free-piston engine, with the following adjustments:

- pumping work is left out as the cycle used is a two stroke;
- compression and gas loads are left out as their effects are accounted for elsewhere in the simulation model;
- crankshaft friction is left out as it is not present in the free-piston engine.

This leaves the frictional losses from the piston, piston rings, valve gear and auxiliaries, giving a friction mean effective pressure (fmep) of approximately 120 kPa. For the bounce chamber, the frictional losses are likely to be lower than for the combustion cylinder since the bounce chamber is working with lower pressures and the sealing requirements are less stringent. A value of half the friction mean effective pressure of the combustion cylinder piston and piston rings was used for the bounce chamber. Frictional losses in the electric machine and from additional bearings that may be required have not been considered.

Having the total mean effective pressure, a friction force can be calculated. The friction force was assumed to be constant over the full cycle, a simplification compared to the real frictional forces which depend on factors such as piston speed and in-cylinder gas pressure. The simplification does not, however, have a large influence on the simulation results because the frictional forces are significantly lower than the other forces acting on the piston, and do therefore not have a large influence on the piston dynamics.

With the driving of valves and auxiliaries included in the frictional work, the estimated free-piston engine friction mean effective pressure in the single piston free-piston engine is around 90 per cent of that in conventional engines.

4.2.3.8 Linear electric machine

The electric machine was modelled simply as a force acting on the piston assembly, and was initially assumed to have a load force profile that is proportional to the speed of the translator. The code allowed the implementation of any desired load force profile, such as a constant load force or a load force acting only during parts of the cycle.

4.2.3.9 Bounce chamber

With the exception of the frictional losses discussed above, the bounce chamber was modelled as a reversible adiabatic compression and expansion of the air trapped within the bounce chamber cylinder. The amount of air in the bounce chamber at the start of compression was allowed to vary, to aid engine control.

4.2.4 Model validation

The output of the simulation model was validated against data from a Volvo TAD1240 six-cylinder, turbocharged diesel engine. Technical data for this engine are shown in Table 4.1. The comparison was carried out with the aim of verifying that the model produces realistic results, and that it is able to predict real trends for varying engine operating conditions. It should be noted that the Volvo TAD1240 is a four-stroke engine, and a comparison of experimental data to those predicted for the free-piston engine was therefore not undertaken.

Stroke	0.150 m
Bore	0.131 m
Operation	4-stroke
Displacement	12.13 dm^3
Compression ratio	17.5:1
Nominal operating speed	1500 rpm
Maximum power	310 kW
Mean piston speed	7.5 m/s

Table 4.1: Volvo Penta TAD1240 GE technical data.

4.3 Simulation results

Using the simulation model described in Section 4.2, simulations of the engine illustrated in Figure 3.1 were performed with varying engine design and operational parameters. This section presents simulation results investigating the basic performance of the engine and the influence of important design variables.

Unless otherwise stated, the engine will have design and specifications as listed in Table 4.2. The main engine design variables were chosen to be similar to those of the Volvo TAD1260 diesel engine, against which the simulation model was partially validated.

Nominal stroke	0.150 m
Cylinder bore	0.131 m
Scavenging ports height	0.022 m
Nominal compression ratio	15:1
Piston assembly mass	22 kg
Bounce chamber bore	0.150 m
Bounce chamber nominal compression ratio	15:1
Exhaust back pressure	1.5×10^5 Pa

Table 4.2: Free-piston engine design specifications.

Figure 4.5 shows the reference scale for piston position used in the remainder of this text, as shown in Figure 4.1. The nominal TDC position is defined at the origin, and x defines the piston distance

below TDC. The nominal BDC position will have a value of x equal to the nominal stroke length (0.150 m). Due to the variable stroke length, it is possible for x to have values outside the nominal stroke, including negative values.

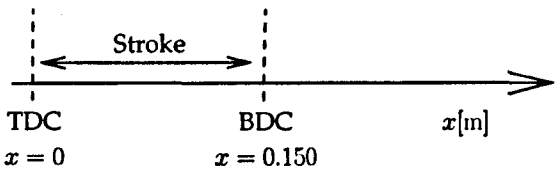

Figure 4.5: Piston position scale used in the simulations, as illustrated in Figure 4.1.

In the simulations both the exhaust valve timing and fuel injection timing were varied in order to optimise engine performance, using controllers within the simulation model. The exhaust valve opening timing was adjusted so that the in-cylinder pressure at the time when the scavenging ports are uncovered is equal to the boost pressure. This maximises the work done on the piston along with preventing backflow of exhaust gases into the intake manifold. The exhaust valves were set to close at the same time as the piston covers the scavenging ports in the compression stroke. Fuel injection timing was set to its optimum value for high efficiency in all the simulated cases.

4.3.1 Basic engine performance

The basic performance of the free-piston engine is shown in Table 4.3. The engine was operating with a fuel-air equivalence ratio of 0.60. The efficiency values presented in the table and those presented below refer to the 'shaft' fuel efficiency of the combustion engine, and losses in the electric machine are ignored.

Speed	30 Hz
Output power	44.4 kW
Mean piston speed	9 m/s
Scavenging efficiency	0.90
Boost pressure	1.68×10^5 Pa
Engine efficiency	0.42

Table 4.3: Simulated engine basic performance.

Figure 4.6 shows the simulated in-cylinder pressure of the combustion cylinder and bounce chamber for one engine cycle. The predicted combustion can be seen to be close to a constant volume process.

Figure 4.7 shows the predicted piston dynamics of the free-piston engine. Figure 4.7a shows the simulated piston motion for one engine cycle, compared to a conventional engine (with a crankshaft radius to connecting rod length ratio of 0.3) running at the same speed. Significant differences can

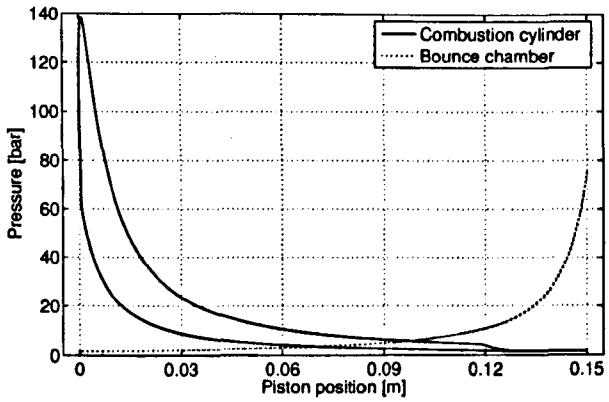

Figure 4.6: Simulated combustion cylinder and bounce chamber pressure for one engine cycle.

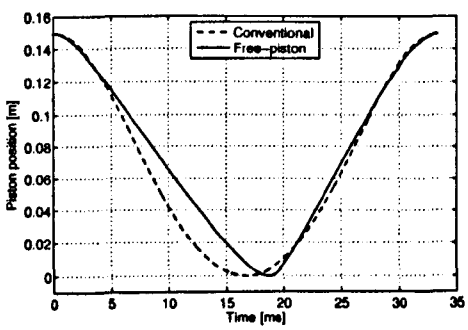

(a) Simulated piston motion for the free-piston engine compared to a conventional engine running at the same speed.

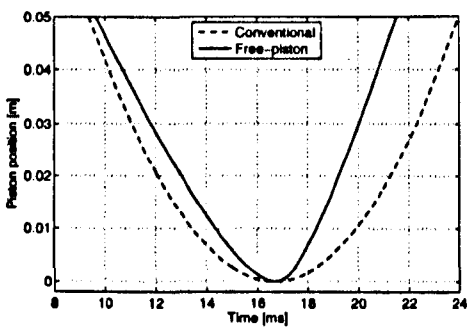

(b) Simulated piston motion close to TDC for a free-piston engine and a conventional engine, normalised around TDC position.

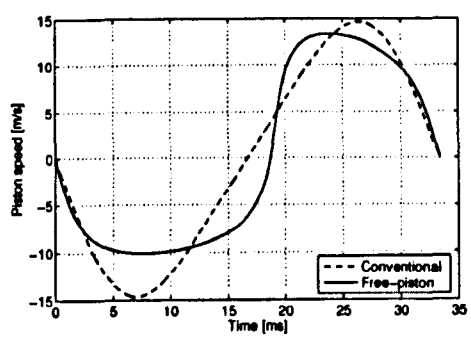

(c) Simulated piston speed profile for the free-piston engine compared to a conventional engine running at the same speed.

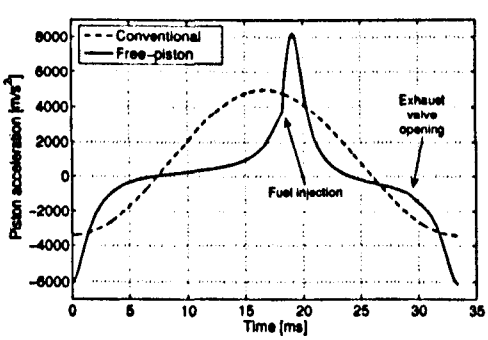

(d) Simulated piston acceleration profile of the free-piston engine compared to a conventional engine running at the same speed.

Figure 4.7: Predicted piston dynamics of the free-piston engine.

be seen, the most important being that the free-piston engine spends shorter time around TDC, where the gas pressure and temperature are at their highest. This is emphasised in Figure 4.7b, which shows the piston motion in the area close to TDC, normalised around the TDC position. It can be seen that the expansion just after TDC is significantly faster for the free-piston engine, due

to the low inertia of the piston assembly.

It can also be seen from the piston motion trajectory that the free-piston engine motion is asymmetrical around TDC, and the engine therefore spends more time in the compression phase than in the expansion phase of the cycle.

Figure 4.7c shows simulated piston speed in the free-piston engine and the piston speed profile of a conventional engine. It can be seen that the peak piston speed is lower in the free-piston engine for the same mean piston speed, and that the speed profile is significantly different. Compared to the conventional engine, the free-piston engine has a speed profile resembling a square wave, with rapid speed changes and long periods of close to constant speed.

Figure 4.7d shows piston acceleration in the free-piston and a conventional engine. As above, significant differences can be seen, in particular shortly after ignition where the unrestricted motion of the piston in the free-piston engine gives a very high acceleration as the combustion cylinder pressure increases. Predicted peak piston acceleration in the free-piston engine is around 60 % higher than that of the conventional engine.

A curiosity of the free-piston engine is that, because the acceleration is directly proportional to in-cylinder gas pressure, events in the combustion chamber can be found on the acceleration graph. Both the fuel injection and the exhaust valve opening can be seen on the graph in Figure 4.7d, at around $t = 18$ ms and $t = 29$ ms respectively.

The predicted piston dynamics correlates well with theoretical and experimental reports from other authors investigating free-piston engines operational characteristics, including Achten et al. [2], Fredriksson and Denbratt [41] and Tikkanen et al. [96].

4.3.2 Engine geometry and design

In an engine design process, knowledge of the influence of different engine geometric variables is of high importance. Although the influence of the main design parameters can be predicted based on experience from conventional engines, their effects on overall engine performance may be different in the free-piston engine due to the particular operating characteristics of this type of engine. This section investigates the influence of the main engine design parameters in the free-piston engine.

Most of the design– and operational parameters in the free-piston engine are highly interconnected, and the system becomes more complicated in this sense than the conventional engine. For example, an increase in moving mass will not only lead to lower engine speed but will also have effects on the stroke length, which in turn influences both the scavenging process and the compression ratio. Changing operational variables, such as fuel mass flow or boost pressure, will have similar effects. Due to this, a parametric study of the free-piston engine design and operational variables is not straight-forward. A number of prerequisites must be decided upon before such investigations can be undertaken.

In the simulations presented below, TDC and BDC positions are controlled to their nominal values by changing the bounce chamber pressure and fuel flow rate respectively. To ensure that the comparison is done under comparable operating conditions, the electric load force is adjusted to achieve a fuel-air equivalence ratio of 0.60 for all cases. The height of the scavenging ports is further adjusted such that a scavenging efficiency of 0.90 is achieved in order to ensure that realistic engine designs are compared. Finally, the exhaust valve opening timing and fuel injection timing are optimised as described above.

4.3.2.1 Moving mass

The engine resembles a spring-mass system and the moving mass is therefore of high importance to engine operation, particularly reciprocating speed. A reported concern with the free-piston engine generator is developing an electric machine with sufficiently low weight, and it is clear that if this cannot be found the engine may not achieve an acceptable power to weight ratio for all applications.

It is expected that an increase in moving mass leads to lower engine speed and therefore a lower engine power output. However, lower speed may give more time for scavenging, allowing lower scavenging ports height and resulting in closer to constant volume combustion, both increasing engine efficiency. It will, however, at the same time lead to higher peak temperatures and pressures, which increase heat transfer losses. An optimal engine speed for high efficiency may therefore be expected.

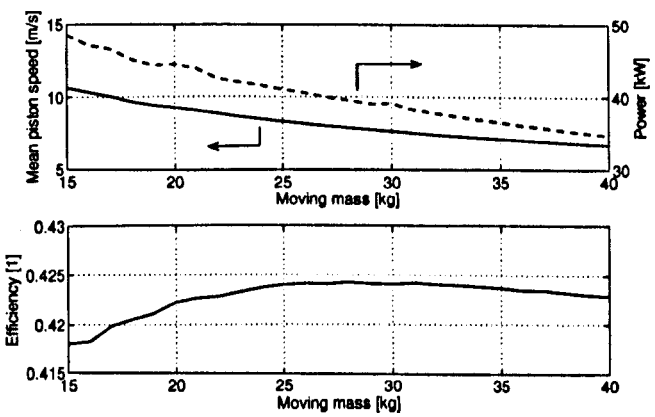

Figure 4.8: Effects of changes in piston assembly mass on engine performance.

Figure 4.8 shows the predicted effects of varying piston assembly mass on engine performance. It can be seen that the spring-mass analogy is valid, as increasing mass leads to a decrease in engine speed and power output.

The results for engine efficiency show that the predicted optimum moving mass for efficiency

is relatively high. This indicates that the requirements of a low-mass electric machine are less stringent in a turbocharged diesel-powered free-piston engine, and that acceptable mean piston speeds and high efficiency can be achieved even for a high moving mass.

4.3.2.2 Compression ratio

The compression ratio is variable during operation in the free-piston engine, but the nominal value must be decided at the design stage. The absence of a crankshaft and the associated load-carrying bearings may allow the free-piston engine to operate with higher compression ratios than conventional engines. Although a higher compression ratio gives higher theoretical cycle efficiency, it increases in-cylinder temperatures and pressures, increasing heat transfer losses, emissions formation, and mechanical stress, and these factors effectively determines the maximum possible compression ratio.

Figure 4.9 shows the effects of varying the nominal compression ratio of the free-piston engine. The simulations predict that an optimal compression ratio can be found, but only minor effects on engine efficiency are found for compression ratios between 15 and 25.

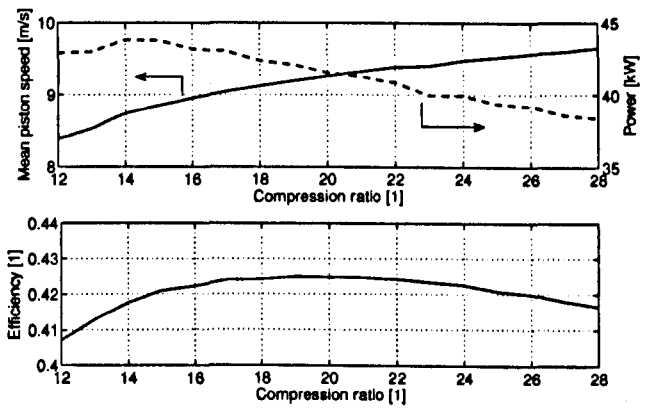

Figure 4.9: Effects of varying nominal compression ratio on engine performance.

An effect that is not obvious is the decrease in engine power output together with increased engine speed. The latter is a result of the combustion cylinder "gas spring" being stiffer, which increases the bouncing frequency in the mass-spring system. The reduced power output is due to the fact that an increased compression ratio leads to an increased expansion ratio, which reduces the energy in the exhaust gases. While this may increase engine efficiency, it reduces the boost pressure and therefore also engine power output since the simulations are run with constant fuel-air equivalence ratio. In the simulations, the exhaust gas temperature drops by around 8 per cent between compression ratios of 15 to 25, giving a reduction in boost pressure by around 4 per cent in the same interval.

4.3.2.3 Exhaust back pressure

The exhaust back pressure of an engine is determined by the size of the turbocharger. The effects of varying exhaust back pressure on engine performance are investigated below, with the assumption that the turbocharger efficiencies are constant for all conditions. An increase in exhaust back pressure is assumed to give higher engine speed, since the pressure forces increase. In addition, significantly higher power output is expected with higher boost pressure, since the engine is running at a constant fuel-air equivalence ratio.

Figure 4.10 shows the effects of varying exhaust back pressure on engine performance. It can be seen that along with the expected increase in engine power output and speed, the efficiency improves with increasing exhaust back pressure. This is due to the fact that the contribution from frictional losses decreases at higher engine power outputs.

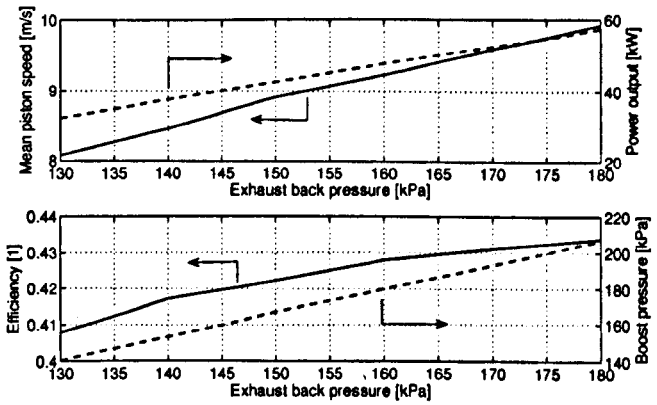

Figure 4.10: Effects of changing exhaust back pressure on engine performance.

Engine performance with higher exhaust back pressures than 180 kPa were not investigated as the upper range of the investigated values produced very high peak cylinder pressures (approaching 20 MPa). Operation on higher exhaust back pressures with constant fuel-air equivalence ratio is therefore not realistic. Further investigations to compare the performance of a highly turbocharged engine running at a low equivalence ratio compared to a moderately turbocharged engine running at high equivalence ratios may be worthwhile.

4.3.2.4 Stroke to bore ratio

The stroke to bore ratio is one of the core design variables in internal combustion engines, relating the combustion chamber surface area to its volume and the piston area to stroke length. Conventional engines with high stroke to bore ratios, such as those found in marine and stationary powerplants, are characterised by high efficiency but low power density. Low stroke to bore ra-

tios, commonly found in small-scale engines, e.g. in automotive applications, allow higher engine speeds, which increase power to weight ratio, but come with a penalty in engine fuel efficiency.

Figure 4.11 shows the effects of varying stroke to bore ratio on engine performance with the engine swept volume kept constant. As expected, higher efficiencies were obtained with an increasing stroke to bore ratio. Despite an increase in mean piston speed, the engine output power is slightly reduced with increasing stroke to bore ratio due to a reduction in engine speed.

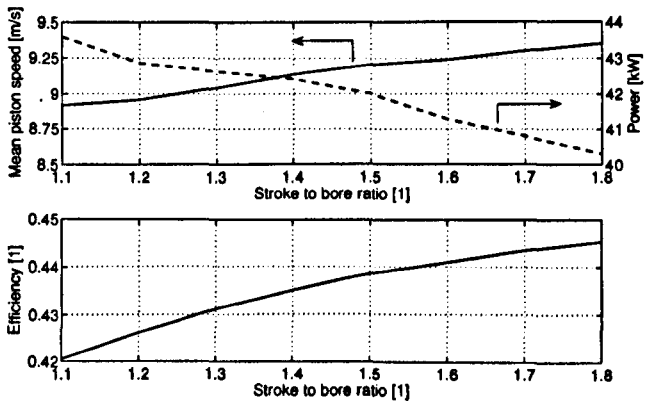

Figure 4.11: Effects of varying free-piston engine stroke to bore ratio with constant swept volume.

4.3.3 Operational variables

A number of operational variables can be controlled during engine operation, including valve timing and fuel injection timing, as is common in conventional engines. In addition, providing an adequate control system can be realised, the stroke in the free-piston engine can be varied by varying the TDC and BDC setpoints. Combined, these may allow extensive operation optimisation possibilities for the free-piston engine.

Control of exhaust valve timing was implemented into the simulation model, and was described in Section 4.3. This optimises the opening and closing of the valves at any operating condition and the effects of varying exhaust valve timing are therefore not further investigated.

4.3.3.1 Effect of variable stroke

The free-piston engine has the potentially valuable feature of variable stroke. This means that the compression ratio of the engine can be altered during operation, to optimise engine performance for any operating condition. This has been mentioned by a number of authors, and suggested advantages include increased part load efficiency and multi-fuel operation possibilities.

Figure 4.12 shows the effect of changing the TDC setpoint for the engine (the figure shows the corresponding effective compression ratio) on engine efficiency at different loads. The simulations

show that the optimum compression ratio varies only slightly with load, and no advantage of increasing the compression ratio at low loads was found. This result is somewhat unexpected, and is due mainly to the influence of the compression ratio on engine speed and turbocharger performance, which for a constant engine load leads to variations in the fuel-air ratio. For high loads a small increase in efficiency can be seen with increasing compression ratio, and in these cases the peak cylinder pressure will limit the maximum compression ratio. The compression ratios for which the peak cylinder pressure exceeded 18 MPa are shown in the figure.

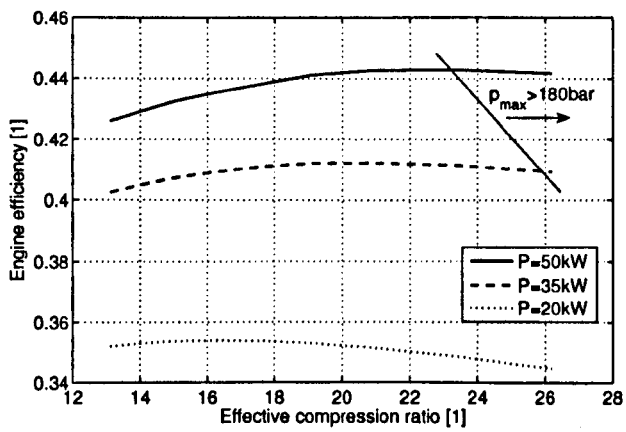

Figure 4.12: Effects of changing effective compression ratio during engine operation at constant load.

Similar simulations were performed for BDC position, but minor variations in the BDC setpoint produced no noticeable effect on engine efficiency.

4.3.3.2 Fuel injection timing

Varying the fuel injection timing is widely used as a tool to optimise engine performance and control emissions formation at varying operating conditions. Most modern diesel engines employ electronic control of fuel injection timing and technology such as common-rail fuel injection systems make the implementation of this relatively simple.

Figure 4.13 shows the effects of varying fuel injection timing on the predicted engine efficiency for different load levels. The simulations indicate that changes in the fuel injection timing do not have a significant effect on engine efficiency. However, a significant increase in the peak in-cylinder gas temperature was observed with advanced injection timing, as can be seen in Figure 4.14, and this will influence emissions formation. It can be seen that an optimal point of fuel injection for high efficiency can be found, and this point varies slightly with load.

In addition to control of the fuel injection timing for operation optimisation purposes it will

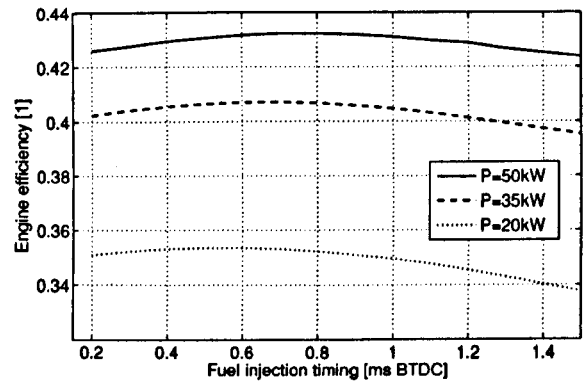

Figure 4.13: Effects of varying fuel injection timing for different engine loads.

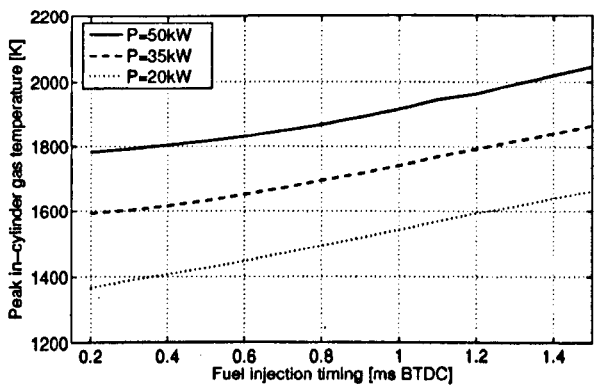

Figure 4.14: Peak in-cylinder gas temperature for varying fuel injection timing.

be necessary to control injection timing during engine start-up and transient operation. Since the reference used to set the fuel injection timing is the measured piston position (equivalent to the crank angle in conventional engines), the injection may not be initiated if the piston fails to reach the point of fuel injection, for example in the case of a rapid load increase. To avoid the engine stopping in such an event, it may be necessary to have a control system advancing fuel injection timing in such a situation and retarding it again when the engine reaches steady state operation. Engine control issues are discussed further in Chapter 6.

4.3.4 Different load profiles

In the simulations presented above the load force from the alternator over the length of the stroke is assumed to be proportional to the instantaneous piston speed. This was based on the assumption of an electric machine coupled to a constant, purely resistive electric load. As discussed in Section 2.1.3.5, the load device can have a different force profile if the electric load force is controllable, for

example by varying the magnetic field strength or through the use of power electronics, or if the load device is of a different type, for example a hydraulic cylinder. It is clear that the load force profile will influence engine operation since it directly influences the piston dynamics. The simulation model allows the use of any load force profile, and in this section the influence of different load force profiles on the operation and performance of the engine will be investigated.

4.3.4.1 Load force proportional to piston speed

Figure 4.15 shows the piston motion profile of the free-piston engine for the original configuration, compared to a crankshaft engine running at the same speed. Figure 4.16 shows an efficiency map of the engine for varying compression ratio and fuel injection timing, with the engine running with a constant power output of 50 kW. As one would expect, an optimum area of operation can be found. These results can be compared to those obtained with different load force profiles in order to investigate the influence of this variable.

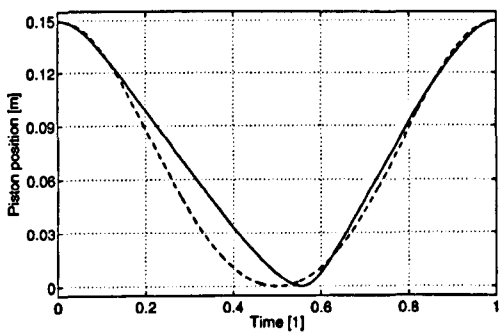

Figure 4.15: Piston motion profile of the free-piston engine with a load force proportional to piston speed, compared to that of a conventional engine (dashed).

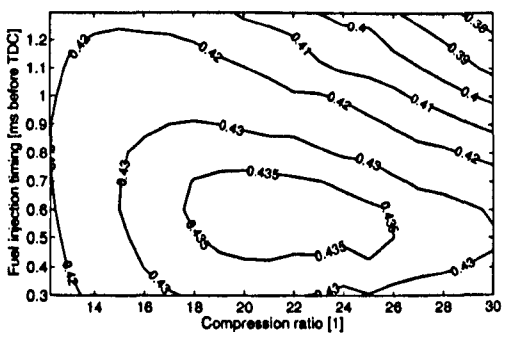

Figure 4.16: Engine efficiency map for varying compression ratios and fuel injection timing with load force proportional to piston speed.

4.3.4.2 Constant load force

A constant load force over the full stroke better represents the properties of a hydraulic load device, consisting of a cylinder working against a constant discharge pressure. It may also be possible for an electric machine to adopt such a force profile, and this may be beneficial as it would have the lowest maximum load force requirements and thereby the lowest translator mass.

Figure 4.17 shows the piston motion profile of the free-piston engine for a constant load force profile, compared to a crankshaft engine running at the same speed. No significant effect on piston motion compared to the case with the load force proportional to piston speed was found. Figure 4.18 shows the engine efficiency map for varying compression ratio and fuel injection timing. Compared to the previous changing load force, a constant force over the full stroke can be seen to give

a very small decrease in optimum engine efficiency. This is due to the speed of the power stroke expansion being slightly lower than in the previous case, giving an increase in heat transfer losses.

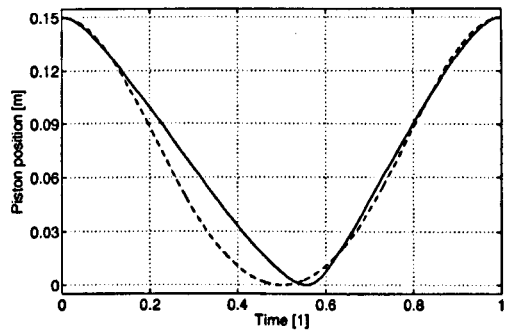

Figure 4.17: Piston motion profile of the free-piston engine with constant load force, compared to that of a conventional engine (dashed).

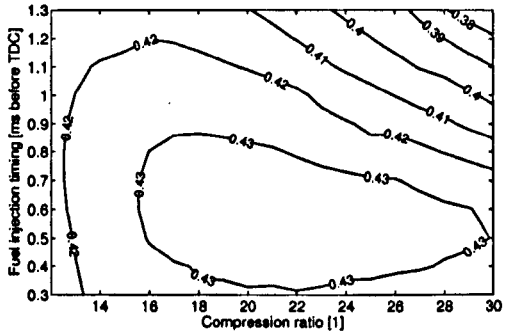

Figure 4.18: Engine efficiency map for varying compression ratios and fuel injection timing with constant load force.

4.3.4.3 Other force profiles

With the use of appropriate power electronics, the electric machine can in theory be controlled to have any load force profile. One could, for example, take out all the power on the first half of the stroke and then let the piston continue to its outer position with no load. This will, however, effectively double the required generator force, which will significantly increase the mass of the translator. This may still be worthwhile if the performance benefits of such an operational strategy outweigh the potential drawbacks of an increased moving mass. Moreover, other load devices may have such characteristics (for example will the load in an air compressor be extracted predominantly in the last half of the stroke), and an investigation into the influence of the load force profile on engine performance is therefore worthwhile.

The mentioned example, taking out all the power on the first half of the stroke, is likely to lead to a lower piston speed just after TDC and thereby a slower power stroke expansion, whereas taking out all the power in the last half of the stroke would have the opposite effect. Manipulating the piston dynamics in this way may influence factors such as the volume change during combustion, the time spent in the high temperature parts of the cycle and, in the other end of the stroke, the time available for scavenging. Although the load force is subordinate to the pressure forces from the cylinders, and thereby only has limited influence on the piston dynamics, some effects on engine performance is expected.

First half of stroke Figure 4.19 shows the piston motion profile when extracting all the load in the first half of the stroke (i.e. in the upper half, around TDC). It can be seen that the expansion process

in this case is slower than in the previous cases and that this takes almost half of the total cycle time, making the piston motion nearly symmetric, like in the crankshaft engine. Figure 4.20 shows the engine efficiency map for this case. Compared to the force profiles investigated previously this force profile can be seen to give slightly lower efficiency, however the differences are minimal.

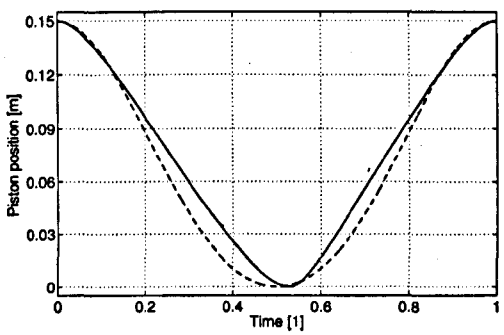

Figure 4.19: Piston motion profile of the free-piston engine with constant load force over the first half of the stroke, compared to that of a conventional engine (dashed).

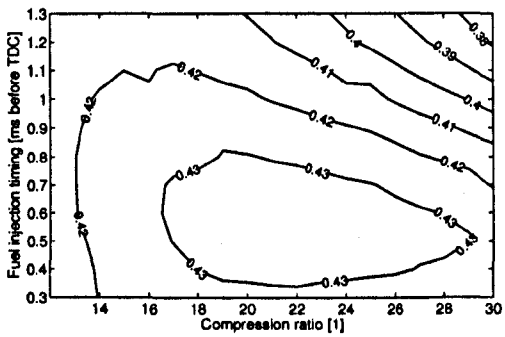

Figure 4.20: Engine efficiency map for varying compression ratios and fuel injection timing with constant load force over the first half of the stroke.

Last half of stroke Figure 4.21 shows clearly the faster expansion when the power is extracted over the last half of the stroke, as one would expect. This leads to a higher degree of asymmetry in the piston motion profile and a larger difference between the time spent in the compression part of the cycle and that spent in the power stroke expansion. Figure 4.22 shows the engine efficiency map for this case. Slightly higher efficiency can be seen for this case, due to lower heat transfer losses resulting from the faster combustion. As above, the differences are only minor between this case and the original.

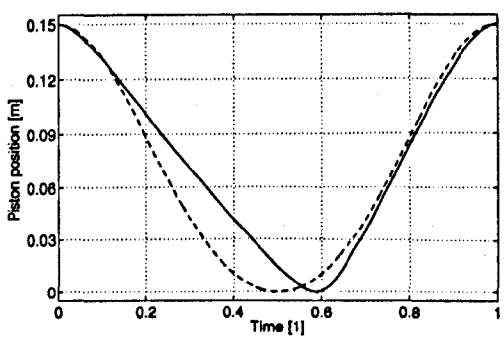

Figure 4.21: Piston motion profile of the free-piston engine with constant load force over the last half of the stroke, compared to that of a conventional engine (dashed).

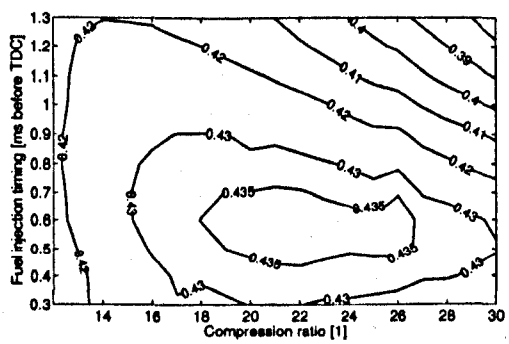

Figure 4.22: Engine efficiency map for varying compression ratios and fuel injection timing with constant load force over the last half of the stroke.

4.3.5 Conventional engine simulation and comparison

To investigate the effects of the particular operating characteristics of the free-piston engine compared to conventional engines, a crankshaft engine simulation subroutine was implemented in the simulation model. The subroutine uses the simulation results for a given free-piston engine configuration and runs a subsequent simulation for an engine with the same configuration and operational variables (bore, stroke, boost pressure, injected fuel mass etc.), but with a piston motion equal to that of a conventional engine (i.e. a crankshaft-driven motion that is not influenced by the in-cylinder pressure).

Using such an approach, some insight into potential performance differences between the free-piston and conventional engines can be gained. It should, however, be noted that the current simulation model was unable to predict effects of the piston motion profile on the gas motion in the combustion chamber. Differences in the gas motion will influence the combustion process and in-cylinder heat transfer, and the results presented in this section should therefore be taken as indicative only. Differences in the in-cylinder processes between free-piston and conventional engines will be investigated in detail in Chapter 5.

The optimum point of fuel injection differs between the two engines due to the differences in piston motion profile, and in order to obtain a realistic comparison each engine was investigated with the injection timing giving the best fuel efficiency. These optimum values were identified through simulation studies and it was found that the free-piston engine required a slightly advanced injection timing compared to the conventional engine.

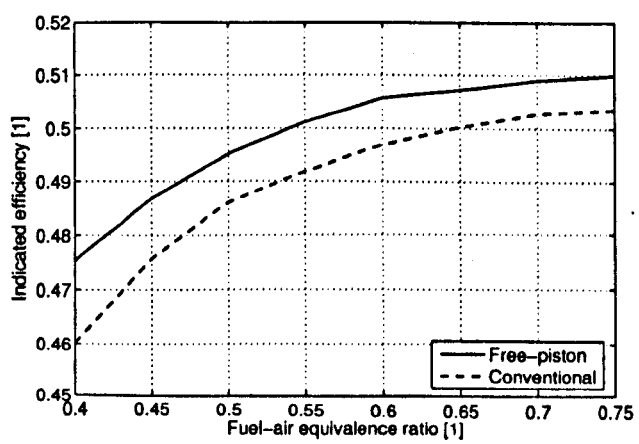

Figure 4.23: Indicated efficiency of the free-piston engine compared to a conventional engine for varying load levels.

Figure 4.23 shows the simulated indicated efficiency of the free-piston engine compared to an identical conventional engine for varying engine load level (fuel-air equivalence ratio). The com-

parison is done on the basis of indicated (in-cylinder) values, since no assumptions have been made for the mechanical efficiency of conventional engines. A slight fuel efficiency advantage is predicted for the free-piston engine over the full load range, and it will be shown below that this is due to reduced heat transfer losses. In addition to this there are potentially lower frictional losses in the free-piston engine which will improve fuel efficiency further.

4.3.5.1 In-cylinder gas temperature and heat transfer losses

The fast power stroke expansion of the free-piston engine reduces the amount of time spent in the high-temperature parts of the cycle, and this possibly reduces in-cylinder heat transfer losses and temperature/time-dependent emissions formation. Using the simulation model, the predicted heat transfer rate from the cylinder and the in-cylinder gas temperature was compared for the free-piston engine and for an equivalent conventional engine.

Figure 4.24 shows the simulated in-cylinder gas temperature and the total heat lost to in-cylinder heat transfer for one cycle, where the latter is shown as a fraction of the injected fuel heat. The graphs are synchronised around the start of combustion. It can be seen that both the peak temperature and the temperature levels during expansion is lower in the free-piston engine, and that this results in lower heat transfer losses. The simulations predict that 17.4 % of the fuel heat is lost to in-cylinder heat transfer in the free-piston engine. For the conventional engine this value is 18.7 %.

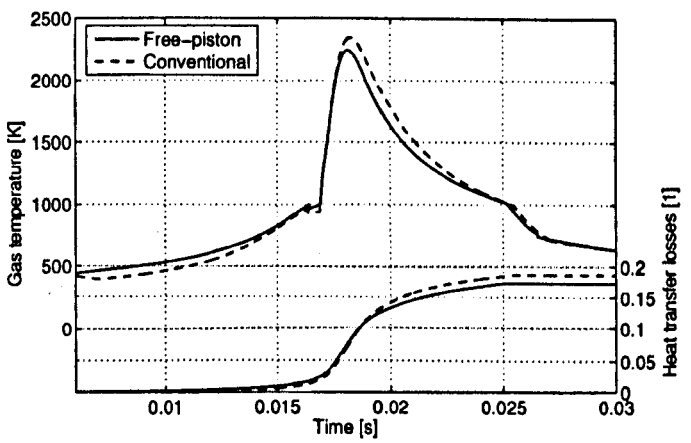

Figure 4.24: In-cylinder gas temperature and heat transfer losses in free-piston and conventional engines.

The simulations further show that the fast expansion of the free-piston engine results in it spending less time in the parts of the cycle where the in-cylinder gas temperatures are high. The amount of time per cycle that the gases in the free-piston engine hold a temperature of above 1500 K is 89 % of that in the conventional engine. (This time period is equal to 10.1 % of the cycle time in the free-

piston engine and 11.3 % in the conventional engine.) For temperatures of above 2000 K, this value is 83 % (with such temperature levels occurring for 4.5 % and 5.4 % of the cycle time respectively). In addition to reducing heat transfer losses, this particular feature of the free-piston engine may lead to a reduction in the formation of temperature/time-dependent emissions, most importantly nitrogen oxides.

4.3.6 Model uncertainties

The simulation model was partially validated against a conventional engine, and some uncertainties will exist in analyses like the one presented here. A particular concern that was noted was the use of models developed for conventional engines in the modelling of a free-piston engine. Reported experimental work on free-piston engines suggests differences in the combustion process, and the modelling of the engine friction in the present study was based on an estimated breakdown of friction mechanisms in conventional engines. Furthermore, it is known that some variation exists between the predictions obtained from different in-cylinder heat transfer correlations [92]. It was therefore worthwhile to investigate the influence of changes in the submodels in these areas and their effects on overall engine performance predictions.

4.3.6.1 Effect of fuel burn rate

Figure 4.25 shows the effect of changing fuel burn rate on engine performance. In addition to changing the total time allowed for combustion (but not the fuel burn pattern) in Equation 4.4, the effect of assuming that all the fuel burns in a single, pre-mixed phase is shown. Such an approach was adopted by Tikkanen et al. [95] and has been supported by experimental results from the same group and from Somhorst and Achten [90].

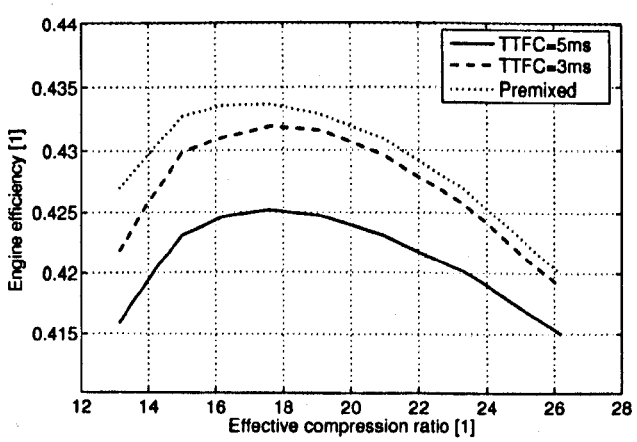

Figure 4.25: Effect of total time for combustion (TTFC) on engine performance predictions.

Some influence on engine performance can be seen and a more rapid combustion will, as expected, improve engine performance. It is further seen that the optimum compression ratio does not change significantly with varying fuel burn rate, indicating that the variable compression ratio may be less beneficial than expected. It should, however, be noted that changing the compression ratio will influence factors that are not predicted here, such as squish effects, which are likely to influence the performance of the engine.

The simulations showed that for high load (fuel-air equivalence ratio of around 0.70), most of the fuel has been burned within around 2 ms with total time for combustion in Equation 4.4 set to 5 ms. With total time for combustion set to 3 ms most of the fuel burns in around 1.5 ms. Somhorst and Achten [90] reported fuel burn rates even higher than this, stating that 90 % of the combustion in their free-piston engine finishes within 1 ms. Figure 4.25 showed that the effect of a higher fuel burn rate is an improvement in engine fuel efficiency.

4.3.6.2 Friction and heat transfer losses

Figures 4.26 and 4.27 show the effects of changes in the friction and heat transfer submodels. In the simulations the heat transfer coefficient and the friction mean effective pressure were changed by a factor as shown in the figures with other engine variables held constant, in order to investigate their influence on the overall predictions. It can be seen that minor errors in any of these have only limited effects on the overall engine performance predictions. A 10 % error in one of the two will produce approximately a 0.5 percentage point error in overall engine efficiency predictions.

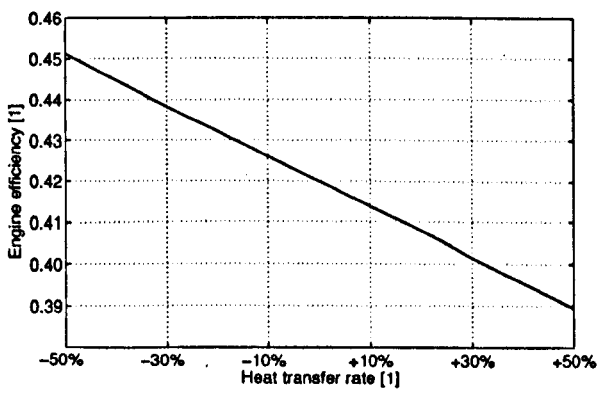

Figure 4.26: Effects of varying heat transfer predictions on simulated engine performance.

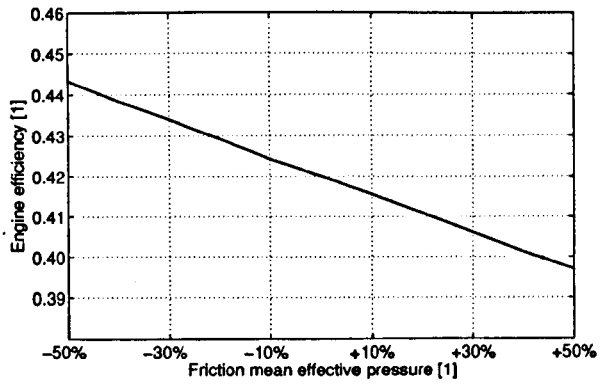

Figure 4.27: Effects of varying frictional losses on simulated engine performance.

4.4 Summary

This chapter presented the derivation of a detailed simulation model for the free-piston engine generator presented in Chapter 3. Extensive simulation results were presented, giving insight into the basic performance of the engine and the effects of engine design parameters and operational variables on engine performance.

It was found that the design and operational variables of the free-piston engine are highly interconnected, and the changing of one input parameter in the simulation model influences most operational variables. Due to the variable stroke, this occurs to a higher degree than what one would expect in a conventional engine.

The trends observed from the simulation results indicate that the heat transfer losses during the high-temperature parts of the cycle are the more influential mechanism determining engine efficiency, compared to the advantages of lower piston speeds during combustion. Both in the comparison between free-piston and conventional engines and in the free-piston simulations it was seen that a faster power stroke expansion leads to improved engine efficiency due to reduced heat transfer losses. This indicates that close to constant volume combustion is achieved for all cases. The mass requirements for the electric machine, a concern with the free-piston engine generator often mentioned by other authors, were found to be less stringent in the current design, due to higher operating pressures.

It was further found that the free-piston engine has potential advantages over conventional technology in terms of fuel efficiency as a result of mechanical simplicity and faster power stroke expansion. Shorter time at elevated temperatures may reduce the formation of exhaust gas emissions, however this must be verified through more detailed modelling or experimental testing. The flexibility of the variable stroke was not found to give significant advantages for normal engine operation, a result that was somewhat unexpected.

Chapter 5

Multidimensional modelling of free-piston engine performance

Some advantages with free-piston engines compared to conventional technology are obvious, such as reduced frictional losses due to a simpler design and fewer moving parts. Other potential advantages, including increased combustion efficiency and reduced exhaust gas emissions, have been claimed by free-piston engine developers and were discussed in Sections 2.1.3.7 and 4.1.1. However, very few reported studies have investigated the influence of the particular free-piston design and operating characteristics on the in-cylinder processes, and a detailed investigation into this is therefore worthwhile.

Many factors influence the combustion and emission formation in combustion engines, making accurate predictions of these processes extremely complex. In this chapter, details of free-piston engine in-cylinder processes will be investigated and directly compared to those of conventional engines in order to identify potential advantages or disadvantages with the free-piston engine concept.

Parts of the work presented in this chapter were presented by Mikalsen and Roskilly [74,76].

5.1 Simulation methodology

Most reported modelling of free-piston engines is based on zero-dimensional, single-zone models, in which the cylinder charge is assumed homogeneous and uniform in temperature and heat is added to the charge according to a pre-defined fuel burn rate. (See Section 4.1 for an overview of reported work.) While this may be sufficient to model basic engine performance, for example in the early stages of a design process, such models do not account for factors such as in-cylinder gas motion and cannot accurately predict emissions formation. Moreover, most such models have been developed for, and calibrated against, conventional engines, and it is questionable whether they are suitable for modelling free-piston engines without modifications.

Modern computational fluid dynamics (CFD) codes provide powerful tools to investigate the highly complex interaction between in-cylinder gas motion, heat transfer, combustion and chemical kinetics in internal combustion engines, and such codes are widely used in engine research. Although computationally intensive, CFD codes are particularly well suited for comparative studies such as the one presented here, where effects of single parameters are to be investigated with other variables constant.

5.1.1 OpenFOAM

The simulations in this work were performed using the open source CFD toolkit OpenFOAM [68]. Written in the object oriented C++ programming language and released under the GNU GPL licence OpenFOAM gives the user considerable power to modify the code to suit specific needs, for example with the implementation of new submodels or modification of existing solvers. Solvers for a wide range of applications are implemented in the toolkit, including fluid flow, electromagnetics, solid mechanics and combustion. Implemented in the toolkit are the Weller model [105] for premixed combustion, the Chalmers PaSR model for diesel combustion [78] and a CHEMKIN-compatible chemistry solver. Jasak et al. [57] described the toolkit and presented examples of the simulation of pre-mixed spark ignition combustion as well as diesel spray and combustion.

Also included in the toolkit are utilities for pre– and post-processing, such as mesh generation and visualisation of results, the latter based on the open source visualisation application ParaView.

5.1.2 Modifications to the OpenFOAM code

Mesh motion functionality for simulation of piston motion in conventional engines is provided with the OpenFOAM code. The piston dynamics of a free-piston engine were investigated in Chapter 4, and it was found that the piston motion in the free-piston engine differs significantly from that of a conventional engine. The predicted piston motion profile of a single piston free-piston engine compared to that of a conventional engine is shown in Figure 5.1. This piston motion profile was described mathematically through least square error fitting to a high-order polynomial and implemented into the OpenFOAM code. This allows a direct comparison between the free-piston and conventional engines for identical engine design and operating conditions.

The comparison in Figure 5.1 was carried out on a time basis since the piston motion in the free-piston engine cannot be measured in crank angles. However, to allow an easier comparison, this time-based piston motion profile was normalised around TDC and mapped on to a crank angle scale, and this notation is used in the investigations described below.

Further modifications to the code and implementation of submodels are described under the appropriate headings below.

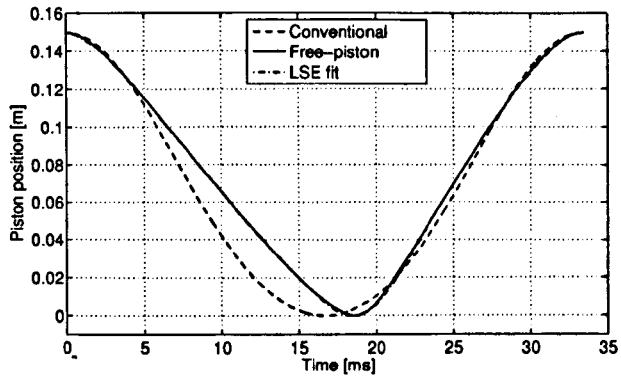

Figure 5.1: Simulated piston motion profile for a single piston free-piston engine and that of a conventional engine. (TDC at position 0.)

5.2 Spark ignited free-piston engine performance

Spark ignited free-piston engines are likely to possess different characteristics than compression ignition engines and it is not obvious that one operating principle is better suited for the free-piston engine than the other. Although the free-piston engines developed in the mid-20th century were diesel powered, many of the recently proposed free-piston engines have been of the spark ignited type. Proposed advantages of spark ignited free-piston engines include multi-fuel capability [25] and reduced exhaust gas emissions [13]. Hence, an investigation into the performance of spark ignited free-piston engines is worthwhile.

5.2.1 Challenges with the design

The free-piston engine is restricted to the two stroke operating principle, since a power stroke is required every cycle. Small two stroke engines, such as those found in small motorcycles, are usually port scavenged to keep the design simple and reliable. Operating with a pre-mixed charge, these engines suffer from short-circuiting, i.e. that parts of the inlet charge passes through the cylinder and out with the exhaust. This gives penalties in both fuel efficiency and exhaust gas emissions, and is a major problem for small, spark ignited two stroke engines. For larger applications, where engine simplicity is less important, the engine can be designed with exhaust valves in the cylinder head. This allows the more efficient uniflow scavenging to be employed, which will reduce the problem of short circuiting, but this problem will always be present in pre-mixed two stroke engines. The emerging technology of direct injection spark ignition (DISI), also known as gasoline direct injection (GDI) will eliminate this problem.

5.2.2 Simulation setup

A simple piston and cylinder design is sufficient for a comparative study such as the one presented here, and a script was written to produce a computational mesh using the mesh generation utility supplied with with OpenFOAM. The engine geometry was assumed to be symmetric around the cylinder axis, allowing a wedge geometry with cyclic boundary conditions to be used. This simplification reduces the computational costs significantly, and the feasibility of such a setup in a spark ignition engine simulation with OpenFOAM was demonstrated by Lucchini [70]. Figure 5.2 shows the computational mesh used in the simulations. A mesh sensitivity analysis was carried out to ensure the accuracy of the predictions, and the mesh used was a 30-degree wedge with 9200 cells, equivalent to more than 110,000 cells for the full cylinder.

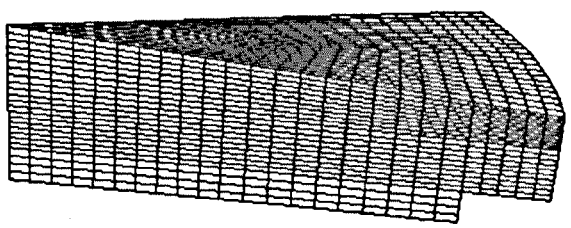

Figure 5.2: Computational mesh for a spark ignited engine CFD simulation.

The modelled engine had a 60 mm bore, a 60 mm stroke, a nominal compression ratio of 8:1, and the fuel used was iso-octane at a fuel-air equivalence ratio of 1. Combustion was modelled using the Weller combustion model [105] with a centrally located spark plug. Turbulence was modelled with a standard k–ϵ model with wall functions, and constant wall temperatures were used. As the engine was a two stroke, the simulations were run between the point of exhaust ports closing and the point of exhaust ports opening. The cylinder charge at the start of compression was assumed to be a homogeneous mixture of fuel and air. Swirl was introduced at the start of compression, and the swirl level was assumed to be constant for all engine speeds.

5.2.3 Engine basic performance

To allow a direct comparison between the free-piston engine and a conventional engine, the engines must run at comparable operating conditions. While all the externally set conditions, such as engine speed and intake air pressure and temperature, are identical, the optimum ignition timing may vary between the two engines. A series of simulations were run to identify the optimum spark timing, and all the results presented below are run at maximum brake torque (MBT) ignition timing. (The influence of spark timing on engine performance can also be seen below in Figure 5.8.)

The simulations showed that the free-piston engine requires advanced spark timing compared

to the conventional engine, which is likely to be due to the faster expansion just after TDC. Figure 5.3 shows the spark timing required for maximum brake torque for the two engines.

Figure 5.3 further shows the predicted indicated efficiency of the two engines. It can be seen that the free-piston engine has a slight efficiency advantage over the conventional engine at low speeds, but that the efficiency of the free-piston engine drops as the speed increases. This is likely due to the effects of volume change during combustion having greater impact at higher speeds. Overall, only very small differences in indicated efficiency between the two engines were found. This is different to the results for the compression ignition free-piston engine studed in Chapter 4, and indicates that the free-piston engine is best suited for diesel engine operation.

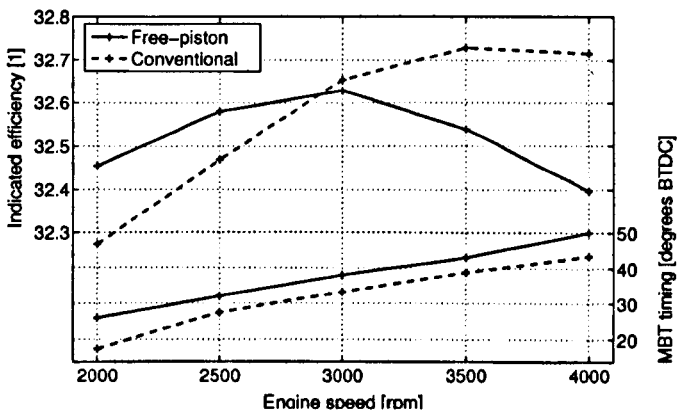

Figure 5.3: Engine indicated efficiency and MBT ignition timing against engine speed for the free-piston engine compared to a conventional engine.

Figure 5.4 shows the in-cylinder gas pressure plot for the two engines. It can be seen that the free-piston engine has a slightly higher peak in-cylinder pressure, due to the advanced spark timing. The pressure drops more rapidly in the free-piston engine due to the faster power stroke expansion.

For some diesel-powered free-piston engines, higher heat release rates compared to conventional engines have been reported [2,96]. It has been suggested that this is due to the high piston acceleration around TDC, increasing in-cylinder gas velocities and turbulence levels. Although the gas motion and turbulence levels in a spark ignition engine are significantly lower than those of a diesel engine, any such differences will influence the flame speed and this may have effects on engine performance. Figure 5.4 also shows the mass fraction burnt for the two engines as a function of crank angle. With the exception of the advanced spark timing in the free-piston engine, no noticeable differences in the fuel burn pattern were found.

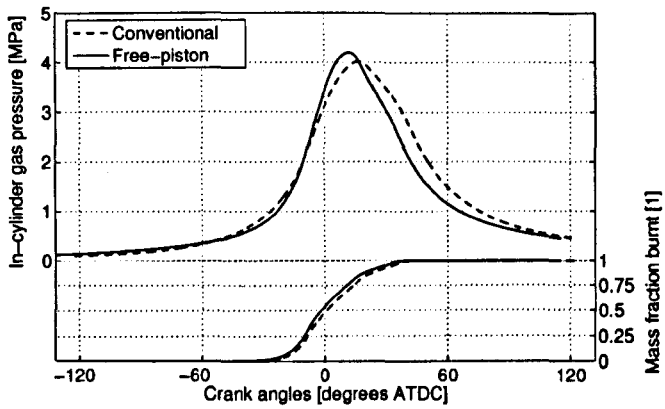

Figure 5.4: Simulated in-cylinder pressure and mass fraction burnt for the free-piston and conventional engines running at 3000rpm.

5.2.4 Part load performance

For lean mixtures (mixtures with fuel-air equivalence ratios of less than 1) the flame speed is reduced, giving a decrease in engine efficiency. Although the flame speed of a mixture peaks for slightly rich of stoichiometric conditions, the indicated efficiency usually peaks for slightly lean mixtures, since the efficiency also depends on factors such as heat transfer losses and the chemical composition of the burnt gases.

Figure 5.5 shows the predicted part load performance of the two engines. For both engines, the efficiency penalty occurs immediately on the lean side of stoichiometric. This is due to the shape of the combustion chamber, giving a relatively long distance for the flame to travel. This poor compactness of the combustion chamber penalises even small reductions in flame speed due to increased volume change during combustion. The faster volume change around TDC in the free-piston engine makes the efficiency drop more rapidly as the charge is diluted, decreasing its part load performance compared to the conventional engine.

Variable stroke length

While the compression ratio in a conventional engine is fixed (with the exception of small variations depending on the valve timings and valve flow characteristics), the free-piston engine can be designed to allow variation practically without limits. The compression ratio can be varied continuously during engine operation by varying the TDC setpoint, and this may provide operation optimisation possibilities at part load.

The limitation in compression ratio lies in the fuel quality and its knock (self-ignition) characteristics, and is commonly between 7:1 and 11:1 for ordinary gasoline fuels [51]. The limitation in compression ratio typically occurs for fuel-air equivalence ratios of around 0.9, i.e. slightly lean of

stoichiometric. For leaner mixtures, the knock limit increases drastically, and may exceed a compression ratio of 15:1 for very lean mixtures [51].

Figure 5.5 shows the simulated part load performance of the free-piston engine with such compression ratio control. For equivalence ratios, ϕ, of 0.9 and lower, the compression ratio was increased linearly between the nominal 8:1 to 10:1 at $\phi = 0.7$. A small efficiency improvement can be seen, however, due to the knock limitations, increasing the compression ratio cannot offset the efficiency disadvantage of the free-piston engine. At very low loads, where the compression ratio can be increased significantly more, these effects are expected to be higher. However, from an engine fuel economy perspective, the load range presented here will be of highest interest.

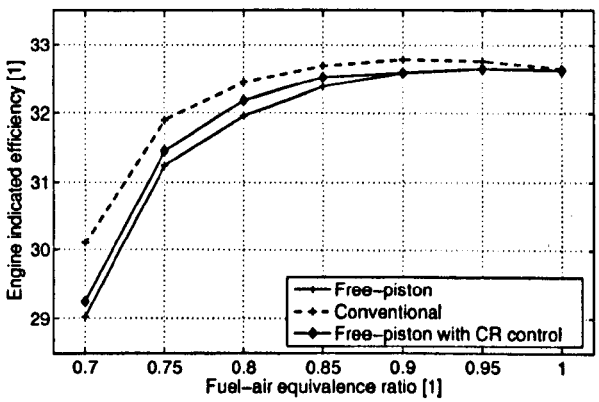

Figure 5.5: Part load efficiency of a free-piston engine, a conventional engine, and a free-piston engine with compression ratio control.

5.2.5 Multi-fuel operation

The high operational flexibility of the free-piston engine may provide significant multi-fuel possibilities. High engine performance can be achieved for a variety of fuels, which allows the operator to select the fuel based on current fuel prices, emission targets or other factors. For example, ethanol-gasoline blends are becoming increasingly common and are widely available at petrol stations in many countries. Utilising the variable compression ratio together with modern engine technology such as electronically controlled, variable spark timing and accurate knock sensors, the engine operation can be optimised based on the properties of a given fuel.

The most important characteristics of a fuel are flame speed, knock limit and heat content. For example, ethanol has a flame speed that is approximately 30 % higher than that of ordinary gasoline fuel, in addition to a higher knock limit. Hydrogen has a flame speed that is one order of magnitude higher than these fuels.

It was seen above that the free-piston engine appeared to suffer more from reduced flame speed

than a conventional engine. To investigate the sensitivity to, and effects of, flame speed in the free-piston and conventional engines, a correction factor was introduced into the OpenFOAM code to modify the calculated flame speed.

Figure 5.6 shows the effects of varying flame speed on engine performance predictions. It can be seen that the free-piston engine has advantages when using fast-burning fuels, since this reduces the negative effects of high volume change of the combustion chamber during combustion, but that the efficiency drops rapidly for lower flame speeds. One reason for the latter is that the ignition timing in the free-piston engine had to be advanced significantly for the combustion process to finish in time, more than in the conventional engine. (The fact that the graphs intersect for a correction factor of around one is coincidental.)

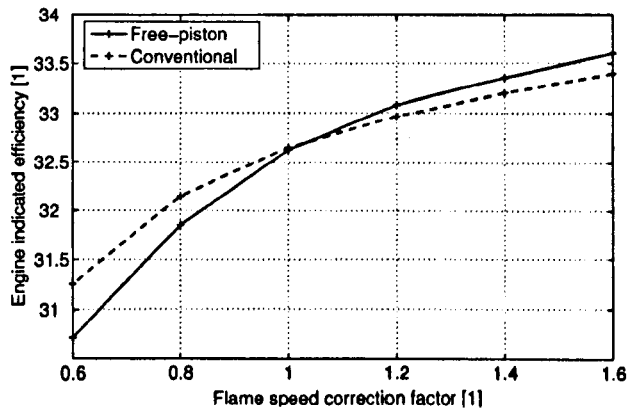

Figure 5.6: Effects of varying flame speed on engine performance.

5.2.6 Engine emissions

The main exhaust gas emissions from spark ignited engines are carbon monoxide (CO), nitrogen oxides (NO_x) and unburnt hydrocarbons (HC). In addition to these comes carbon dioxide (CO_2), which is a product of hydrocarbon fuel combustion and can only be reduced by improving fuel efficiency or using an alternative fuel.

HC emissions mainly result from incomplete combustion, e.g. in crevices within the cylinder. The operational differences between free-piston and conventional engines are not believed to result in differences in HC emissions formation, and these are therefore not further investigated here. The formation of CO and NO_x emissions depend highly on the temperature of the in-cylinder gases and the time spent in the high-temperature parts of the cycle, and may therefore be influenced by the particular operating characteristics of the free-piston engine.

Methodology

A solver for the chemical composition of the in-cylinder gases was implemented within the OpenFOAM code, based on the approach presented by Olikara and Borman [81]. The equilibrium concentrations for a set of species were estimated and used to solve the kinetics of NO_x and CO formation and destruction. 10 species were considered: CO_2, H_2O, N_2, O_2, CO, H_2, H, O, OH and NO.

Nitrogen oxides The formation of nitrogen oxides in internal combustion engines is kinetically controlled and highly temperature dependent, and the formation and destruction of NO_x is too slow for the gases to reach equilibrium states during the engine cycle. NO_x will be formed in the parts of the cycle where gas temperatures are high (i.e. around TDC), and, as the gases are rapidly cooled during the expansion stroke, the NO_x tends to 'freeze' as the reaction rates for NO_x destruction is reduced with the decreasing temperature.

The particular operational characteristics of the free-piston engine may influence the NO_x formation and destruction. Firstly, if the free-piston engine spends less time in the high-temperature parts of the cycle, this may decrease NO_x formation. Secondly, however, the fast expansion may increase the 'freezing' effects, reducing the destruction rate of NO_x.

The extended Zeldovich mechanism is commonly used to model the formation of nitrogen oxides in internal combustion engines. This states that the main reactions governing the formation (and destruction) of nitrogen oxides are [51]:

$$\mathrm{O} + \mathrm{N_2} \underset{k_1^-}{\overset{k_1^+}{\rightleftharpoons}} \mathrm{NO} + \mathrm{N}$$

$$\mathrm{N} + \mathrm{O_2} \underset{k_2^-}{\overset{k_2^+}{\rightleftharpoons}} \mathrm{NO} + \mathrm{O}$$

$$\mathrm{N} + \mathrm{OH} \underset{k_3^-}{\overset{k_3^+}{\rightleftharpoons}} \mathrm{NO} + \mathrm{H}$$

Heywood [51] described how these, with the approximation of steady state concentration of N and the assumption that the other species are in chemical equilibrium, can be reduced to give the formation rate of NO:

$$\frac{\mathrm{d[NO]}}{\mathrm{d}t} = 2k_1^+[\mathrm{O}][\mathrm{N_2}]\frac{1 - [\mathrm{NO}]^2/(K[\mathrm{O_2}][\mathrm{N_2}])}{1 + k_1^-[\mathrm{NO}]/k_2^+[\mathrm{O_2}] + k_3^+[\mathrm{OH}]}$$

where $K = (k_1^+/k_1^-)(k_2^+/k_2^-)$ and the brackets denote species concentrations. Rate constants are [51]

k_1^+	$7.6 \times 10^{13} \exp\left(\frac{-38000}{T}\right)$	k_1^-	1.6×10^{13}
k_2^+	$6.4 \times 10^{9} T \exp\left(\frac{-3150}{T}\right)$	k_2^-	$1.5 \times 10^{9} T \exp\left(\frac{-19500}{T}\right)$
k_3^+	4.1×10^{13}	k_3^-	$2.0 \times 10^{14} \exp\left(\frac{-23650}{T}\right)$

where T is the gas temperature.

Carbon monoxide Carbon monoxide, CO, emissions in spark ignition engines are mainly a problem when the engine is operating with rich mixtures. Carbon monoxide is formed in the high-temperature parts of the cycle, and oxidised to CO_2 at a rate slower than the formation rate. Heywood [51] stated that carbon monoxide concentration stays close to the equilibrium value during the combustion and the beginning of expansion, but that it becomes kinetically controlled in the last parts of the expansion, where the gas temperatures are lower. Heywood showed that the CO concentration remains in approximate equilibrium until around 60 degrees ATDC, and that the CO effectively freezes as the exhaust gas exits the cylinder and the oxidation stops due to low temperature. The faster power stroke expansion in the free-piston engine may therefore influence the level of carbon monoxide emissions.

Ramos [85] described the main oxidation reactions for CO:

$$\mathrm{CO} + \mathrm{OH} \underset{k_4^-}{\overset{k_4^+}{\rightleftharpoons}} \mathrm{CO_2} + \mathrm{H}$$

$$\mathrm{CO_2} + \mathrm{O} \underset{k_5^-}{\overset{k_5^+}{\rightleftharpoons}} \mathrm{CO} + \mathrm{O_2}$$

If the other species are assumed to be in chemical equilibrium, the formation of CO can be expressed as

$$\frac{\mathrm{d[CO]}}{\mathrm{d}t} = C - D[\mathrm{CO}] \tag{5.1}$$

where

$$C = R_1 + R_2$$

$$D = \frac{R_1 + R_2}{[\mathrm{CO}]_e}$$

where the subscript e denotes equilibrium concentration, and

$$R_1 = k_4^+[\mathrm{CO}]_e[\mathrm{OH}]_e = k_4^-[\mathrm{CO_2}]_e[\mathrm{H}]_e$$
$$R_2 = k_5^+[\mathrm{CO_2}]_e[\mathrm{O}]_e = k_5^-[\mathrm{CO}]_e[\mathrm{O_2}]_e,$$

and the rate constants are [12]

k_4^+	$6.76 \times 10^{10} \exp\left(\frac{T}{1102}\right)$
k_5^-	$2.5 \times 10^{12} \exp\left(\frac{-24055}{T}\right)$

Chemical equilibrium calculations In order to predict NO_x and CO formation, the concentrations of a number of other species must be estimated. These are commonly assumed to be in chemical equilibrium, and their concentrations can be found using a set of reaction equations with appropriate equilibrium constants. For the 8 remaining species, consisting of 4 chemical elements, 4 independent chemical reactions can be written. The following reactions were chosen [38]:

$$\frac{1}{2}\mathrm{H_2} \rightleftharpoons \mathrm{H}$$
$$\frac{1}{2}\mathrm{O_2} \rightleftharpoons \mathrm{O}$$
$$\frac{1}{2}\mathrm{H_2} + \frac{1}{2}\mathrm{O_2} \rightleftharpoons \mathrm{OH}$$
$$\mathrm{H_2} + \frac{1}{2}\mathrm{O_2} \rightleftharpoons \mathrm{H_2O}$$

Together with the four element balance equations this gives eight equations with eight unknowns. This set of equations was solved using Newton-Raphson iteration. The chemical composition was solved for each cell in the domain, giving a significant penalty in computational time. For this investigation, the simplified mesh and the limited number of simulations required made this approach acceptable.

Engine emissions simulation results

Figure 5.7 shows the predicted concentration of NO_x and CO emissions in the cylinder gases at the time of exhaust port opening. As above, the engine simulations were run at MBT ignition timing, with no exhaust gas recirculation and at stoichiometric conditions, giving somewhat high NO_x emissions levels. Similarly, the predicted CO emissions were lower that what one would expect

from an actual engine due to the assumption of a perfectly homogeneous mixture and stoichiometric conditions. It can be seen from the figure that noticeable differences between free-piston and conventional engines could be found neither in the NO_x nor in the CO emission levels.

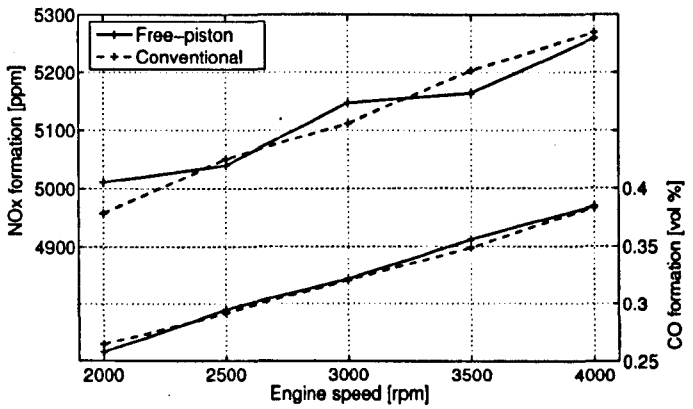

Figure 5.7: Predicted engine emissions from the free-piston and conventional engines.

Baruah [13] reported that a significant reduction in NO_x emissions could be obtained in the free-piston engine due to the fact that the ignition timing could be retarded with low penalties in engine efficiency. It was shown above that the MBT ignition timing is advanced in the free-piston engine compared to the conventional engine, and it was found that the free-piston engine has no advantages in terms of emissions compared to conventional engines at MBT spark timing. Simulations were run to investigate the sensitivity of the free-piston engine to changes in the spark timing compared to that of a conventional engine, and the effects of spark timing on engine emissions.

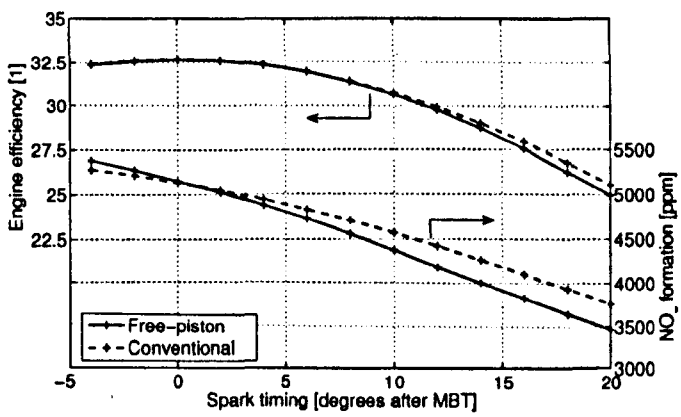

Figure 5.8: Engine sensitivity to changes in spark timing and effects on NO_x emissions formation.

Figure 5.8 shows the effects of advancing or retarding spark ignition timing for both engine types. It can be seen that the efficiency penalty of retarding spark timing is similar for the two

engines, but that the free-piston engine benefits slightly more from this in terms of NO_x emissions than the conventional engine.

5.2.7 Summary

The performance of a spark ignited free-piston engine was simulated and directly compared to that simulated for a conventional engine of identical design. The aim of the work was to investigate potential advantages of the free-piston engine and identify effects of the particular piston motion profile of such engines. The simulations showed only minor differences in engine performance, and no thermodynamic advantages were identified. It was found that the free-piston engine suffers more from reductions in flame speed, such as that occurring at part load operation. The variable compression ratio in the free-piston engine could only partly compensate for this, due to the fuel knock limit. For faster-burning fuels, the free-piston engine showed a slight performance advantage over the conventional engine.

Carbon monoxide and nitrogen oxide emissions were investigated but only minor differences were found between free-piston and conventional engines. The free-piston engine was found to benefit slightly more from retarded spark timing with regards to nitrogen oxide emissions, but the advantages over conventional engines suggested by other authors could not be identified.

The variable compression ratio in the free-piston engine provides extensive operation optimisation possibilities if operating on varying fuels. The multi-fuel possibilities are, in addition to the reduced frictional losses from the simple free-piston design, considered the main advantages of this concept. The feasibility of a pre-mixed, two stroke free-piston engine was also questioned due to the potential challenges in achieving efficient scavenging in a such an engine.

5.3 Free-piston diesel engine performance

The mid-20th century free-piston engines were without exception diesel engines, and the engine investigated in this work, described in Chapter 3, was a diesel engine aimed for large-scale applications. Diesel engines differ from spark ignited engines in several respects, one of the most important being the influence of gas motion within the cylinder on the combustion process. The operating characteristics of the free-piston engine may influence this, and other authors have reported experimental results suggesting differences in the in-cylinder processes between free-piston and conventional engines. Notably, enhanced in-cylinder gas motion in the free-piston engine has been suggested, giving advantages of improved fuel-air mixing, faster combustion, and reduced emissions formation. A detailed investigation into the differences between free-piston and conventional diesel engines is therefore of interest.

5.3.1 Free-piston engine combustion

Although discussed briefly by some free-piston engine developers, very few studies investigating the details of the combustion process in free-piston diesel engines have been reported. Some reports suggesting differences in the combustion process and performance between free-piston engines and conventional engines exist, however they are mainly based on experimental from free-piston engines (or prototypes of such engines), and do not present a direct comparison to conventional engines.

The differences in the piston motion profile between the free-piston engine and conventional engines have been documented by a number of authors, and the free-piston engine is known to have higher piston acceleration around TDC and a faster power stroke expansion. This may, as discussed in Section 2.1.3.7, influence the in-cylinder gas motion and the combustion process and, consequently, the performance of the engine.

5.3.1.1 The combustion process in free-piston diesel engines

Somhorst and Achten [90] investigated the combustion process in a hydraulic free-piston engine and reported differences when comparing the results to those of a conventional engine. The authors stated that most of the fuel in the free-piston engine burns in the pre-mixed phase, resulting in a very high rate of heat release with pressure gradients of two to five times those of a comparable conventional engine. It was suggested that this is due to the high piston velocities around TDC, increasing in-cylinder gas motion and turbulence levels [2, 90]. Tikkanen et al. [96] reported the same behaviour in a dual piston free-piston engine and stated that combustion takes place predominantly in a single, pre-mixed phase.

Free-piston engine combustion was also studied in the mid-20th century free-piston engines and differences when compared to conventional engines are reported by a number of authors. Discussing the free-piston engine multi-fuel possibilities, Flynn [61] described the successful operation of a free-piston engine on a range of fuels including gasoline, diesel fuel, crude oil and even vegetable and animal oils, and stated that "It seems that these engines do not care whether they get fuel with octane or cetane numbers". Fleming and Bayer [39] reported abnormal combustion leading to mechanical problems in the free-piston engine, and stated that thermodynamic models had to be modified to fit free-piston engine data due to long ignition delays and high heat release rates. The authors described how the performance was improved with changes made to the injection system. Fleming and Bayer further compared the operational sensitivity of the free-piston engine and a conventional engine to external parameters, and stated that when recreating the conditions under which the free-piston engine was successfully operated in a conventional engine, this engine would not run.

5.3.1.2 HCCI mode operation

The operational flexibility of the free-piston engine, with its variable compression ratio and lower requirements for accurate ignition timing control, suggest that this concept is well suited for alternative fuels and homogeneous charge compression ignition (HCCI) operation. A particular feature of the free-piston engine is that the combustion work contributes to the work required to slow down the piston around TDC and accelerate it downwards. Hence, a delay in the pressure rise from combustion (late ignition) will delay the speed reversal at TDC and give an increased compression ratio, whereas an early pressure rise will reduce the maximum compression ratio. Due to these self-regulatory characteristics, the free-piston engine will be less sensitive to variations in ignition timing, which is the main challenge associated with the use of HCCI in conventional engines.

The successful operation of a free-piston diesel engine in direct injection HCCI mode was described by Hibi and Ito [52]. Theoretical and computational investigations into the concept were presented by among other Kleemann et al. [64], Fredriksson [40] and Golovitchev et al. [45]. As this investigation is concerned only with conventional diesel operation, the reader is referred to the reports mentioned above for further information on HCCI free-piston engines.

5.3.2 Simulation setup

An engine with the same design and identical design variables as that investigated in Section 4.3 was chosen and a CFD simulation case was set up using OpenFOAM. A standard bowl-in-piston configuration was assumed and a computational mesh, shown in Figure 5.9a, was created. The design had a bowl diameter to bore ratio of 0.60 and a minimum clearance between the piston and cylinder head of 2 mm (equal to 1.33 % of the stroke length). The piston and cylinder were designed to be symmetric around the cylinder axis, allowing a wedge geometry with cyclic boundary conditions to be used. An eight-hole injector was assumed, and the mesh represented a sector of 45 degrees (1/8 of the cylinder) and consists of 60,000 cells, equivalent to 480,000 cells for the full cylinder.

In addition, a low-squish configuration of similar design but with a bowl diameter to bore ratio of 0.75, shown in Figure 5.9b, was defined to investigate the influence of the piston and cylinder design on the free-piston engine performance.

Turbulence was modelled with a standard k-ϵ model and swirl was introduced at the start of compression with a swirl/rpm ratio of 3.0. As the engine operates on a two-stroke cycle, the simulations were run from the point of inlet ports closure (approximately 130 degrees before top dead centre).

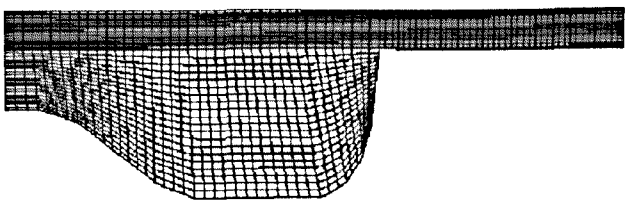

(a) Basic bowl-in-piston configuration.

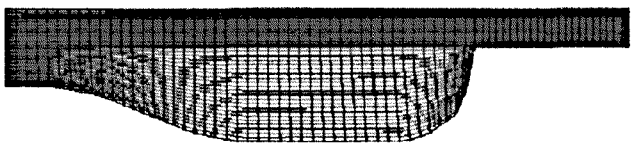

(b) Low squish bowl-in-piston configuration.

Figure 5.9: Computational meshes describing the investigated piston geometries.

5.3.2.1 Model validation

A grid sensitivity analysis was performed to ensure the accuracy of the predictions and the independence of the solution from the mesh density. The validity of the simulation model was further investigated by modelling a Volvo TAD1260 diesel engine and comparing the predictions to experimental data from this engine. The Volvo engine has main design parameters similar to those of the free-piston engine investigated here, and the simulation results showed good agreement with the experimental data.

5.3.3 Simulation results

A number of simulations were run with the aim of identifying potential differences in the in-cylinder processes between free-piston and conventional engines. Cold-flow simulations (full engine cycles without fuel injection) were performed to investigate the influence of the piston motion profile on the in-cylinder gas motion. Fuel injection was subsequently introduced to investigate differences in the combustion process.

5.3.3.1 In-cylinder gas motion

In-cylinder gas motion has a high influence on engine performance in both spark ignition and compression ignition engines. The in-cylinder flow during combustion directly affects the fuel-air mixing, the combustion process and the heat transfer between the gases and cylinder walls, which all influence engine efficiency and emissions formation. In diesel engines, high in-cylinder gas velocities are generally desireable because the performance advantages due to increased fuel-air mixing and faster combustion usually outweigh the additional in-cylinder heat transfer losses and pumping losses in the intake system. The intake system (valves and/or ports), piston crown and

cylinder head in modern engines are therefore carefully designed to optimise engine performance.

In-cylinder gas motion is typically divided into swirl effects and squish effects. Swirl is the rotational motion of the in-cylinder gases around the cylinder axis, and is a result of the intake system giving the gases an angular momentum as they enter the cylinder. In diesel engines the effects of swirl are commonly enhanced by using a bowl-in-piston design which forces the gases in towards the centre of the cylinder axis as the piston approaches TDC. The angular momentum of the gases is preserved, resulting in an increase in gas velocity.

Squish is the radial (inwards) motion of the gas as it is forced into the cylinder bowl when the piston approaches TDC and the clearance to the cylinder head decreases. For engines with a wide squish band (i.e. a low bowl diameter to cylinder bore ratio) and small clearance between the piston and cylinder head, the squish effects can be significant. These effects depend heavily on the piston velocity.

A detailed discussion on in-cylinder gas motion and its effects on engine performance was presented by Heywood [51]. Numerous studies of the fluid flow in internal combustion engines using CFD techniques have been presented. A comprehensive overview was presented by Arcoumanis and Whitelaw [8].

Gas motion in the free-piston engine It has been suggested that the reported differences in the combustion process between free-piston and conventional engines are related to the in-cylinder gas motion. Such differences are likely to be found mainly in the squish effects, since swirl levels are decided predominantly by the initial swirl generated by the intake system. The swirl momentum losses during the compression stroke will not be largely influenced by the piston motion profile differences between the free-piston and conventional engines.

The squish effects occur at the last stages of the compression stroke, where the clearance between the piston and cylinder head decreases rapidly, and depend heavily on the instantaneous piston speed.

Figure 5.10 shows the predicted piston speed for the free-piston engine and a conventional engine plotted against piston position. It can be seen that the piston speed in the conventional engine is higher than that of the free-piston engine for most of the compression stroke but that the free-piston engine piston speed is slightly higher very close to TDC. Differences in the squish effects between the two engines may therefore be expected.

As the piston is reversed at TDC and accelerates downwards, a low-pressure region above the squish band is created and gas from the piston bowl flows back towards the cylinder liner region. This reverse squish is critical for the last stages of combustion when the swirl levels have decayed [8]. The faster power stroke expansion in the free-piston engine may enhance this effect, and this may benefit the combustion process in the free-piston engine.

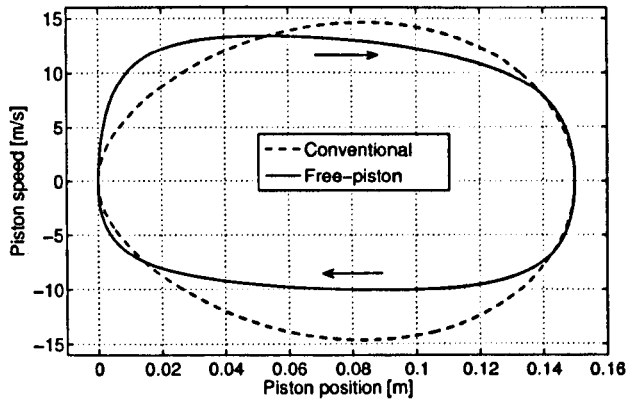

Figure 5.10: Predicted piston speed for the free-piston engine and a comparable conventional engine.

In-cylinder flow simulations A series of simulations were run over a range of engine speeds and for varying initial swirl levels with the two computational meshes. It was found that the differences between the two engine designs were present for all investigated cases, and that the relative differences in gas motion were not largely influenced by these variables.

Figure 5.11 shows the predicted in-cylinder gas motion in the upper half of the cycle (i.e. around TDC) for the free-piston engine and a conventional engine with the same piston and cylinder design. Figure 5.11a shows the average in-cylinder gas velocity in the two engines. The two main contributors to the gas motion are the swirl and the displacement of gas as the piston moves. At the start of compression the average gas velocities in the two engines are equal, however since the piston velocity in the compression stroke is higher in the conventional engine the average gas velocities are higher. It can further be seen how the swirl decays rapidly around TDC. After TDC the higher piston velocity in the free-piston engine leads to slightly higher average gas velocities. Overall, however, only minor differences are found.

Figure 5.11b shows the average radial (inwards) velocity of the in-cylinder gases, or squish. At the start of compression this value is equal to zero but as the cylinder volume and shape change, gas flows in the radial direction, into or out of the piston bowl. Slightly higher squish effects can be seen in the free-piston engine during the late stages of compression, with the average radial velocity being around 15 % higher than that in the conventional engine. The reverse squish, occurring early in the expansion stroke, can be seen to be markedly higher in the free-piston engine, with the peak average radial velocity being around 30 % higher than that in the conventional engine. It was found that in order to achieve a level of squish and reverse squish equal to that of the free-piston engine operating at 1500 rpm (25 Hz), the speed of the conventional engine had to be increased to around 1900 rpm.

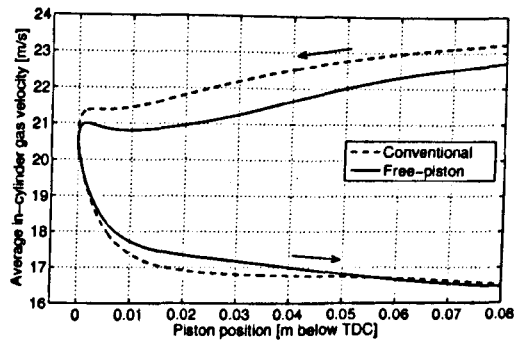

(a) Average in-cylinder gas velocity.

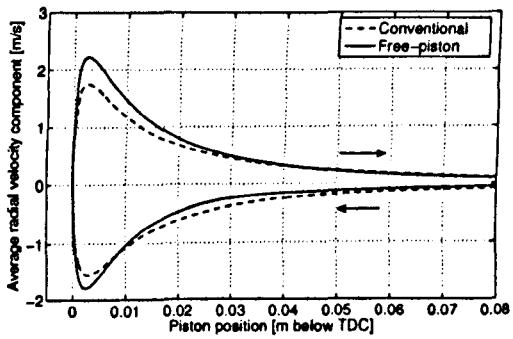

(b) Average radial velocity of the in-cylinder gases (squish).

Figure 5.11: Predicted in-cylinder gas motion.

Figure 5.12 shows the similar plots for the low-squish combustion chamber. The same trends as above can be seen, and it is clear that the differences between the free-piston engine and the conventional engine is not largely influenced by the piston design.

5.3.3.2 The combustion process

Having investigated in-cylinder gas motion, fuel injection was introduced in order to investigate effects of the piston motion profile on the combustion process in the free-piston engine. The combustion process depends on a number of factors, one of the most important being the fuel injector properties. A standard common rail injection system was assumed and appropriate specifications such as injection pressure, nozzle diameter and fuel mass flow profile were chosen. An injection duration of 25 crank angle degrees was assumed, and the fuel used was n-heptane, C_7H_{16}. Combustion was modelled with the Chalmers PaSR model [78] and the chemistry model consisted of 15 species and 39 reactions. The full chemical mechanism used is shown in Listing A.1 in Appendix A. For details of the modelling of sub-processes such as the fuel spray and chemical kinetics in OpenFOAM, the reader is referred to [57] and [68].

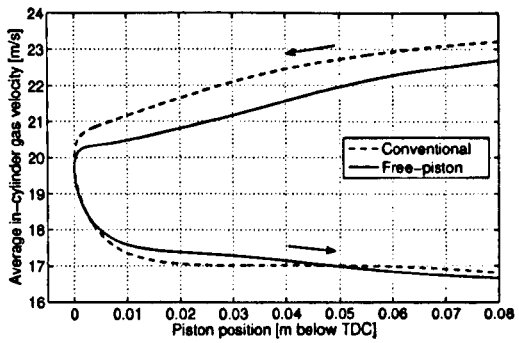

(a) Average in-cylinder gas velocity.

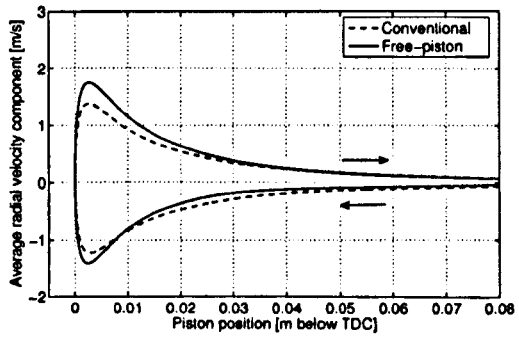

(b) Average radial velocity of the in-cylinder gases (squish).

Figure 5.12: Predicted in-cylinder gas motion for low-squish piston.

Fuel injection timing In order to evaluate the performance of the engines under comparable operating conditions, the fuel injection timing must be set individually for the crankshaft and free-piston engines. Previous work has indicated that in spark ignition free-piston engines, the spark timing has to be significantly advanced compared to the conventional engine due to the faster power stroke expansion. Zero-dimensional modelling of the current engine indicated that the fuel injection timing in the free-piston diesel engine should be slightly advanced when compared to that of a similar conventional engine [75].

Simulations were run to investigate the influence of fuel injection timing and identify the optimum fuel injection timing for both engines, where optimum timing refers to the start-of-injection timing giving the highest indicated efficiency, i.e. maximum net work produced by the cycle. (This is also known as maximum brake torque, MBT, timing.) It was found that the optimum timing differs only very little between the free-piston and the conventional engines, with the free-piston engine requiring a slightly more advanced injection timing. The injection timing found for optimum efficiency were -21 and -19 crank angle degrees ATDC for the free-piston and conventional engines respectively.

In a real engine, the injection timing is likely to be retarded slightly compared to this value in order to reduce exhaust gas emissions formation and avoid excessive in-cylinder gas pressures.

This is acceptable because retarding the injection timing can reduce the peak in-cylinder gas temperatures significantly, with only minor penalties in fuel economy. In the free-piston engine the effects of retarding fuel injection may, however, be different than in the conventional engine due to the faster power stroke expansion.

Figure 5.13 shows the predicted effects of variations in the fuel injection timing on engine performance. It can be seen that the free-piston engine is slightly more sensitive to changes in injection timing.

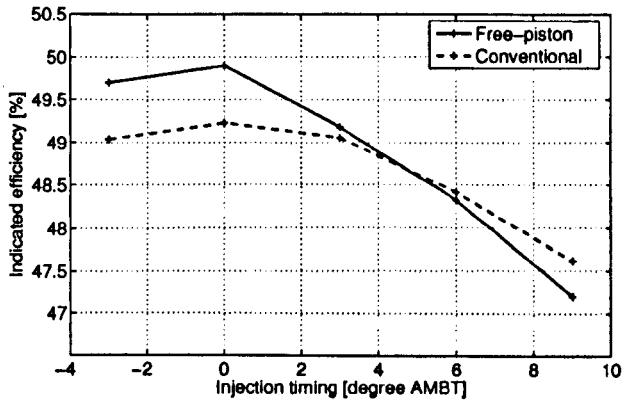

Figure 5.13: Effects of variations in fuel injection timing (relative to MBT timing) on engine performance.

The figure also shows that a slight efficiency advantage was predicted for the free-piston engine compared to the conventional engine. This is consistent with earlier findings [75], and is due mainly to the free-piston engine spending less time in the high-temperature parts of the cycle which reduces in-cylinder heat transfer losses. It shows that the reduced heat transfer losses outweigh the disadvantages associated with increased volume change during combustion in the free-piston engine.

Combustion progress Figure 5.14 shows the predicted in-cylinder gas pressure and the heat release rate for the free-piston and conventional engines with the optimum injection timing. It can be seen that ignition takes place later in the free-piston engine despite the earlier injection, which is due to a longer ignition delay. This results in a higher initial burn rate, since the amount of fuel that burns in the pre-mixed phase depends on the ignition delay.

The reason for the longer ignition delay is the piston motion profile of the free-piston engine, with a higher piston speed and a more rapid compression close to TDC, which lead to a lower compression ratio at the start of injection. It was found that the state of the air within the cylinder at the start of fuel injection was around 35 bar and 820 K for the free-piston engine and 42 bar and

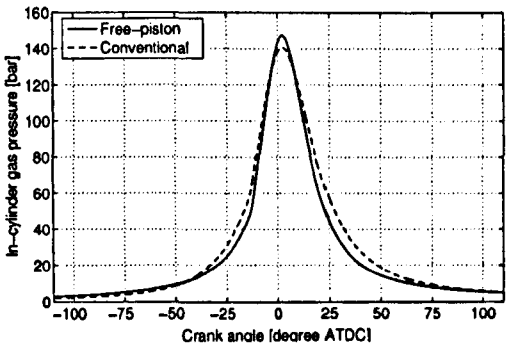

(a) In-cylinder gas pressure.

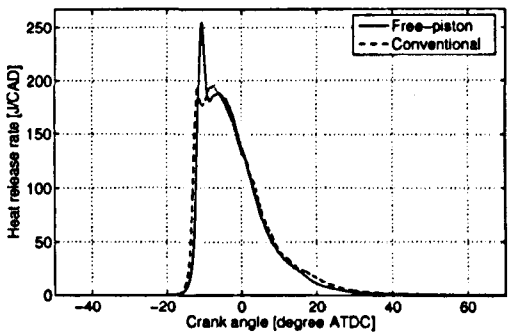

(b) Heat release rate.

Figure 5.14: Predicted in-cylinder gas pressure and heat release rate at MBT injection timing.

855 K for the conventional one.

The trend of an increased heat release rate in the pre-mixed phase is consistent with the experimental findings of Achten et al. [2], Tikkanen et al. [96] and Fleming and Bayer [39], discussed previously. It should be noted that, as the simulated engine was turbocharged, the ignition delay and the fraction of fuel burnt in the pre-mixed phase was lower than what would be expected in a naturally aspirated engine. Hence, for a non-turbocharged engine one would expect these effects to be more dominant.

With the exception of the longer ignition delay, no significant differences in the combustion process were found. The enhanced squish and reverse squish were not found to have any noticeable influence on the progress of the combustion process, and the fuel burn rate in the late stages of combustion can be seen to be similar for the two engines.

Figure 5.15 shows the pressure plot and heat release rate for the engines with the fuel injection timing retarded by 6 crank angle degrees compared to the optimum one. In this case the compression ratio at the start of injection is similar for the two engines, leading to comparable ignition delays, and Figure 5.15b shows that no noticeable differences can be found in the combustion progress.

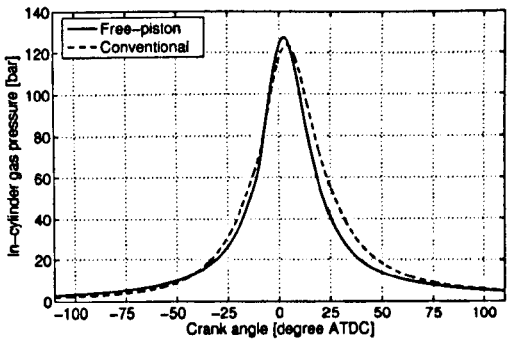

(a) In-cylinder gas pressure.

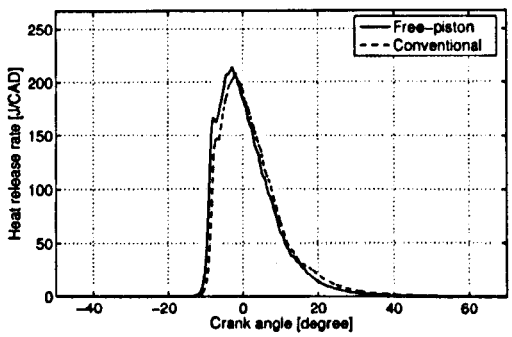

(b) Heat release rate.

Figure 5.15: Predicted in-cylinder gas pressure and heat release rate for retarded injection timing.

5.3.3.3 Predicted engine exhaust gas emissions

The main exhaust gas emissions of concern from an environmental and health perspective produced by diesel engines are nitrogen oxides and particulates, of which nitrogen oxides, NO_x, are usually regarded the most critical in large scale engines. Both particulates and NO_x are formed mainly during the diffusion combustion phase, and their formation depends heavily on the local temperature and concentration of fuel and oxygen in the reaction zone.

The formation of these emissions may be influenced by the operating characteristics of the free-piston engine in two ways. Firstly, the differences in in-cylinder gas motion may influence the fuel-air mixing and temperature distribution within the cylinder. Secondly, the faster power stroke expansion reduces the time available for emissions formation.

A more comprehensive study with a more detailed chemistry model is required to fully investigate the details of emissions formation in the free-piston engine, such as the trade-off between particulates, NO_x emissions and engine efficiency. However, the current simulated chemical mechanism includes the main formation equations for NO_x (the extended Zeldovich mechanism), and some indications of potential differences in the formation of nitrogen oxides between free-piston engines and conventional engines could therefore be obtained with the current simulation setup.

Figure 5.16 shows the predicted concentration of nitrogen oxide, NO within the cylinder for

the free-piston and conventional engines. A significant emissions reduction potential can be seen for the free-piston engine. The free-piston engine also appears to benefit more from the retarded injection timing, however it should be noted that the efficiency penalty is higher for this engine, as shown in Figure 5.13.

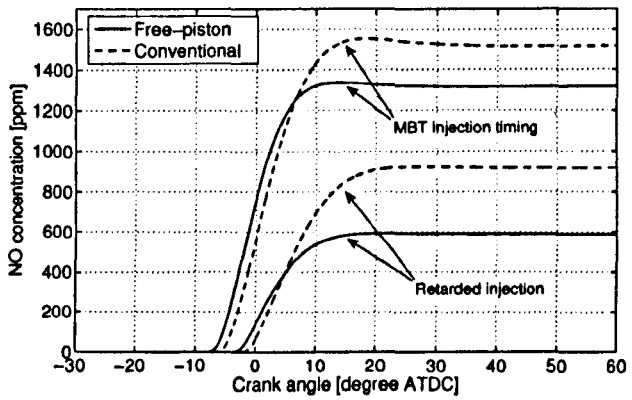

Figure 5.16: Predicted average in-cylinder NO concentration.

A number of factors influence the NO formation, including the fuel injection timing, the in-cylinder gas motion, and the temperature and pressure reduction from the expansion. A more detailed investigation is therefore required to identify details of the emissions formation in free-piston engines and potential advantages over conventional engines. The formation of other exhaust gas emissions, most importantly particulates, should also be investigated. The results presented here suggest that a more detailed study will be worthwhile.

5.3.4 Summary

The in-cylinder gas motion, combustion process and nitrogen oxides formation in a free-piston diesel engine was investigated. The results were compared to those predicted for a similar conventional engine in order to identify potential differences in engine performance.

The piston motion profile in the free-piston engine was found to influence in-cylinder gas motion to some degree, with potential advantages of enhanced squish and reverse squish effects. The combustion process was not found to be largely influenced by this, however increased ignition delays were found in the free-piston engine due to a lower compression ratio at the start of fuel injection. A slight fuel efficiency advantage was found for the free-piston engine, which is consistent with the findings in Chapter 4.

The nitrogen oxides formation in free-piston and conventional engines was briefly investigated, and potential advantages for the free-piston engine were found. It was stated that a more detailed investigation is required to identify details of the emissions formation in such engines. Other topics

that should be further investigated include the effects of the variable compression ratio and the potential for operation optimisation, along with the use of alternative or low-quality fuels.

5.4 Coupled dynamic–multidimensional simulation

Engine CFD codes may be useful in the study of innovative engine design, for example identifying the detailed influence of the particular piston motion profile in free-piston engines, as presented previously in Sections 5.2 and 5.3. The mesh motion algorithms implemented in such CFD codes are, however, usually time-dependent only, determining the piston motion from an analytic expression. In the case of free-piston engines, the motion of the piston is influenced by a number of operational variables and the investigations presented previously assumed that, for example, a change in ignition timing was followed by adjustments in other operational variables to maintain factors such as engine speed and compression ratio constant. For a fully parametric study of single operating variables, such as injection timing or the effect of cycle-to-cycle variations in the combustion process, solution-dependent mesh motion is required.

Existing work on CFD modelling of free-piston engines, including that presented previously, commonly employs a piston motion profile obtained from a dynamic engine model, which is expressed mathematically as a function of time and implemented in the CFD code. Examples of such work include the reports of Bergman et al. [15], Fredriksson [40] and Kleemann et al. [64]. While it is possible to investigate general free-piston engine performance using such an approach, fully parametric studies of single operational variables requires an iterative approach in which the CFD solution is fed back to the dynamic model to update the piston motion solution until convergence is achieved. For investigations over a wide range of engine operational variables, such a strategy is likely to be both laborious and computationally intensive.

This section presents an engine simulation model suitable for detailed investigations into free-piston engine performance by implementing a solver for the piston dynamics into the engine CFD code.

5.4.1 Modelling engine dynamics

As discussed in Chapter 4, the motion of the piston assembly in the free-piston engine is governed by the interaction of the forces acting on it, and can be described by using Newton's 2nd law. Figure 5.17 shows the free body diagram of the piston assembly in the dual piston free-piston engine generator illustrated in Figure 2.20. The main forces acting on the piston assembly are the cylinder pressure force, the force from the load device, the force from the rebound device (which is the second cylinder in dual piston engines) and frictional forces. Frictional forces are subordinate

to the other three and do not have a large influence on engine dynamics, and they were therefore ignored here. The motion of the piston assembly can be found using

$$F_{C1} - F_L - F_{C2} = m\frac{\mathrm{d}^2x}{\mathrm{d}t^2} \tag{5.2}$$

where m is the mass of the piston assembly and x is its position. The pressure force from the combustion chamber was predicted by the CFD code, and the forces that need to be represented in the model are therefore the load force and the rebound force (where, in the dual piston engine case, the rebound force will be the pressure force from the other cylinder).

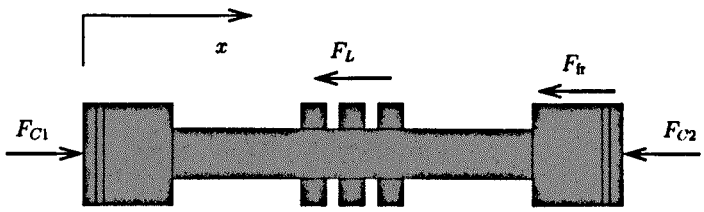

Figure 5.17: Free body diagram of free-piston engine piston assembly.

5.4.1.1 Rebound force

For single piston hydraulic free-piston engines, such as the one illustrated in Figure 2.17, the rebound force will be provided by a hydraulic cylinder. With a constant hydraulic supply pressure, the force from such a cylinder is commonly assumed to be constant over the full stroke.

For engines with a bounce chamber as a rebound device, or dual piston engines where the opposite cylinder is driving the compression, the rebound force will depend on the bounce chamber gas pressure. In such engines the rebound force will be high when the combustion cylinder is at the BDC and the bounce chamber pressure is high, and will decay as the bounce chamber pressure is reduced during the engine compression stroke. Figure 5.18 illustrates the force profiles of these two types of rebound devices. The shaded areas represent the compression energy.

Both types of rebound devices were implemented in the model. In the case of a hydraulic rebound device, the rebound force F_R was assumed to be constant over the full stroke, i.e.

$$F_R = k,$$

where k is a constant.

For a gas-filled rebound device, i.e. a bounce chamber cylinder or a second combustion cylinder, the gas in the bounce chamber can be approximated to follow a polytropic expansion, such that

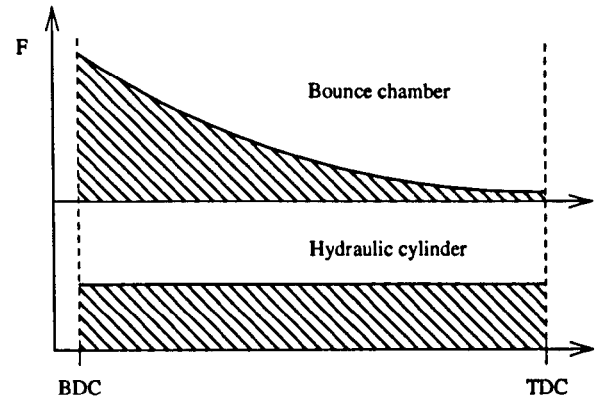

Figure 5.18: Illustration of the force profiles of free-piston engine rebound devices.

$$pV^{\gamma} = \text{constant}$$

where p is the gas pressure, V is the bounce chamber cylinder volume and γ is the ratio of specific heats. Hence, the pressure at any point can be related to the instantaneous volume of the rebound cylinder by

$$p = p_0 \left(\frac{V_0}{V}\right)^{\gamma}$$

where subscript 0 indicates some initial condition, here taken as the BDC position for the combustion cylinder.

The instantaneous rebound cylinder volume can be described in terms of the initial volume V_0, the piston area A_p and the distance x which the piston has travelled from the initial position:

$$V = V_0 + A_p x.$$

The nominal compression (and expansion) ratio R_C of the rebound cylinder can be expressed by

$$R_C = \frac{V_0 + A_p S}{V_0}$$

where S is the engine nominal stroke length, making $A_p S$ equal to the swept volume. Using this, the rebound cylinder pressure can be expressed in terms of piston position, initial rebound cylinder pressure and compression ratio:

$$p = p_0 \left(\frac{S}{S + x(R_C - 1)}\right)^{\gamma}.$$

Knowing that the rebound cylinder force is proportional to the cylinder pressure, $F_R \propto p$, this expression can be modified to express rebound force directly.

5.4.1.2 Load force

The properties of the load device, such as moving mass and load force profile, will have a high influence on the engine dynamics, and different load devices will have different dynamic properties. A hydraulic cylinder working against a constant discharge pressure can, as above, be modelled as a constant load force acting against the motion of the piston assembly. The load force profile of an electric machine will depend on details of the machine and the electric load coupled to it, however the load force in such devices is commonly assumed to be proportional to the instantaneous speed of the translator. Figure 5.19 illustrates the force profiles of these two types of load devices. The shaded areas represent the output load energy.

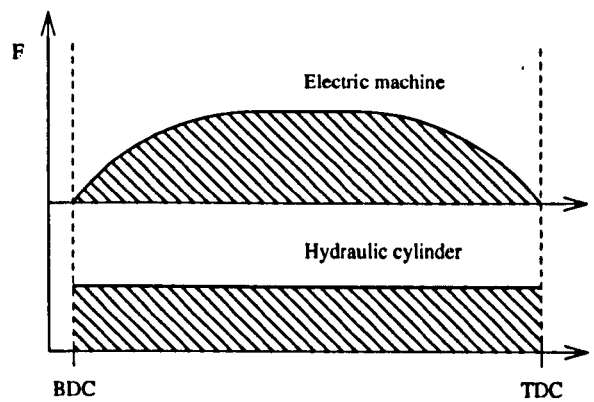

Figure 5.19: Illustration of the force profiles of free-piston engine loads.

For a hydraulic load device, the load force, F_L, is assumed to be constant, but with the direction determined by the direction of motion of the piston assembly:

$$F_L = \begin{cases} -k & \text{if } \dot{x} > 0 \\ 0 & \text{if } \dot{x} = 0 \\ k & \text{if } \dot{x} < 0 \end{cases}$$

In the case of an electric machine, the load force is assumed to be proportional to the translator velocity:

$$F_L = k\dot{x}.$$

5.4.1.3 Implementation into the CFD code

The simulations started at BDC, for which the computational mesh was defined and appropriate initial conditions, such as start-of-compression pressure, temperature and swirl level, were chosen. In the original code, the piston motion was calculated from a mathematical expression defining the position of the piston as a function of time, and the mesh was subsequently updated at each timestep. This expression was replaced by the solving of Equation 5.2 numerically. The piston acceleration was given by

$$\ddot{x} = (pA_p - F_{C2} - F_L)/m \tag{5.3}$$

where F_{C2} is the rebound force, F_L is the load force, p is gas pressure in the combustion cylinder and A_p is the combustion cylinder piston area. The expressions for F_{C2} and F_L are functions of x and $\dot{x}$, depending on the choice of rebound and load devices, as discussed above. This equation was integrated at each timestep to give piston speed and position.

Standard forward Euler integration was found to be sufficiently accurate, due to the solving of the equations for fluid flow and combustion requiring significantly shorter timesteps than those needed for an accurate solution of Equation 5.3.

The dynamic model requires the user to specify

- the mass of the piston assembly;
- the type of rebound device, along with the appropriate constants;
- the type of load device, along with the appropriate constants.

In addition to this information the user is required to input CFD simulation specific data.

5.4.2 Simulation results

The free-piston engine is, as discussed previously, effectively restricted to the two-stroke operating principle and such engines are therefore best suited for direct injection operation. The coupled dynamic-multidimensional simulation model will, however, be demonstrated using a pre-mixed, spark ignition engine solver, due to its significantly lower computational costs, allowing simulation over a wider range of operating conditions to fully investigate the capabilities of the coupled solver.

The results presented below are those predicted for a free-piston engine generator, similar to that shown in Figure 2.20. Simulations were also run for a hydraulic free-piston engine and the same trends as those presented below were found, albeit with minor differences in the piston motion profile due to differences in piston assembly mass (a hydraulic free-piston engine will have a lower moving mass than a free-piston engine generator) and the dynamic characteristics of the load and rebound devices.

5.4.2.1 Case setup

A mesh describing a simplified piston and cylinder configuration, similar to that used in Section 5.2, was generated. The cylinder geometry was assumed to be symmetric around the cylinder axis, allowing a wedge geometry with cyclic boundary conditions to be used. The mesh described a 30-degree sector and consisted of 15,400 cells, equivalent to more than 180,000 cells for the full cylinder. The shape of the computational mesh is the same as that shown in Figure 5.2.

The engine chosen had a bore of 81 mm and a stroke of 81 mm, and a nominal compression ratio of 8:1. The fuel used was iso-octane at a fuel-air equivalence ratio of 1. Turbulence was modelled with a standard k–ϵ model with wall functions, and constant wall temperatures were used. As the engine was two-stroke, the in-cylinder pressure when the intake ports were open was assumed equal to the intake pressure (taken as atmospheric pressure).

5.4.2.2 Influence of compression energy

The compression energy can be varied during operation in most free-piston engine designs. In hydraulic free-piston engines the hydraulic supply pressure may be variable, and in free-piston engines using a gas-filled bounce chamber, a high-pressure gas supply may allow control of the amount of gas in the bounce chamber. In dual piston engines the compression energy will depend on the combustion energy from the opposite cylinder.

Figure 5.20 shows the influence of the compression energy on engine operation with the spark timing and all other variables kept constant. Figure 5.20a shows the effects of variations in the compression energy on the piston motion profile. It can be seen that the compression energy influences both the TDC position (i.e. the compression ratio), as one would expect, and also the cycle time. A 10 % change in the compression energy gives approximately a 1 Hz change in operating frequency. Although not a major change, this effect is of high importance if the frequency of the engine is to be controlled, for example to control the electric output or engine vibrations.

Figure 5.20b shows the influence of the compression energy on the compression ratio of the engine. It can be seen that, provided that the compression energy can be accurately controlled, effective compression ratio control can be achieved in free-piston engines.

5.4.2.3 Influence of ignition timing

One of the most important operational variables is the spark timing, and this variable is commonly electronically controlled in modern combustion engines to optimise engine fuel efficiency and minimise emissions formation. In the free-piston engine, it is expected that the spark timing has influence on the piston motion as it controls the release of the combustion energy, which contributes to the downwards acceleration of the piston around TDC.

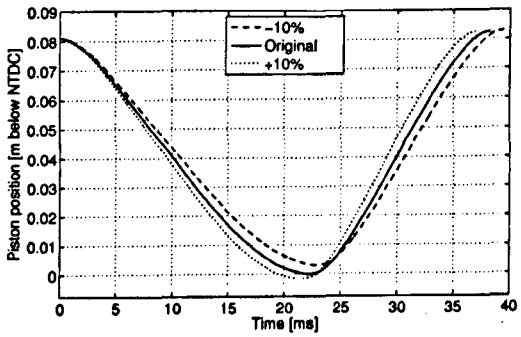

(a) Effect on piston motion. (Piston position shown as distance below nominal TDC (NTDC).)

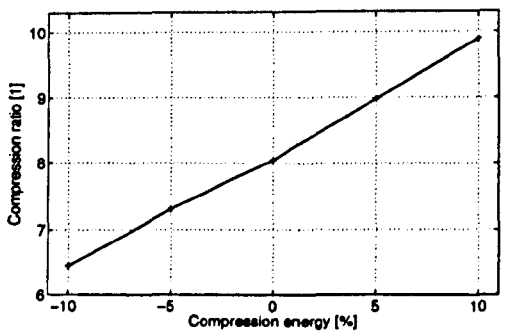

(b) Effect on engine compression ratio.

Figure 5.20: Effects of variations in engine compression energy.

Figure 5.21 shows the influence of the spark timing on engine operation. Figure 5.21a shows the piston motion profiles for variations in spark timing, with the spark timing varied with the equivalent of 20 crank angle degrees (CAD). A clear influence on the piston motion can be seen. The effect of the variation in the spark timing on engine compression ratio is shown in Figure 5.21b. The effect of advanced spark timing is a rapid decrease in compression ratio, as the high pressure from combustion slows down and returns the piston before it reaches the nominal TDC. Retarding the spark timing allows the piston to reach its nominal TDC, but increases the cycle time since the acceleration around TDC is reduced.

5.4.2.4 Engine operation optimisation

Having a model which allows simulations to be run for a range of engine operating conditions, operation optimisation possibilities can be investigated. Such analyses are commonly used to determine the optimum operating point for conventional engines, where variables such as ignition timing and engine speed can be varied for a given engine load in order to optimise engine efficiency and/or emissions formation. In the free-piston engine, the main operating variables available for operation optimisation purposes are the ignition timing and the compression energy.

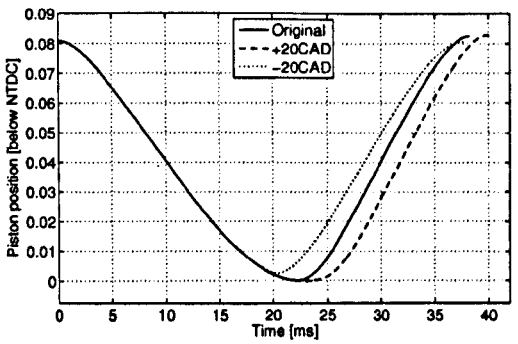

(a) Effect on piston motion. (Piston position shown as distance below nominal TDC (NTDC).)

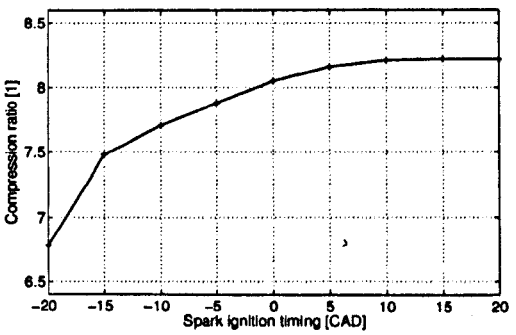

(b) Effect on compression ratio.

Figure 5.21: Effects of variations in spark timing.

Figure 5.22 shows the predicted engine indicated efficiency for variations in ignition timing and compression energy. It can be seen that an optimum ignition timing can be found for a given compression energy, and that increased compression ratio improves the efficiency, which is the expected result.

With variable compression ratio, the peak in-cylinder pressure will be of high importance in the free-piston engine. Although the compression ratio in the spark ignited free-piston engine is likely to be limited by the fuel knock limit, in free-piston diesel engines the peak in-cylinder gas pressure is likely to be the limiting factor.

Figure 5.23 shows the peak in-cylinder gas pressure for varying ignition timing and compression energy. It can be seen that increased compression energy leads to higher peak pressures, however for retarded ignition timing this effect is reduced. For highly advanced ignition timing, it can be seen that the peak pressure is reduced due to the early pressure rise reducing the maximum compression ratio.

The plots shown in Figures 5.22 and 5.23 were examples of operating maps that can give insight into the performance of the free-piston engine and its operation optimisation possibilities. Similar performance maps can be produced for engine emissions formation or other engine operational variables of interest.

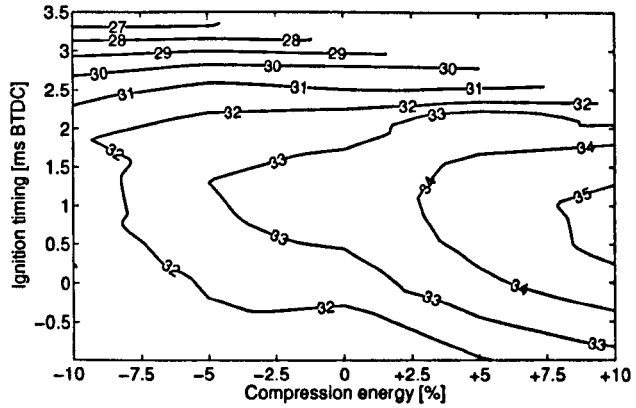

Figure 5.22: Engine indicated efficiency (per cent) map for varying compression energy and ignition timing.

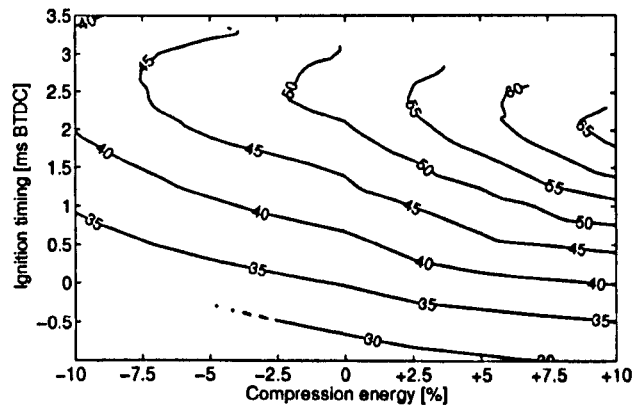

Figure 5.23: Peak in-cylinder pressure (bar) for varying compression energy and ignition timing.

5.4.3 Summary

A coupled dynamic-multidimensional simulation model for the simulation of free-piston engines was described. The model is based on the OpenFOAM CFD code, but incorporates solution-dependent mesh motion in order to model the influence of engine operational variables on the piston motion. The use of the coupled solver was demonstrated with the simulation of a spark ignited free-piston engine, and predictions of the influence of some operational variables on engine performance were presented.

The coupled solver provides a powerful tool to investigate the operating characteristics and performance of free-piston engines. In the case of free-piston diesel engines, the effects of changes in TDC position and compression ratio are expected to be higher than in spark ignited engines, due to the higher influence of the in-cylinder gas motion on the combustion process. With changes in

TDC position, the clearance distance ('squish band') between the piston and cylinder head changes, influencing squish and reverse squish in the combustion chamber. With the coupled dynamic-multidimensional solver, detailed investigations into the effects of such changes on the combustion process and engine performance can be undertaken.

Chapter 6

Engine control

The absence of the crank mechanism in the free-piston engine means that the positions of the combustion piston TDC and BDC are not fixed, but will vary according to the engine operating conditions and may be influenced by disturbances. While the variable stroke may be advantageous in terms of engine optimisation, it sets high requirements on the engine control system. It is clear that if an appropriate control system, able to keep TDC and BDC positions within the required operating range, cannot be realised, the free-piston engine concept will not be feasible.

In addition to the control of the TDC and BDC, which is critical for engine operation, comes the control of a number of other variables required for operation optimisation of the engine. These may include control of engine speed, fuel injection timing and valve timing. For the free-piston engine to be competitive against conventional technology, appropriate control of these variables must be realised.

This chapter presents an investigation into the dynamics and control of the free-piston engine, using the established simulation model to investigate the effects of the different control variables and the feasibility of proposed control strategies.

6.1 The control challenge

In conventional engines the crankshaft mechanism provides piston motion control, defining both the outer positions of the piston motion (TDC and BDC) and the piston motion profile. Due to the high inertia of the crankshaft system, the piston motion cannot be significantly influenced in the timeframe of one cycle. In the free-piston engine the piston motion is determined by the instantaneous sum of the forces acting on the piston assembly, and the piston motion may therefore be influenced by the progress of the combustion process. Moreover, the piston motion profile may be different for different operating conditions. Variations between consecutive cycles due to cycle-to-cycle variations in the in-cylinder processes are also possible.

Achieving sufficient engine control over the full load range has been a reported problem in free-

piston air compressors and gas generators, and several of these engines were constant-power units with simple on/off control [22,37,99]. Other reports have described load dumping when operating at part load [6,61]. The performance of the controlled free-piston engine over the full operating range is therefore an area of particular interest.

6.1.1 Control objectives in free-piston engines

Control of TDC and BDC positions is crucial for the operation of the free-piston engine. The TDC position must be controlled within tight limits to ensure sufficient compression, required for fuel autoignition and efficient combustion, while avoiding excessive in-cylinder gas pressures. Similarly, as the free-piston engine in practice is restricted to the two stroke operating principle, the BDC position must be controlled to ensure efficient scavenging of the cylinder. Moreover, if the piston travels far outside the nominal TDC and BDC positions, this may lead to mechanical contact between the piston and the cylinder head, which may be fatal for the engine. The clearance between the piston and cylinder head at TDC is very small in diesel engines, typically between 1 and 2 per cent of the stroke length (equivalent to 1.5–3 mm in the engine investigated here).

A secondary control objective is the speed of the engine. This may be required to provide control of the fluid flow in hydraulic engines, or the electrical frequency in free-piston engine generators.

Finally, in order to optimise engine operation and fully utilise the operational flexibility of the free-piston engine, a supervisory control system is required to control variables such as fuel injection timing, compression ratio setpoint and valve timing.

6.1.2 Control of single piston engines

The excellent controllability of single piston hydraulic free-piston engines has been demonstrated by some authors, including Achten et al. [2]. The hydraulic cylinder acts as both load and rebound device using an advanced hydraulic control system, and the compression energy can be accurately controlled. Since the piston velocity at BDC is zero and the compression stroke starts only when the hydraulic energy is released, frequency control can be applied by pausing the piston at BDC. This "Pulse Pause Modulation" control, described in more detail in Chapter 2, allows the engine to operate at optimum conditions at all load levels, giving very high part load efficiency.

6.1.3 Control of dual piston engines

Bouncing-type free-piston engines, i.e. dual piston engines or single piston engines using a bounce chamber, will have characteristics similar to those of a spring-mass system, and the control of such engines is significantly more complicated than for the hydraulic single piston engine. Since the

compression energy is delivered directly or indirectly from the combustion power stroke, the combustion energy needs to be accurately controlled in order to achieve control of the compression ratio. Cycle-to-cycle variations in the combustion process may also be present, and this may be a problem for engine controllability and influence the performance.

Speed control of such engines may represent a further challenge. Many of the old free-piston engines were reported to be effectively constant-speed machines. If the engine speed range is limited, this may be a problem, for example in hydraulic applications which require flow control. For loads where a constant speed is desired, such as electric generators, this may, however, be an advantage.

The control of a dual piston hydraulic free-piston engine was investigated by Tikkanen and Vilenius [97] using a simplified model based on energy balances. The aim of the work was to achieve compression ratio control for the engine, and it was demonstrated how acceptable performance could be achieved for moderate load changes by modifying the fuel mass flow. Cycle-to-cycle variations in dual piston free-piston engines have been reported by Tikkanen et al. [96] and Clark et al. [31], although neither reported that these were large enough to cause problems with engine operation.

Johansen et al. [59] derived a mathematical model of a single piston free-piston gas generator and investigated control issues in such an engine. Experimental results from a single cylinder test engine were reported and details of the engine control structure were outlined [60]. It was demonstrated how sufficient piston motion and engine optimisation control was obtained by controlling the fuel mass flow and the amount of air trapped in the bounce chamber.

6.2 Detailed control objectives and engine control structure

The engine under investigation was described in Chapter 3 and illustrated in Figure 3.1. Like any plant, a number of inputs and outputs to the system can be defined. At the lowest level, the main inputs to the engine include the signals to the fuel injection system, determining fuel injection timing and mass of fuel to be injected, and the signals to the bounce chamber pressure control valves, whose opening and closing timing determine the amount of gas trapped in the bounce chamber. These make up the available control variables for the engine. The main disturbance is the load force from the linear electric machine, which for the purpose of this investigation is assumed not to be controllable[1].

[1]Some level of control of the electric machine will have to be implemented in the unit to aid starting. If sufficient engine control cannot be achieved with the control variables at hand, it may be possible to apply load control on the electric machine with the implementation of appropriate power electronics, to aid engine control.

6.2.1 Engine control objectives

A piston motion control system must be established, and the main control objectives are TDC position, BDC position and engine speed. TDC position will be of the highest importance, BDC position control is slightly less stringent, whereas the speed is not critical for safe engine operation. Supervisory control objectives include the optimisation of engine operation for all load conditions.

6.2.1.1 TDC control

It is clear that variations in TDC position will have a large effect on engine operation, since such variations will influence the engine compression ratio. Potential consequences of insufficient TDC control are excessive in-cylinder gas pressures or, in the worst case, the piston hitting the cylinder head if the stroke is too long. If the stroke is too short and a sufficiently high compression ratio is not achieved, the fuel may fail to autoignite and the engine will stop.

Figure 6.1 shows the effect of variations in TDC position on the compression ratio in the current engine. It can be seen that even small variations in TDC position lead to large changes in engine compression ratio. A typical clearance between the piston and cylinder head at TDC in this engine would be 2–3 mm. (It may, however, be necessary to use a piston with a flatter profile in the free-piston engine, to give more clearance and avoid critical situations during transient operation.) Accurate control of TDC position is therefore of high importance to engine operation.

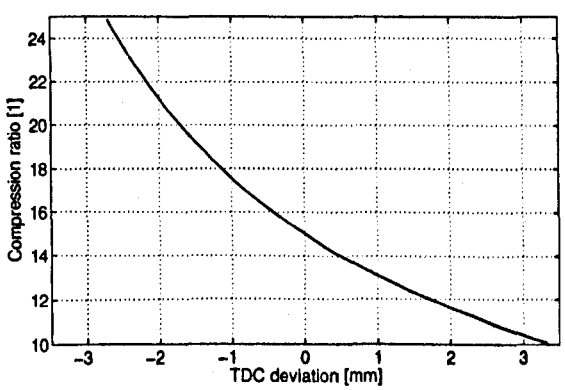

Figure 6.1: Effect of varying TDC position on engine compression ratio.

Variable TDC setpoint Unlike in conventional engines, the TDC setpoint can be varied for varying engine load. At low loads, the compression ratio can be increased without experiencing excessive peak gas pressures. This has been demonstrated by other authors, including Tikkanen and Vilenius [97], who varied nominal compression ratio from 15:1 at full load to 30:1 at lower loads.

In this work, the compression ratio setpoint was varied linearly between values of 20:1 at 10% load and 15:1 at 100% load. Figure 6.2 shows the compression ratio setpoint for different loads.

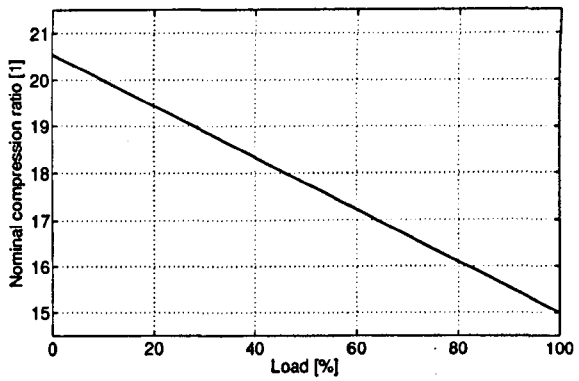

Figure 6.2: Engine compression ratio setpoint.

6.2.1.2 BDC control

At the lower end of the stroke, the BDC position will also effect the engine performance. The requirements are not as stringent as those for TDC position since the engine can be designed to allow some variation in BDC position without danger of mechanical damage. In the current engine, the nominal clearance distance between the bounce chamber piston and cylinder head at BDC was 10 mm, i.e. significantly higher than the clearance distance in the combustion cylinder.

In terms of engine performance, changing the BDC position will mainly influence the time and port area available for scavenging, and small variations in BDC position will not have a significant influence on overall engine performance. The scavenging ports height in the engine investigated in this work was 22 mm, and the critical BDC deviation, for which scavenging would completely fail, was therefore one order of magnitude higher than a typical critical deviation for TDC position.

6.2.1.3 Speed control

Speed control of the engine may be required, depending on the requirements of the load device. Unlike in hydraulic free-piston engines, where a wide speed range will be desired to allow flow control, the free-piston engine generator is likely to benefit from a close to constant operating speed. A factor of interest will therefore be if a constant speed can be achieved and maintained through the full load range for the current engine design.

Furthermore, the engine investigated here was intended to be modular, in such a way that a number of units can be operated in parallel to increase the power output. If the engine speed can

be accurately controlled, vibrations from the plant can be reduced or cancelled out by running the units in different phases.

6.2.1.4 Operation optimisation

At a higher level, a supervisory control system is required to optimise engine performance for any given operating point, in conventional combustion engines typically achieved by adjusting variables such as fuel injection and valve timing. Unlike conventional engines, however, operation optimisation of the free-piston engine may include varying the compression ratio and stroke length.

6.2.2 Control structure

Figure 6.3 illustrates the proposed control structure for the free-piston engine, showing low-level control, piston motion control and supervisory control systems. The control structure is similar to that presented by Johansen et al. [60], however the current engine differs from that presented by Johansen et al. in some respects, most importantly in the interaction between the engine and the load.

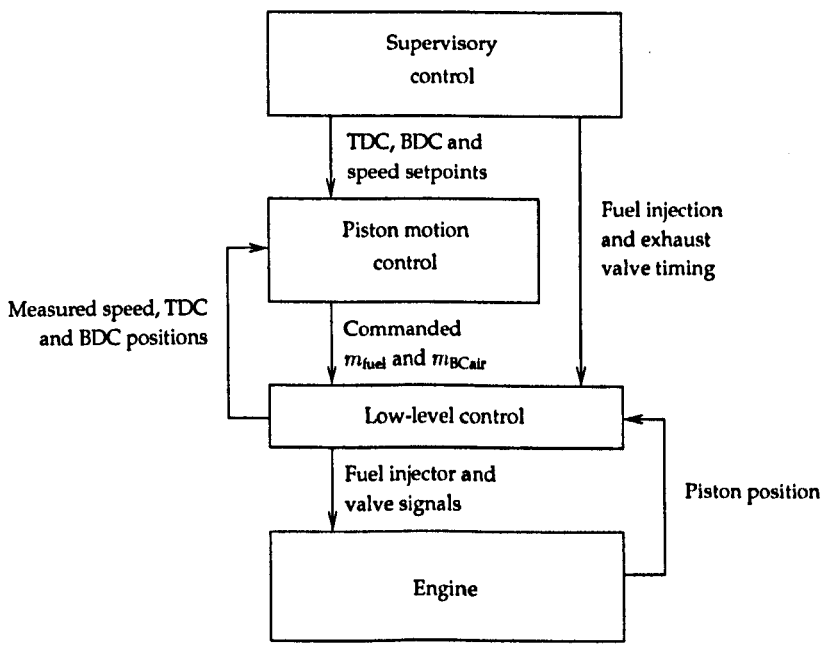

Figure 6.3: Free-piston engine control structure.

The low-level control will read the piston position continuously and provide the signals for the fuel injector, bounce chamber pressure control valves and exhaust valves based on the commanded values. It will further calculate TDC and BDC positions along with engine speed, and feed this information to the piston motion control system.

The piston motion control system receives setpoints for TDC, BDC and engine speed from the supervisory control system and manipulates the command signals for the supply of fuel, m_{fuel}, and bounce chamber trapped air, m_{BCair}.

Finally, the supervisory control system sets the TDC, BDC and speed setpoints according to the operating conditions (such as load and speed) of the engine. Fuel injection timing and exhaust valve timing are reserved for engine optimisation purposes and is therefore also set by the supervisory control system.

6.2.3 Investigating engine control issues

In order to investigate engine dynamics and control over a number of consecutive cycles, the simulation model must be able to accurately predict engine performance during transient operation. Changes in operational variables in the free-piston engine will, unlike in conventional engines, lead to changes in stroke length and TDC and BDC positions, thus affecting both scavenging and compression ratio.

As described in Chapter 4, the simulation model predicted the effects of changes in BDC position and time available for scavenging, and the effects of poor scavenging on the following combustion. Furthermore, the effect of changes in compression ratio and fuel-air equivalence ratio on the ignition delay and the combustion process were accounted for.

Providing the dynamics of the input variables can be realistically represented, the simulation model provides a powerful tool for investigating free-piston engine control issues.

6.3 Model analyses

The control variables of the engine have been identified, and their effects on engine operation, along with those of the load force disturbance, must be determined in order to investigate possible control strategies.

6.3.1 Fuel mass flow

Controlling the mass of fuel injected per cycle is commonly used in conventional diesel engines to control engine speed or power output. Modern engine technology, such as electronically controlled common rail fuel injection systems, makes the implementation of fuel mass flow control straightforward and allows high flexibility in the control of this variable.

The fuel mass control variable is discrete in nature, as it can only be varied once per engine cycle. Hence, if a disturbance occurs just after the fuel injector command signals are set, corrections can only begin to take action one full cycle later.

Varying the amount of fuel injected will influence the amount of energy in the combustion gases. If one considers the power stroke, the amount of combustion energy will influence the amount of compression energy stored in the bounce chamber, and the fuel mass control variable is therefore likely to influence the BDC position. Furthermore, changes in the compression of the bounce chamber gases will influence the available compression energy for the next cycle, hence a change in the subsequent TDC position is also expected from a change in fuel mass input. Finally, changes in the pressure levels in the cylinders will influence piston acceleration and engine speed.

Figure 6.4 shows the effect of changes in fuel mass per cycle on piston stroke length and engine speed. It can be seen that changes in the fuel mass as expected have a large effect on engine operation and lead to changes in stroke length, TDC and BDC positions, and engine speed.

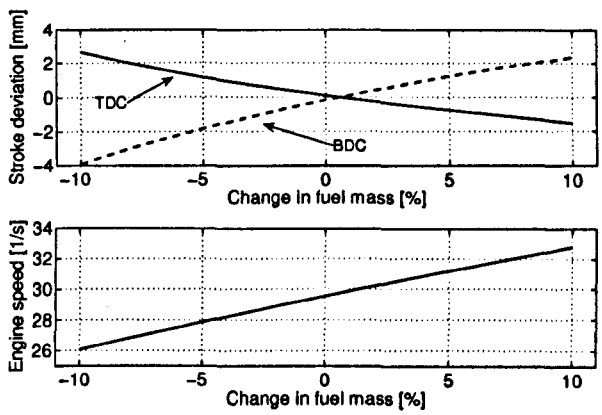

Figure 6.4: Steady state engine response to changes in the mass of fuel per injection.

6.3.2 Fuel injection timing

The fuel injection timing will have an influence on piston motion, since in controls the timing of the energy release which slows down the piston and accelerates it downwards. An influence of fuel injection timing on TDC position is therefore expected. The timing of the energy release has, however, a large influence on the in-cylinder gas temperature, and therefore also engine efficiency and emissions formation, and it is in conventional engines commonly used as a tool to optimise engine performance. It is therefore likely to be unsuitable as a main control variable for the speed or stroke length in the free-piston engine due to the potential penalty in exhaust gas emissions and fuel consumption.

Figure 6.5 shows the steady state effects of changes in fuel injection timing. It can be seen that fuel injection timing has some effect on TDC and BDC position, but very little effect on engine speed. A large penalty in the temperature levels within the cylinder is, however, also seen with advanced fuel injection timing, and this will heavily influence both engine efficiency and exhaust

gas emissions. This control variable was therefore in this investigation assumed to be available only for engine optimisation purposes and not for piston motion control.

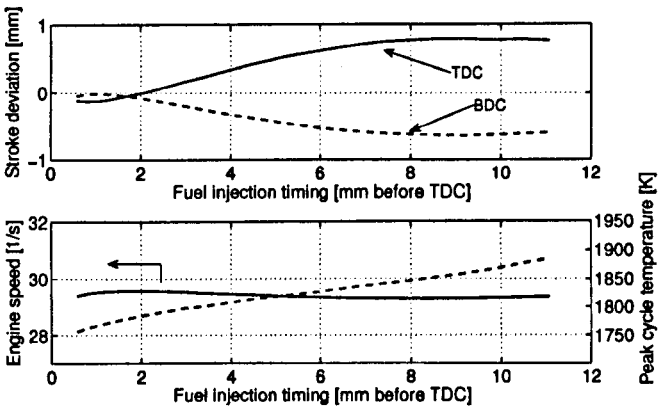

Figure 6.5: Steady state effects of changes in fuel injection timing.

6.3.3 Bounce chamber trapped air

Variations in the amount of trapped air in the bounce chamber will change the stiffness of the bounce chamber gas spring. Considering the power expansion stroke, such variations will influence the process of energy storage in the bounce chamber and the point at which the piston is stopped and the return motion starts. Changing the amount of air in the bounce chamber pressure is therefore likely to influence the engine BDC position. Less influence on TDC position would be expected, since the amount of compression energy stored in the bounce chamber is determined mainly by the combustion process. Changing the pressure levels in the bounce chamber may, however, influence piston accelerations, which will influence engine speed.

The amount of air in the bounce chamber can, if a sufficient high pressure supply is available, be controlled continuously throughout the stroke. Due to the high pressures in the bounce chamber when compressed, it is, however, likely that control of the bounce chamber air mass will be limited to the part of the cycle when the piston is around TDC of the combustion cylinder.

For the bounce chamber pressure to be useful as a control variable, a method of controlling the amount of air trapped is required. One uncomplicated method is to control the opening and closing of the high-pressure supply valve relative to the TDC, as illustrated in Figure 6.6. As the piston approaches TDC, the valve to the high-pressure supply is opened and the pressure in the bounce chamber becomes equal to the supply pressure. As the piston moves downwards, air will be rejected back into the high-pressure supply line and by varying the closing timing of the pressure control valve the amount of air retained in the bounce chamber can be controlled.

Using this method, control of the amount of air in the bounce chamber can be achieved on a

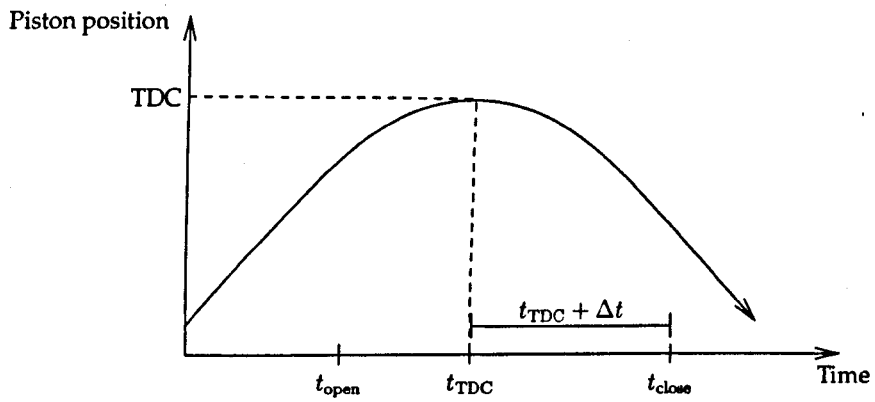

Figure 6.6: Control of bounce chamber trapped air through pressure control valves timing.

cycle-to-cycle basis, and the operation of only one pressure control valve is required. No knowledge of the amount of air trapped in the bounce chamber or the supply air pressure is required, since the bounce chamber pressure control can be related to valve timing only and any offset can be corrected using an integrator in the control loop.

This method will, however, introduce pumping losses for the gas flowing through the pressure control valve. An alternative method was described by Johansen et al. [59], in which an estimator for the mass of air in the bounce chamber was implemented. A control circuit was made to control both low-pressure and high-pressure bounce chamber supply valves, allowing the introduction or rejection of air as necessary. While minimising pumping losses, this method requires a more complex control system with the operation of two pressure control valves, and may also have higher time delays in the control response. It has therefore not been investigated further in this work.

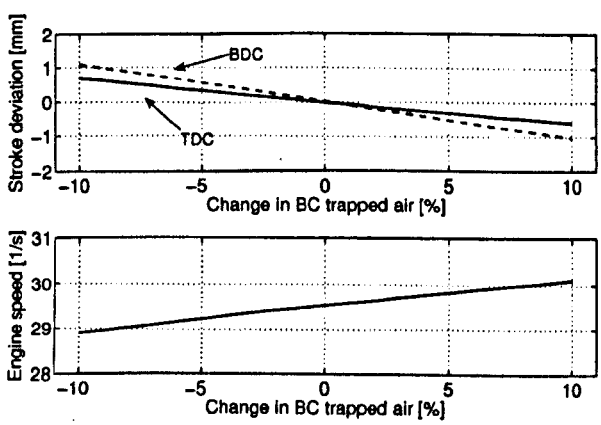

Figure 6.7: Steady state effects of variations in bounce chamber trapped air mass.

Figure 6.7 shows the steady state effects of changes in the amount of air trapped in the bounce chamber. It can be seen that this variable has some effect on TDC and BDC positions, with a slightly

higher influence on BDC position. Having somewhat similar effects on the TDC and BDC positions, the stroke length is not significantly influenced by the bounce chamber trapped air. Some influence on engine speed can also be seen.

6.3.4 Load force

The characteristics of the load force from the electric machine will depend on the type of electric machine and the electric load coupled to it. While it may be possible to control the electric load force using power electronics, and such control is likely to be available due to the necessary implementation of a starting system, the load force is in the investigations presented here treated as a disturbance only. If sufficient engine control can be achieved using the other control variables at hand, this will clearly be the desired solution.

The amount of energy extracted through the load will heavily influence engine operation. If a full cycle is considered, an increase in electric load force will reduce the amount of compression energy available, leading to a lower compression ratio in both the combustion cylinder and the bounce chamber. The load force is therefore likely to influence both TDC and BDC positions, where an increased load force will lead to a shorter stroke length and vice versa. Engine speed will also be influenced due to changes in the pressure levels in the cylinders.

Figure 6.8 shows the steady state effects on the engine from variations in the electric load force. A high influence both on engine speed and TDC and BDC positions can be seen, with the magnitude of the engine response being comparable to that resulting from changes in fuel mass.

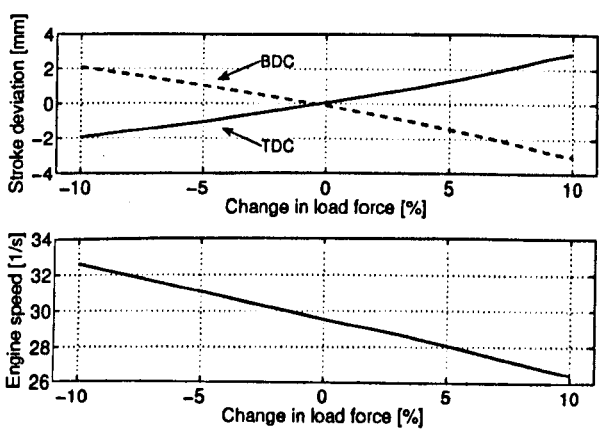

Figure 6.8: Steady state effects of varying electric load force.

6.3.5 Engine dynamics

The dynamic response of the engine to changes in the disturbance and control variables is of high importance, since it determines the feasibility of given control variables to counteract disturbances sufficiently fast enough to avoid situations critical to engine operation.

A series of tests were performed on the simulation model, introducing step changes in the input variables fuel mass, bounce chamber trapped air mass, and load force. It was found that the responses of all output variables (TDC, BDC and speed) resembled first-order or overdamped second-order systems, except the response in BDC position following changes in bounce chamber pressure, which resembled a slightly underdamped second-order system (i.e. having a minor overshoot in the response).

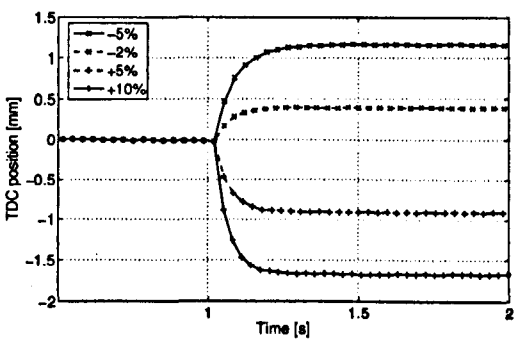

(a) Engine response to a step change in mass of fuel per injection. (Ticks show consecutive TDC position readings.)

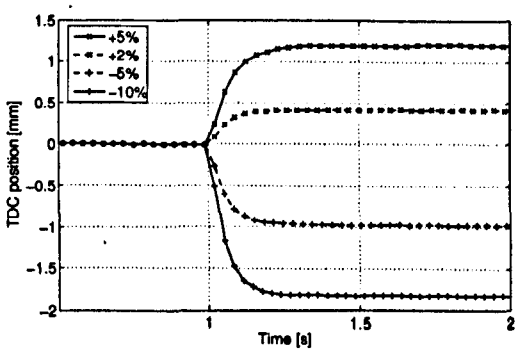

(b) Engine response to a step change in electric load force. (Ticks show consecutive TDC position readings.)

Figure 6.9: Examples of engine dynamic response.

Examples of the engine response to a step change in fuel mass flow and electric load force are shown in Figure 6.9. In both figures the change was imposed at time $t = 1\,\mathrm{s}$. The minor delay in the engine response for the fuel mass input due to its discrete nature can be seen, whereas for the load force the response is instant. It can be noted that the responses for fuel mass and load force are very similar, both in terms of steady state and transient response. The speed of response for the fuel mass input is slightly higher than that of the load force, however the initial delay in the

response to changes in fuel mass gives an overall similar speed of response for the two. The speed of response for the bounce chamber trapped air input was found to be similar to these. The full set of engine dynamic response tests can be found in Appendix B.

6.3.6 System nonlinearities

The system gain for all the input variables depends on the engine operating conditions, mainly the load, and this will be of high importance in the design of the controller. The gain defines the ratio of the magnitude of response in an operational variable to the magnitude of change in an input variable, for example

$$\Delta \text{TDC} = k\,\Delta m_{\text{fuel}}$$

for the effect of fuel mass changes on TDC position, where k is the gain.

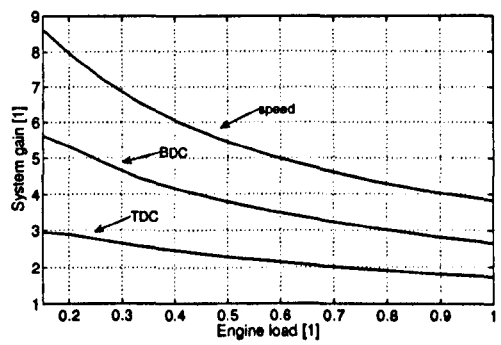

(a) Gain for fuel mass flow input.

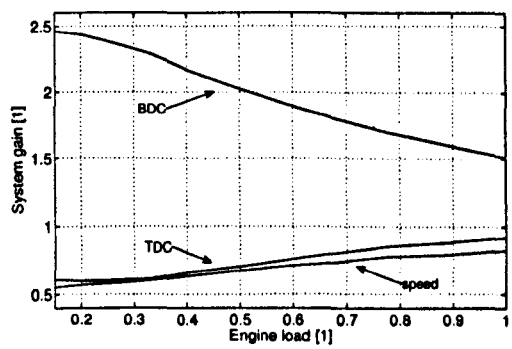

(b) Gain for bounce chamber pressure input.

Figure 6.10: Plant nonlinear gain.

Figure 6.10 shows the gain for the control variables over the engine load range. Some nonlinearity can be seen for all input variables which suggests that advanced control techniques may need to be applied to achieve good performance over the full load range. The very similar influence of the load force and the fuel mass flow may, however, reduce this problem.

Alternatives to correct for the problem of nonlinearities include the application of adaptive control techniques such as gain scheduling.

6.4 Controller design and controlled engine performance

It is clear that a controller is critical for engine operation. The investigations above showed that even a 10 % change in the electric load force produced a TDC position error that is probably unacceptably large (see Figure 6.9). The performance requirements for the control system will depend on the specific engine design, most importantly the clearance between the piston and the cylinder head at TDC.

As mentioned above, a typical TDC clearance value for an engine such as the one presented here would be 1.5–3 mm. Figure 6.1 showed that a TDC deviation of ±1 mm is equivalent to a compression ratio range of around 13-18, which is probably acceptable in most cases. Maintaining the TDC position within ±1 mm of the TDC setpoint was therefore chosen as an initial design guideline. The requirements for BDC position is more relaxed, and a target of ±3 mm was chosen.

When adding a feedback loop with a controller to the free-piston engine plant, a system as that illustrated in Figure 6.11 is obtained.

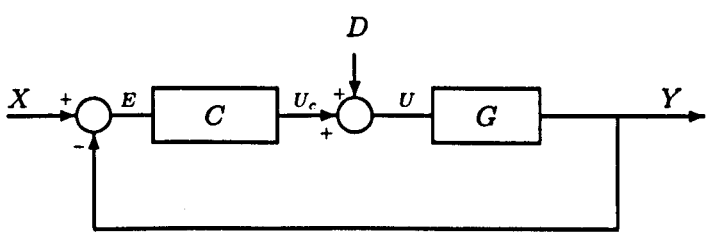

Figure 6.11: Feedback control system.

The engine plant, G, has three inputs and three outputs, hence G is a 3 × 3 matrix. The output vector, Y, contains engine speed, TDC and BDC positions, and can be written as

$$Y = \begin{bmatrix} \text{speed} \\ \text{TDC} \\ \text{BDC} \end{bmatrix}, \tag{6.1}$$

and the input to the engine, U consists of fuel mass per injection, bounce chamber trapped air mass and electric load force, hence

$$U = \begin{bmatrix} m_{\text{fuel}} \\ m_{\text{BCair}} \\ F_{\text{mag}} \end{bmatrix}. \tag{6.2}$$

X contains the setpoints for the three output variables, i.e.

$$X = \begin{bmatrix} \text{speed}_{\text{SP}} \\ \text{TDC}_{\text{SP}} \\ \text{BDC}_{\text{SP}} \end{bmatrix}, \tag{6.3}$$

and the output from the controller, U_c, is the two controllable plant inputs:

$$U_c = \begin{bmatrix} m_{\text{fuel}} \\ m_{\text{BCair}} \\ 0 \end{bmatrix}. \tag{6.4}$$

Consequently, the disturbance, D, is the electric load force

$$D = \begin{bmatrix} 0 \\ 0 \\ F_{\text{mag}} \end{bmatrix}. \tag{6.5}$$

The controller matrix will be a 3×3 matrix:

$$C = \begin{bmatrix} C_{11} & C_{12} & C_{13} \\ C_{21} & C_{22} & C_{23} \\ 0 & 0 & 0 \end{bmatrix}.$$

6.4.1 Decentralised control

Depending on the level of interaction in the plant, multiple-input multiple-output (MIMO) systems can in many cases be reduced to a set of single-input single-output (SISO) loops for which standard SISO control systems can be designed. This may simplify the work in designing the control system, and the successful application of decentralised control in a free-piston engine was reported by Johansen et al. [59]. Decentralised control has been used throughout this work.

6.4.1.1 Pairing of inputs and outputs

Analytical methods to find the best pairing of intputs and outputs exist, however in the current system physical reasoning can be used to find the best coupling. Of the two control variables, the fuel mass is the more powerful since it has a higher influence on all the operational variables, along

with a fast response. Of the control objectives, the TDC position is that with the highest priority, since this is most critical to engine operation and must be controlled within tight limits. The fuel mass should therefore be coupled to the TDC error signal.

This leaves the bounce chamber trapped air mass to control BDC position. The engine speed is, as discussed above, not critical for engine operation and having only two control variables available, the engine speed cannot be controlled with conventional methods.

The controller matrix becomes:

$$C = \begin{bmatrix} 0 & C_{12} & 0 \\ 0 & 0 & C_{23} \\ 0 & 0 & 0 \end{bmatrix}$$

where C_{12} is the coupling between the TDC error signal and the fuel mass command signal, and C_{23} is the coupling between BDC signal and the bounce chamber trapped air mass demand.

Simulations showed the feasibility of this control strategy, with the TDC and BDC positions being controllable over the full load range (where the load was varied by changing the load force). Figure 6.12 shows the demand on the control variables over the load range. Figure 6.13 shows the resulting engine speed, for which no control variable is available. It can be seen that the speed variations over the load range are significant.

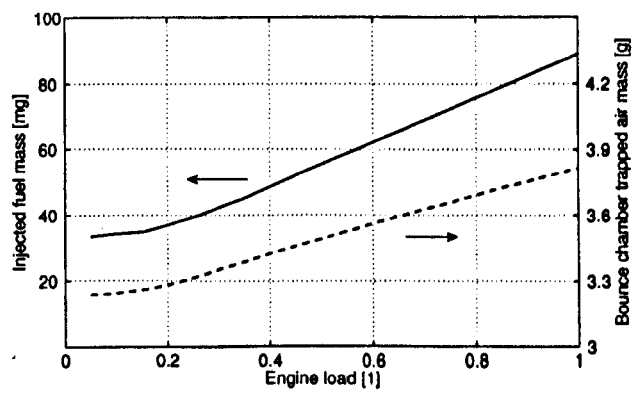

Figure 6.12: Injected fuel mass per cycle and bounce chamber trapped air mass for the controlled engine.

6.4.2 Speed control through varying stroke length

Johansen et al. [59] suggested varying the TDC and BDC setpoints to control engine stroke length and thereby influencing engine speed, utilising the fact that the stroke length and bouncing frequency in the free-piston engine are interconnected.

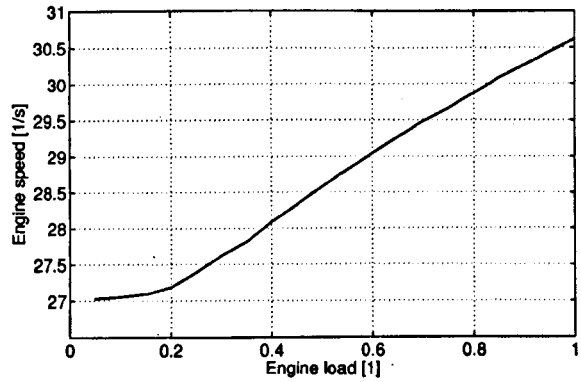

Figure 6.13: Engine speed with TDC and BDC control.

The TDC position has, as mentioned above, a high influence on engine performance and control of the TDC setpoint is restricted for engine optimisation purposes. The BDC can be varied over a significantly larger range without major penalties in engine performance. In the current simulated engine design, the distance from the BDC setpoint to the point of scavenging ports opening was 22 mm, whereas the clearance distance to the bounce chamber cylinder head was 10 mm. The BDC setpoint can therefore be varied significantly without risk of damage to the engine, however such variations may influence engine performance.

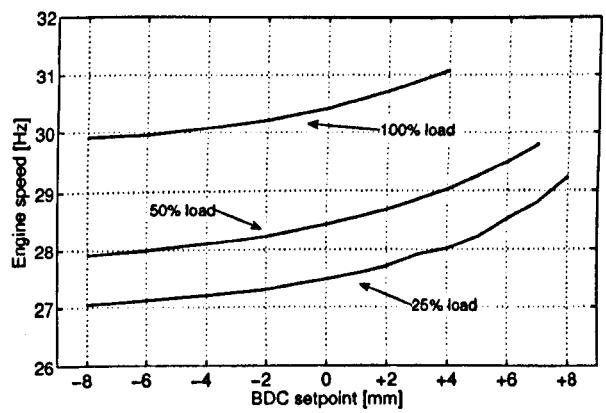

Figure 6.14: Control of engine speed through varying BDC setpoint for different loads.

Figure 6.14 shows the effects of varying BDC setpoint on engine speed at different loads. It can be seen that at a given load, the speed can only be varied over a very limited range when adopting this control method. A speed of for example 30 Hz would not be possible to maintain over the full load range even if large changes in BDC setpoint were allowed. Furthermore, the required changes in the BDC setpoint lead to reduced scavenging time and port area at high loads, whereas the BDC setpoint is below its nominal value at low loads where a reduction in scavenging performance

would be more acceptable.

It was found that this method could be applied successfully and without major effects on engine performance only for a very limited load range, from full load and down to around 90 % load. Hence, this method of speed control would only be feasible for effectively constant power applications.

6.4.3 Engine dynamics

The engine dynamic response to a load change depends heavily on the dynamics of the load force, which for the free-piston engine generator are determined by the electric system. Details of this are not known at an early design stage, but it is clear that electric systems have very low time delays and may therefore impose rapid changes in engine load. It is, however, likely that the output power has to be conditioned, which may allow the implementation of energy storage devices to dampen disturbances on the engine if necessary.

A general investigation of the controlled engine's ability to reject disturbances was undertaken, in order to gain insight into the necessity of additional measures in the electric system to aid engine control.

Characteristics of the engine inputs

The characteristics of the inputs to the engine plant and their influence on its response differ in some respects to textbook examples in control systems design. Firstly, for any load change there will be a change of setpoint in TDC position. This setpoint change must take place immediately to avoid excessive in-cylinder pressures[2]. This was implemented in the simulation model such that a load change triggers an instant change of TDC setpoint. Such simultaneous changes of load and system setpoint add to the requirements set on the controller.

Secondly, the characteristics of the free-piston engine generator are such that the timing of the load change will have an influence on the engine response. Since the control variables are set only once per engine cycle, if a load change occurs shortly after a control variable is set there may be a significant delay before controller action will take affect. If one considers the TDC control variable, the fuel mass flow demand, which is set at BDC, two consecutive engine cycles starting at BDC will include the following events:

[2]An instant TDC setpoint change is strictly necessary only for load increases, since operating at a compression ratio lower than nominal at part load will not be damaging for the engine (providing that the compression is sufficiently high for fuel autoignition). It has, however, in this work been assumed that any load change requires an immediate TDC setpoint change.

First cycle	(1) BDC.
	(2) Compression stroke.
	(3) TDC, where TDC position is read.
	(4) Power stroke expansion.
Second cycle	(5) BDC, where the controller action for TDC controller is set.
	(6) Compression stroke.
	(7) TDC.
	(8) Power stroke expansion.
	(9) BDC.

If a load change occurs during (1) or (2), the TDC position at (3) will be influenced and trigger a control response at (5) to correct for the error at the next fuel injection (at (7)). While this may be a significant delay, if the load change occurs just after (3), the controller action will not begin until (9) and the correction will not take place until the following TDC, two full cycles after the disturbance occurred.

All the simulations following were carried out with the load change occurring at TDC, and therefore represent 'worst case' scenario for the control problem.

6.4.4 Proportional, integral and derivative feedback control

Proportional, integral and derivative (PID) feedback control is widely used in industry and, although having some limitations, has proved to provide excellent performance for a wide range of applications. The implementation of PID control is uncomplicated, and initial tuning can be performed using well-known empirical rules. Johansen et al. [59] demonstrated satisfactory performance of PI and PID control of a free-piston application similar to that investigated here.

To investigate the feasibility of PID controller in the free-piston engine, such controllers were implemented in both control loops in the simulation model. PID control was implemented by setting the relevant elements of the controller matrix C in the standard feedback control system to a sum of a proportional, an integral and a derivative gain term. I.e. for the controller matrix element mn:

$$C_{mn} = k_p \cdot e(t) + k_i \int_0^t e(t)\,\mathrm{d}t + k_d \frac{\mathrm{d}e(t)}{\mathrm{d}t},$$

where $e(t)$ is the error signal component of the vector E.

The feasibility of PID control in the free-piston engine

PID controllers are generally robust, but the derivative controller term can be sensitive to measurement noise and will produce very large controller responses to step changes in setpoint, since the theoretical derivative response to a step change is infinite. Methods do, however, exist to correct for this and avoid the actuators saturating. (The saturation point in the TDC controller loop will be the point at which the fuel-air equivalence ratio is equal to one and injecting more fuel will not produce more power.)

After testing the controller performance, it was found that the particular feature of simultaneous changes in load disturbance and TDC setpoint do represent a challenge for the PID controller. The characteristics of the load and setpoint changes are such that with instant TDC setpoint changes, an initial error will be produced which is opposite to that produced by the load, and therefore trigger an initial control response opposite to the desired one. This limits the gain of the proportional controller term and, in particular, the derivative term due to the initial control response enhancing the error created by the load change. This can be seen in the results shown in Figure 6.15.

For an engine with a constant compression ratio setpoint this will not be a problem, however in the current engine, using only minor changes in compression ratio and TDC setpoint, the derivative gain had to be reduced to a level at which the derivative action did not improve controller performance. If a higher degree of compression ratio control is desired, these problems will be more serious.

Although methods may exist to improve the performance or correct for these problems, for example delaying the TDC setpoint change (which would increase the risk of excessive in-cylinder pressures during transient operation), the feasibility of a PID controller for the free-piston application is questionable.

Controller performance

Due to the very limited effect of the derivative gain term in the TDC control loop, the performance was investigated using a PI controller only. For the BDC control loop, a PI controller was found to perform satisfactorily. Both controllers were manually tuned to minimise the peak errors in TDC and BDC positions.

Figure 6.15 shows the engine dynamic response to a 15 per cent step change in the load at time $t = 1\,\mathrm{s}$, with the engine originally operating at 80 % of full load. The response of the BDC control loop can be seen to be acceptable, with the peak error not reaching values critical for engine operation. The settings of this controller were adjusted to give a response slightly slower (more overdamped) than that possible, in order to minimise the disturbance on the TDC loop.

For the TDC controller, the setpoint change which creates the initial undesired error, as dis-

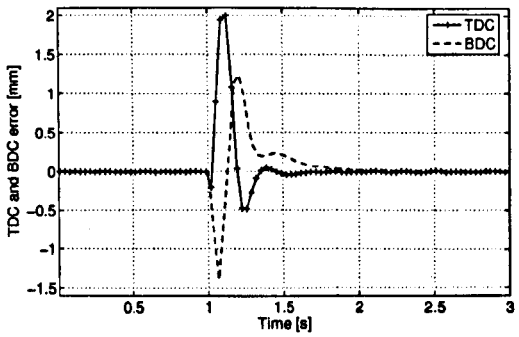

(a) Engine response to a step increase in load.

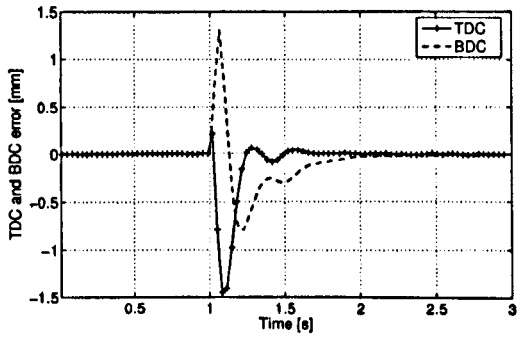

(b) Engine response to a step decrease in load.

Figure 6.15: Engine response to a 15 per cent step change in load with PI controller.

cussed above, can be seen just after $t = 1$ s. A high peak error in the TDC error is further seen, and it was found that this could not be avoided with the current controller due to the delay between the disturbance taking place and the control response. For the load increase case, the peak error of approximately 2 mm is equivalent to a drop in compression ratio to circa 12. While this is still sufficient for fuel autoignition, it will clearly have negative effects on the combustion process and emissions formation. For a rapid load decrease, the increased compression ratio combined with the controller failing to reduce the amount of injected fuel sufficiently fast leads to a significant increase in the peak in-cylinder gas pressure. In this case, the peak pressure reached a value of approximately 180 bar, which is probably unacceptable in a real engine.

The settling times for both control loops were found to be acceptable.

6.4.5 Pseudo-derivative feedback control

The concept of pseudo-derivative feedback (PDF) control was proposed by Phelan [84]. It is an alternative to integral control with derivative feedback (a system in which the feedback signal is differentiated and not the error signal, also known as velocity feedback). Although not being in extensive use, PDF control is generally reported to have better load handling capabilities than PI control whereas PI control has better setpoint tracking performance. (See Phelan [84], Setiawan et

al. [89] and Ohm [80] for further analyses and examples.) In the current system the load disturbance is the greater challenge due to the high peak error produced by rapid load changes. Rapid setpoint changes will only occur as a response to a load change.

Figure 6.16 illustrates the pseudo-derivative feedback control system. The controller in the forward path, C, incorporates an integral term only, and a negative feedback of the output state is added after the controller. The feedback gain matrix K is

$$K = \begin{bmatrix} 0 & K_{12} & 0 \\ 0 & 0 & K_{23} \\ 0 & 0 & 0 \end{bmatrix},$$

where K_{12} and K_{23} contain proportional gain terms only.

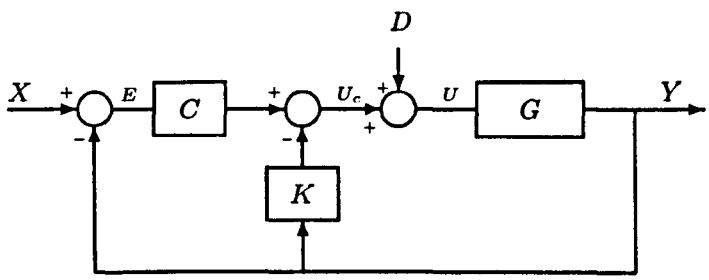

Figure 6.16: Pseudo-derivative feedback control system.

A feature of PDF control that may make it more suitable for the free-piston engine application than PI control is that it is less sensitive to rapid setpoint changes. Since the controller in the forward path, C, does not contain a proportional or derivative term, the speed of response to setpoint changes will be lower than in the PI controller.

Controller performance

Figure 6.17 shows the engine dynamic response to a 15 per cent step change in the load with a manually tuned PDF controller, a similar situation to that investigated previously for the PI controller. A slightly better response than that obtained with the PI controller was found, however the high peak error can not be avoided. Therefore, only a minor improvement in the compression ratio drop for the load increase case and the high peak pressure for the load decrease was found for the PDF controller. A direct comparison of controller performance on these operational variables is shown below in Figure 6.21.

The high peak errors seen are due to the time delay between the observation of the error and the controller correction, making the feedback control loop too slow to satisfactorily correct for this. In relation to the discussion on controller delay above, it can be seen from the TDC error graph that

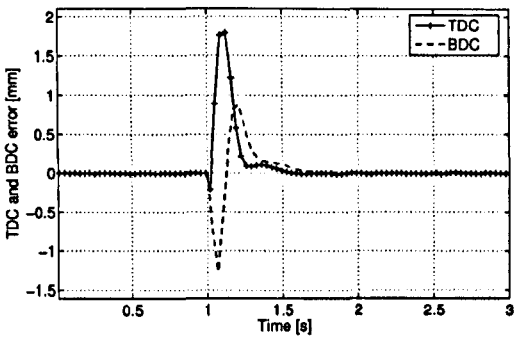

(a) Engine response to a step increase in load.

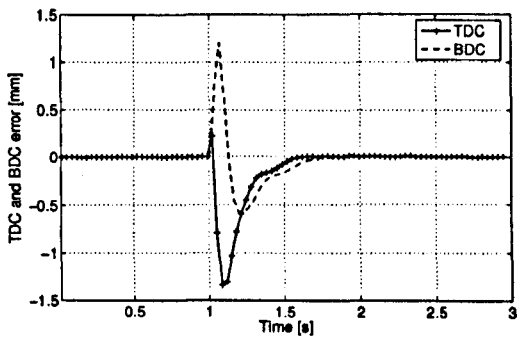

(b) Engine response to a step decrease in load.

Figure 6.17: Engine response to a 15 per cent step change in load with PDF controller.

after two cycles, when the controller action will first take effect, the error is already nearly 1 mm (the ticks on the graph represent TDC position readings). It is therefore clear that a standard feedback control loop is unable to correct for the initial error peak.

PDF controllers have been reported to give more smooth actuator action than a PI controller. Since the actuator transfers energy to or from the plant, optimising the actuator action to minimise energy consumption is of high importance in many plants. In the free-piston engine, this will mainly be an issue for the fuel mass control variable. In addition to engine fuel consumption, the amount of fuel injected is of high importance for the formation of engine emissions and particulates during transient engine operation. Furthermore, the fuel mass control variable relies on there being a sufficient amount of air in the cylinder for the fuel to burn. For high engine loads this control variable will be operating close to saturation.

Figure 6.18 shows the actuator action for the PI and PDF controllers for a 15 per cent step increase in load with the engine originally operating at 80 % load, similar to the situations above. The undesirable initial control response of the PI controller shortly after the load change can be seen, although the magnitude is low in this case since there is only a limited change in TDC setpoint.

The PDF controller can be seen to have a significantly smoother controller response, with a

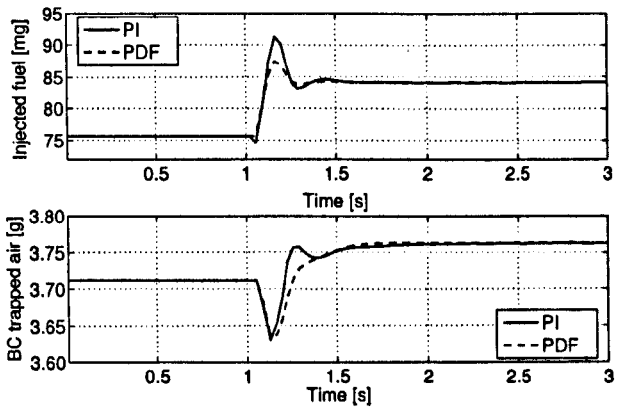

Figure 6.18: Actuator action for a 15 per cent step increase in load with PI and PDF controllers.

peak overshoot in the fuel mass demand, when compared to the final value, of approximately half the value of the PI controller. For this step increase in load from 80 % to 92 % of full load, the PI controller response does in fact surpass the fuel mass injected per cycle at full load, which is around 89 mg. This further indicates that the PDF controller is a better option for the free-piston engine plant than the PI controller.

6.4.6 Disturbance feedforward

The above investigation indicated that the time delay between the load disturbance and the corrective action from the controller makes the initial error peak difficult to avoid with feedback control only. This suggests the use of disturbance feedforward, which, providing that the disturbance can be accurately measured, allows corrective action to begin before the error is measured by the controller.

Goodwin et al. [46] stated that "feedforward control is generally agreed to be the single most useful concept in practical control-system design, beyond the use of elementary feedback ideas", but warned that it can be sensitive to modelling errors. The very similar influence of the fuel mass control variable and load force disturbance on the free-piston engine plant does, however, suggest that disturbance feedforward is well suited for the free-piston engine controller.

The measurement of the electric load force in the linear electric generator is trivial, and can be obtained by measuring the current and voltage at the generator output. Information on generator load is likely to be needed anyway for engine optimisation purposes by the supervisory control system, and also to apply adaptive control such as gain scheduling which may be necessary.

It should be noted that although the fuel demand signal can be manipulated immediately following a load change by the feedforward loop, there may still be a delay of up to one full cycle between this change and the corrective action due to the fuel injection occurring only once per

engine cycle.

Implementation

Disturbance feedforward in the free-piston engine plant was realised by letting the disturbance D influence the fuel mass and bounce chamber air mass demand signals. Figure 6.19 illustrates the pseudo-derivative feedback control system with an added feedforward gain term.

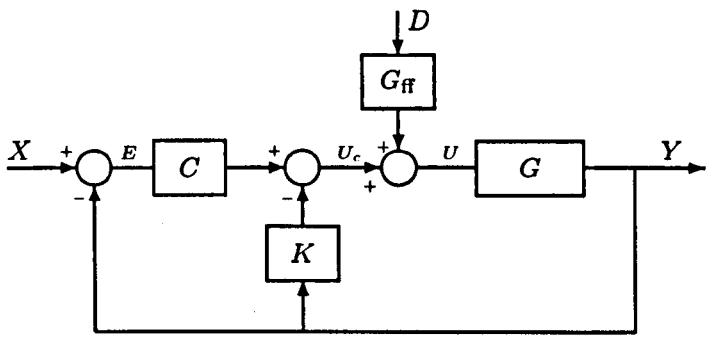

Figure 6.19: Pseudo-derivative feedback control system with disturbance feedforward.

The feedforward gain matrix G_{ff} is

$$G_{ff} = \begin{bmatrix} 0 & 0 & k_1 \\ 0 & 0 & k_2 \\ 0 & 0 & 1 \end{bmatrix},$$

where k_1 and k_2 are constants. k_1 regulates the influence of load changes on the fuel mass control variable and k_2 on the bounce chamber trapped air mass.

Controller performance

Figure 6.20 shows the engine response to a 15 % step change in load, similar to that investigated previously, with PDF control and disturbance feedforward, both with manually tuned coefficients. A significant improvement when compared to feedback control only can be seen, with a large reduction in the peak error and a reduced settling time.

Influence of controller performance on engine operational parameters

It has been demonstrated how the different controllers perform in maintaining TDC and BDC positions within certain limits. For the TDC position, the objective of the controller is to maintain the engine compression ratio within a given range in order to (a) ensure fuel autoignition, and (b) avoid excessive in-cylinder gas pressures.

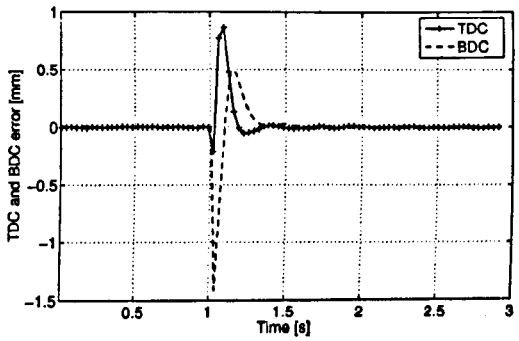

(a) Engine response to a step increase in load.

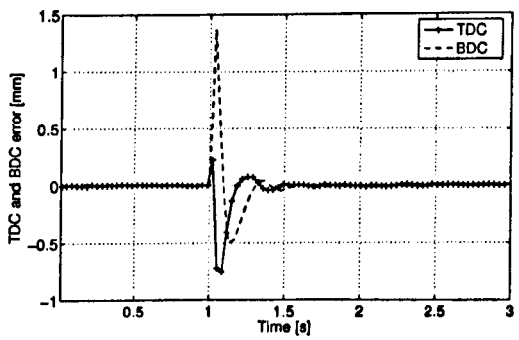

(b) Engine response to a step decrease in load.

Figure 6.20: Engine response to a 15 per cent step change in load with PDF control and disturbance feedforward.

Figure 6.21 shows the engine compression ratio and peak in-cylinder gas pressure during engine transient operation for a similar load change as that investigated above. The same trends as above can be seen for the different controllers, with the pseudo-derivative feedback controller with disturbance feedforward providing a significantly better response than feedback only control.

Figure 6.21a shows that the compression ratio drops rapidly following a load increase due to the error in TDC position. This reduction in compression ratio may influence the combustion progress or even lead to failure of the fuel to ignite, which may cause the engine to stop. For a turbocharged engine like the one investigated here, even a significant reduction in compression ratio (even down to 10:1) may not represent a problem for engine operation other than leading to reduced efficiency, but for crankcase-scavenged engines, measures may need to be implemented to avoid rapid load increases due to the risk of the engine stopping.

Figure 6.21b shows the in-cylinder gas pressure following a load decrease. Very high pressure peaks can be seen due to the rapid increase in compression ratio. An increase in compression ratio and peak in-cylinder pressure may, unlike a compression ratio reduction, lead to mechanical damage to the engine and load decreases are therefore the more critical situation. The peak in-cylinder pressure will, however, depend on both the compression ratio (given by the TDC error) and the fuel injection rate. Hence, if the compression ratio is excessively high due to a TDC error, this may

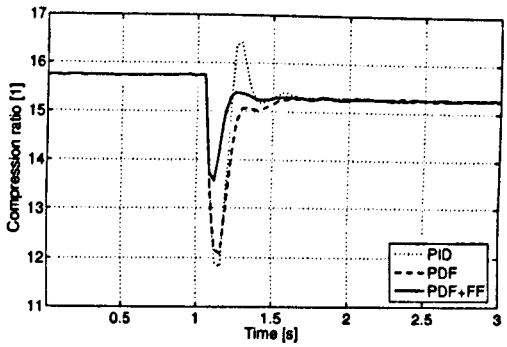

(a) Effect of a 15 % step increase in load on engine compression ratio.

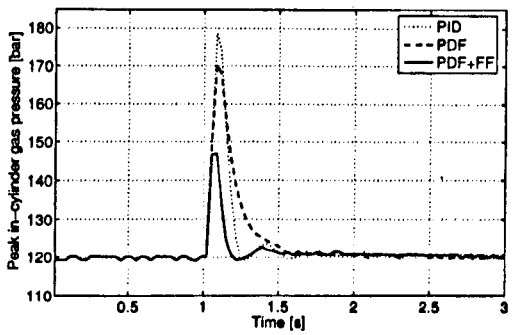

(b) Effect of a 15 % step decrease in load on in-cylinder gas pressure.

Figure 6.21: Effects of engine load changes on compression ratio and in-cylinder gas pressure.

not be a problem if the fuel mass injected can be reduced at the same time. It may therefore be possible to implement a control circuit that measures the piston motion (for example by measuring the piston velocity at some point prior to TDC) and reduces the amount of fuel injected if there is a danger of excessive gas pressures.

6.4.7 Ramp load changes

In the investigations above it was found that even a relatively small load change of 15 % produced significant TDC and BDC position errors due to the harsh characteristics of a step change. In a real system, the load changes may be larger, but will occur over a finite time, which may be possible to influence in the operation of the engine or in the design of the electric system. A better representation of a change in the load demand may be a ramp change between two load levels, where the slope of the ramp determines how rapid the load change is.

Figure 6.22 illustrates a ramp load increase between load levels L_1 and L_2. The difference between t_2 and t_1 will determine how rapid the load change occurs, and a time constant, being the difference between the two, can be defined. As the time constant tends to zero, the load change will resemble a step change, and this is the most challenging disturbance that the engine can experience.

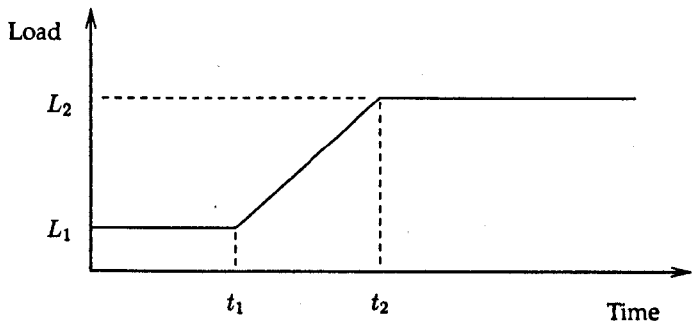

Figure 6.22: Illustration of a ramp load change.

Using such a method, it is possible to investigate how small one can make t for given performance criteria to be fulfilled. This information may be used as a design guideline for the electric system.

Figure 6.23 shows the engine response to a linear change in engine load between 20 % and 100 % over 0.5 s using the PDF controller with disturbance feedforward and manually tuned coefficients. It can be seen that when the load change occurs over a period of time, as opposed to the harsh step change investigated above, the engine can cope with significantly higher load changes while maintaining the TDC and BDC positions within an acceptable range.

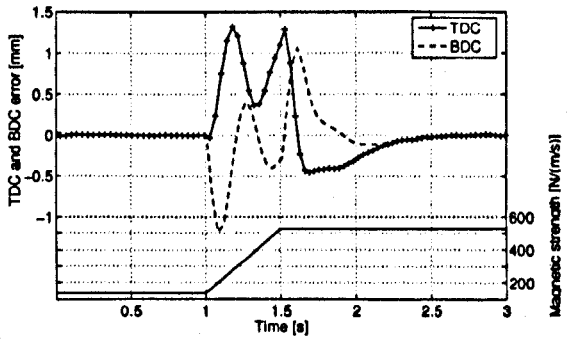

(a) Engine response for a linearly increasing load.

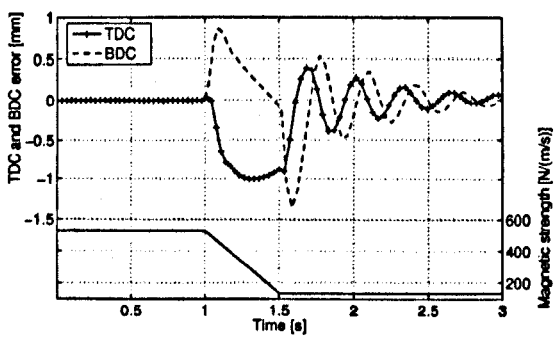

(b) Engine response for a linearly decreasing load.

Figure 6.23: Engine response to a ramp change in load between 20 % and 100 % over 0.5 s.

The effects of the plant nonlinearities over the load range can be seen, with the engine exhibiting a significantly more oscillatory behaviour at low loads. This suggests that gain scheduling would have the possibility of improving controller performance over the full load range. Having a measurement system for the electric load for the feedforward loop, such gain scheduling should not be complicated to implement.

6.4.8 Further improving engine controlled performance

Clearly, there are other approaches to the control problem that can be investigated, both multivariable control and decentralised, SISO control beyond standard techniques. Here, a basic investigation was presented based on well-known methods, which showed acceptable performance for moderate disturbances. The most obvious method of ensuring stable engine operation for dynamically varying loads is to implement load storage devices in the electric circuit, and thereby smooth the load demands on the engine.

Improvements in the proposed controller are possible. In the above investigations, the controller was manually tuned to achieve acceptable performance. With controller coefficients in both the feedback and disturbance feedforward loops, and two controller loops in the system, the tuning is a multivariable optimisation problem. There is clearly potential for improvement in the tuning of the controllers. Furthermore, the implementation of gain scheduling, where the controller gain values would be adjusted as a function of engine load, is possible to give better controller performance over the full load range. The controllers investigated above were tuned at a single operating condition, at a load of 80 % of the full load.

It appears that to further improve the performance, a different approach to the problem beyond the ideas of state feedback would be necessary in order to eliminate the problems that are due to the delay in controller response. If a continuous measurement of the piston position is available, information of the piston motion along with the engine load can be used to predict the dead centre position for example at the half-stroke point. This may be particularly useful to avoid excessive combustion pressures, by delaying the fuel injection if a high compression ratio is predicted. The influence of this on engine operation should, however, be further investigated.

6.5 Cycle-to-cycle variations

Another control-related issue that has not been thoroughly investigated is the smoothness of operation in the free-piston engine. Cycle-to-cycle variations can occur in for example the amount of fuel injected and the progress of the combustion process, and such variations will have an effect on

engine performance. Unlike in conventional engines, any such variations will have a direct influence on the following cycle in the free-piston engine, and this type of engine may be more prone to cycle-to-cycle variations and potentially instability if such errors accumulate.

Some experimental reports have described high cycle-to-cycle variations in the operation of bouncing-type free-piston engines. However, it is not clear whether this is due to the free-piston engine characteristics or to the experimental apparatus. Using a detailed simulation model such as the one developed in this work, the influence of single variables can be investigated without the disturbance of variations in other operational variables.

A common measure of engine smoothness in operation is the variation in indicated mean effective pressure and peak in-cylinder pressure between cycles. This is commonly measured in terms of a coefficient of variation, COV, defined as [51]:

$$\mathrm{COV}_{\mathrm{imep}} = \frac{\sigma_{\mathrm{imep}}}{\overline{\mathrm{imep}}}$$

where imep is the engine indicated mean effective pressure, σ_{imep} denotes the standard deviation of imep and $\overline{\mathrm{imep}}$ is the average value, or mean. It can be defined similarly for other operational variables. Heywood [51] stated that vehicle driveability problems usually occur for $\mathrm{COV}_{\mathrm{imep}}$ higher than around 10 per cent.

Simulations were run for the free-piston engine and for an equivalent conventional engine, using a similar strategy as that described in Section 4.3.5. The engines were run in steady state operation with no controllers active and variations in the fuel mass was implemented in the simulation model using a random number generator and adding or subtracting an amount of fuel according to this. The simulations were run for a number of cycles, for which the appropriate data was logged and the COV finally calculated.

Figure 6.24 shows the effect of variations in the injected fuel mass on the indicated mean effective pressure and the peak in-cylinder gas pressure. Figure 6.24a shows that the indicated mean effective pressure varies with the amount of fuel injected, as one would expect, but that the variations in the free-piston engine are only slightly higher than those of the conventional one. With modern fuel injection systems one would expect a variability in the fuel mass in the lower half of the investigated range, and operational problems due to this are therefore not expected.

Figure 6.24b shows that the variations in peak in-cylinder gas pressure are significantly higher for the free-piston engine than for the conventional one. This is due to the variations in indicated mean effective pressure, which is a measure of the combustion energy from the cycle, influencing the compression ratio for the next cycle. The combination of random variations in both compression ratio and injected fuel gives significantly higher peak pressure variations in the free-piston engine.

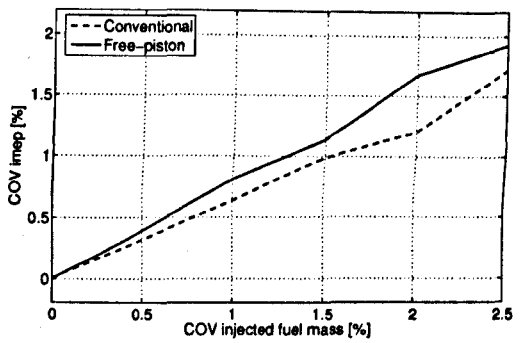

(a) Effect of variations in fuel mass on indicated mean effective pressure.

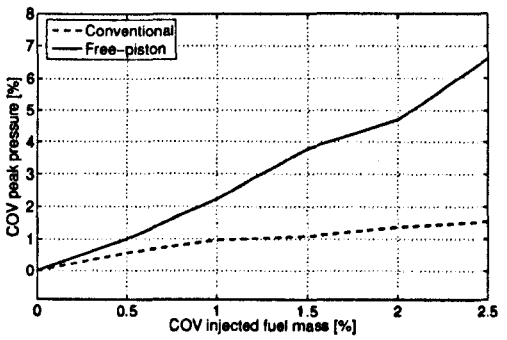

(b) Effect of variations in fuel mass on peak in-cylinder gas pressure.

Figure 6.24: Effects of variations in injected fuel mass.

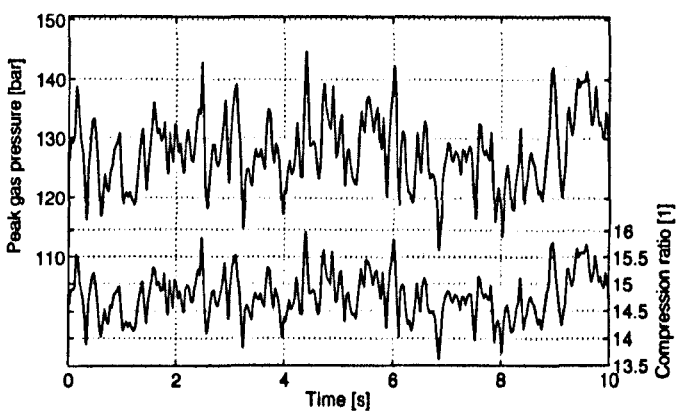

Figure 6.25: Example of operational sequence for the free-piston engine.

Figure 6.25 shows an example of an operational sequence for the free-piston engine with a COV in injected fuel mass of 2 %. It can be seen that even with the relative high COV used here, the peak pressures obtained are not critical for the engine. The figure also shows the variations in engine compression ratio, which means that there is some variation in engine TDC position. The variation is only minimal but may disturb the engine controller and may therefore have to be taken into

account in the design of the control system.

6.6 Summary

An investigation into the dynamics and control of the free-piston engine generator presented in Chapter 3 was presented. Control objectives for the engine were outlined and a control strategy proposed. Control variables were identified, and their influence on engine operation investigated, along with that of engine disturbances, using the full-cycle simulation model described in Chapter 4.

The control strategy, based on standard feedback ideas, was found to give adequate performance for moderate load changes, however the use of disturbance feedforward was crucial to achieve a satisfactory dynamic response. It was found that with a standard control approach the dynamics of the load changes should be limited by applying load storage devices in the electric circuit.

Chapter 7

Conclusions

This thesis has presented a detailed investigation into the free-piston engine concept and its potential advantages over conventional technology for electric power generation in medium and large scale applications. The details of the findings have been summarised at the end of each chapter. Here they will be recapped and evaluated in relation to the feasibility of the free-piston engine concept and the performance of such engines, and recommendations for further work will be presented.

7.1 Summary of the results

Chapter 2 presented a comprehensive background study, reviewing reported free-piston engine applications and their performance. The particular features of the free-piston engine were discussed, and potential advantages and challenges compared to conventional technology identified. It was found that both the hydraulic free-piston engine and the free-piston engine generator appear to be feasible concepts, however that the latter relies on engine control issues being resolved in order to realise optimal performance. Based on this background study, a proposed design for a free-piston engine generator was presented in Chapter 3. A single piston configuration with a variable pressure, gas-filled bounce chamber was chosen, due to its potential advantages in terms of engine control.

In Chapter 4, the development of a full-cycle simulation model of the free-piston engine was described, and comprehensive simulation results were presented. The basic performance and operational characteristics of the engine were investigated, along with the influence of the main design variables. It was found that the design and operational variables of the free-piston engine are strongly interconnected, with changes in any variable influencing many aspects of engine operation. This strong interconnection makes the system more complex than conventional engines and complicates both the engine design process and engine control. The potential problem of low power to weight ratio due to high moving mass, previously reported by other researchers, was not

found to be the case with the turbocharged free-piston diesel engine. A minor efficiency advantage over conventional engines was predicted, due to faster power stroke expansion.

Chapter 5 presented an investigation into the in-cylinder processes of the free-piston engine, including gas flow, combustion and emissions formation, using a multidimensional simulation model. Both spark ignition and compression ignition (diesel) engines were investigated and directly compared to predictions for conventional engines in order to identify potential advantages of the free-piston engine concept. No significant differences in performance could be found for the spark ignition free-piston engine, and the feasibility of spark ignited free-piston engines was questioned due to short-circuiting of the inlet charge in pre-mixed, two-stroke engines. For free-piston diesel engines, a slight fuel efficiency advantage was predicted, similar to that found in Chapter 4. Potential reductions in the formation of nitrogen oxides were also found for the free-piston diesel engine, due to the enhanced in-cylinder gas motion in such engines and the faster power stroke expansion. It was stated that a more comprehensive study is required to fully investigate the emissions formation in such free-piston engines. Finally, a coupled dynamic–multidimensional simulation model allowing the simulation of free-piston engines over a wide range of operating conditions was described and its use briefly demonstrated.

Chapter 6 studied issues related to engine control, an often reported challenge with free-piston engines. Control variables and disturbances were identified and different control strategies were tested using the full-cycle simulation model. It was found that the free-piston engine generator is controllable and that performance acceptable for constant power applications can be achieved using standard feedback control with disturbance feedforward. The engine is, however, very sensitive to rapid load changes and energy storage devices may therefore need to be employed to smooth engine load in applications with variable load demands. The influence of cycle-to-cycle variations in the combustion process was investigated but not found to be critical for engine operation.

7.2 The feasibility of the free-piston engine concept

There seems to be little doubt that the free-piston engine is a feasible concept, with potential advantages over conventional technology. The main advantages of the free-piston engine lie in the simplicity of the unit, giving reduced frictional losses and operation optimisation possibilities. In addition, both the results presented in this thesis and work reported by other authors indicate potential inherent thermodynamic and emissions formation advantages in free-piston diesel engines. The main challenge is clearly that of engine control, which must be resolved not only to a level of maintaining stable engine operation for all operating conditions but also such that the advantages of engine operation optimisation can be realised.

Of the previously reported modern free-piston engine developments, the single piston hy-

draulic free-piston engine appears to be the most promising. Such units have shown favourable performance when compared to conventional technology, and control issues for these engines have been fully resolved. Much research is, however, underway on free-piston engine generators, as such units have a significant appeal due to the widespread use of highly efficient electric power distribution networks and electric machinery. The main incentives for the development of innovative engine technology such as the free-piston engine, namely high fuel prices and stringent emissions legislation, are likely to continue to drive research and development efforts within free-piston engine technology in the years to come.

7.3 Recommendations for further work

Although the free-piston engine concept appears to be a promising candidate for power generation in various applications, significant development efforts are required for it to become a realistic alternative to the highly developed conventional internal combustion engine technology. In order for continuing development of this unconventional engine concept, both the challenges and the potential advantages associated with it must be studied in further detail. This thesis has contributed with some fundamental investigations into the operational characteristics and performance of a free-piston engine generator. It was found that there are two main areas that need further investigation:

- engine combustion and emissions formation, and
- engine control issues.

For both these, the development of an experimental engine will be of high importance in order to validate theoretical and computational predictions.

7.3.1 Further work on combustion and emissions formation

Both the current work and reports from other authors have indicated potential advantages of the free-piston diesel engine in terms of fuel efficiency and emissions formation, and details of these processes should be studied in more detail. In particular, the trade-off between nitrogen oxide emissions, particulates, and engine efficiency will be of high interest. Due to the particular operating characteristics of the free-piston engine, this trade-off may be different than that known from conventional engines.

Furthermore, the potential for operation optimisation in the free-piston engine should be studied in more detail, with the benefits of the variable compression ratio being the factor of main interest. Varying the TDC position will influence the gas motion within the cylinder (in particular squish effects), and the effects of such variations on the combustion and emissions formation

should be further investigated. Along with this comes the use of alternative– or low-quality fuels and the potential of optimising engine operation for any given fuel, in order to, for example, allow the use of fuel with lower quality than that required in conventional engines. Much of this work can be done using computational models, however eventually it is essential that the results be verified through experimental testing.

7.3.2 Further work on engine control

The development of an experimental test engine will be of high importance in the investigation into engine control issues. This will allow the validation of the results obtained from the simulation model, along with further investigations into engine operational stability, sensitivity to disturbances and the feasibility of the proposed control strategies. This will give more accurate information on the need for power electronics and energy storage to reduce load variations on the engine.

Further work in engine control may also include theoretical and computational studies investigating more advanced control strategies. In particular, the application of multivariable and nonlinear control should be investigated, as such controllers are likely to perform better with the free-piston engine plant than the simple linear SISO controllers used in this work.

Finally, topics related to system integration should be investigated, and will include the design of the electric machine, conditioning of the electric output, and the integration into a power grid. This will require knowledge of the application of the free-piston engine generator, for example if it is to be used as a single electric generator in a small application or in a large, multi-unit powerplant. This information will give insight into the requirements for the engine to cope with load variations and to which extent these can be avoided using power electronics.

References

[1] P.A.J. Achten. A review of free piston engine concepts. *SAE Paper 941776, Society of Automotive Engineers*, 1994.

[2] P.A.J. Achten, J.P.J. van den Oever, J. Potma, and G.E.M. Vael. Horsepower with brains: The design of the Chiron free piston engine. *SAE Paper 2000-01-2545, Society of Automotive Engineers*, 2000.

[3] H.T. Aichlmayr. *Design Considerations, Modeling, and Analysis of Micro-Homogeneous Charge Compression Ignition Combustion Free-Piston Engines.* PhD thesis, The University of Minnesota, 2002.

[4] H.T. Aichlmayr, D.B. Kittelson, and M.R. Zachariah. Miniature free-piston homogenous charge compression ignition engine-compressor concept—part 1: performance estimation and design considerations unique to small dimensions. *Chemical Engineering Science*, 57:4161–4171, 2002.

[5] H.T. Aichlmayr, D.B. Kittelson, and M.R. Zachariah. Miniature free-piston homogenous charge compression ignition engine-compressor concept—part 2: modeling HCCI combustion in small scales with detailed homogenous gas phase chemical kinetics. *Chemical Engineering Science*, 57:4173–4186, 2002.

[6] C.A. Amann. Evaluating alternative internal combustion engines: 1950-1975. *Journal of Engineering for Gas Turbines and Power*, 121:540–545, 1999.

[7] K.D. Annen, D.B. Stickler, and J. Woodroffe. Miniature internal combustion engine (MICE) for portable electric power. *In: 23rd Army Science Conference, Orlando, Florida, USA*, 2002.

[8] C. Arcoumanis and J.H. Whitelaw. Fluid mechanics of internal combustion engines — a review. *Proc. Inst. Mech. Eng.*, 201:57–74, 1987.

[9] W. Arshad, C. Sadarangani, T. Bäckström, and P. Thelin. Finding an appropriate electrical machine for a free piston generator. In *Proceedings of the International Battery, Hybrid and Fuelcell Electric Vehicle Symposium & Exhibition, EVS-19*, Busan, Korea, October 2002.

[10] W. Arshad, P. Thelin, T. Bäckström, and C. Sadarangani. Use of transverse-flux machines in a free-piston generator. In *Proceedings of the IEEE International Electric Machines and Drives Conference IEMDC*, Madison, Wisconsin, USA, June 2003.

[11] W. Arshad, P. Thelin, and C. Sadarangani. Alternative electrical machine solutions for a free piston generator. In *The Sixth International Power Engineering Conference (IPEC2003)*, Singapore, November 2003.

[12] I. Arsie, C. Pianese, and G. Rizzo. Models for the prediction of performance and emissions in a spark ignition engine — a sequentially structured approach. *SAE paper 980779, Society of Automotive Engineers*, 1998.

[13] P.C. Baruah. A free-piston engine hydraulic pump for an automotive propulsion system. *SAE Paper 880658, Society of Automotive Engineers*, 1988.

[14] N.H. Beachley and F.J. Fronczak. Design of a free-piston engine-pump. *SAE Paper 921740, Society of Automotive Engineers*, 1992.

[15] M. Bergman, J. Fredriksson, and V.I. Golovitchev. Performance and emission formation evaluation of a diesel-fueled free piston engine using CFD. *JSAE Paper 20065454, JSAE Annual Spring Congress, Yokohama, Japan*, 2006.

[16] P. Van Blarigan. Free-piston engine. US Patent 6199519, 2001.

[17] P. Van Blarigan, N. Paradiso, and S. Goldsborough. Homogeneous charge compression ignition with a free piston: A new approach to ideal otto cycle performance. *SAE Paper 982484, Society of Automotive Engineers*, 1998.

[18] R. Bock. Gas cushioned free piston type engine. US Patent 4128083, 1978.

[19] I. Boldea and S.A. Nasar. Permanent-magnet linear alternators. Part 2: Design guidelines. *IEEE Transactions on Aerospace and Electronic Systems*, 23:79–82, 1987.

[20] I. Boldea and S.A. Nasar. *Linear electric actuators and generators*. Cambridge University Press, 1997.

[21] A. Braun. Free piston engine with antiknock means. US Patent 3,853,100, 1974.

[22] A.T. Braun and P.H. Schweitzer. The Braun linear engine. *SAE paper 730185, Society of Automotive Engineers*, 1973.

[23] H. Brunner, J. Dantlgraber, A. Feuser, H. Fichtl, R. Schäffer, and A. Winger. Renaissance einer Kolbenmachine. *Antriebstechnik*, 4:66–70, 2005.

[24] H. Brunner, A. Winger, A. Feuser, J. Dantlgraber, and R. Schäffer. Thermohydraulische Freikolbenmaschine als Primäraggregat für mobilhydraulische Antriebe. *In: 4th International Fluid Power Conference Dresden – Intelligent Solutions by Fluid Power*, 2004.

[25] D. Carter and E. Wechner. The free piston power pack: Sustainable power for hybrid electric vehicles. *SAE Paper 2003-01-3277, Society of Automotive Engineers*, 2003.

[26] W.R. Cawthorne. *Optimization of a brushless permanent magnet linear alternator for use with a linear internal combustion engine.* PhD thesis, University of West Virginia, 1999.

[27] W.R. Cawthorne, P. Famouri, J. Chen, N.N. Clark, T.I. McDaniel, R.J. Atkinson, S. Nandkumar, C.M. Atkinson, and S. Petreanu. Development of a linear alternator-engine for hybrid electric vehicle applications. *IEEE Transactions on Vehicular Technology*, 48(6):1797–1802, 1999.

[28] A. Chen, W. Arshad, P. Thelin, and P. Zheng. Analysis and optimization of a longitudinal flux linear generator for hybrid electric vehicle applications. In *IEEE VTS Vehicle Power and Propulsion symposium, VPP 04*, Paris, France, October 2004.

[29] N. Clark, S. Nandkumar, C. Atkinson, R. Atkinson, T. McDaniel, S. Petreanu, P. Famouri, and W.R. Cawthorne. Fundamental analysis of a linear two-cylinder internal combustion engine. *SAE Paper 982692, Society of Automotive Engineers*, 1998.

[30] N. Clark, S. Nandkumar, C. Atkinson, R. Atkinson, T. McDaniel, S. Petreanu, P. Famouri, and W.R. Cawthorne. Modelling and development of a linear engine. *In: Proc. of the ASME Spring Conference, Internal Combustion Engine Division*, 30(2):49–57, 1998.

[31] N. Clark, S. Nandkumar, C. Atkinson, R. Atkinson, T. McDaniel, S. Petreanu, P. Famouri, and W.R. Cawthorne. Operation of a small-bore two-stroke linear engine. *Proc. of the Fall Technical Conference of the ASME Internal Combustion Engine Division*, 31(1):33–40, 1998.

[32] N. Clark, S. Nandkumar, C. Atkinson, R. Atkinson, T. McDaniel, S. Petreanu, P. Famouri, and W.R. Cawthorne. Numerical simulation of a two-stroke linear engine-alternator combination. *SAE Paper 1999-01-0921, Society of Automotive Engineers*, 1999.

[33] Deere & Company. Company web site. `http://www.deere.com`, 2007.

[34] Y. Deng and K. Deng. Free-piston engine without compressor. US Patent 4924956, 1990.

[35] J.F. Kos et al. A computer controlled, optimized hybrid engine. *In: AIAA Intersociety Energy Conversion Engineering Conference, Monterey, CA*, pages 955–960, 1994.

[36] P. Famouri, W.R. Cawthorne, N. Clark, S. Nandkumar, C. Atkinson, R. Atkinson, T. McDaniel, and S. Petreanu. Design and testing of a novel linear alternator and engine system for remote

electrical power generation. *Proc. of the IEEE Power Engineering Society winter meeting*, pages 108–112, 1999.

[37] H.O. Farmer. Free-piston compressor-engines. *Proceedings of the Institution of Mechanical Engineers*, 156:253–271, 1947.

[38] C.R. Ferguson. *Internal combustion engines: applied thermodynamics.* John Wiley & Sons., 2000.

[39] J.D. Fleming and R.J. Bayer. Diesel combustion phenomena as studied in free piston gasifiers. *SAE Paper 630449, Society of Automotive Engineers*, 1963.

[40] J. Fredriksson. *Modeling of a free piston energy converter.* PhD thesis, Chalmers University of Technology, 2006.

[41] J. Fredriksson and I. Denbratt. Simulation of a two-stroke free piston engine. *SAE Paper 2004-01-1871, Society of Automotive Engineers*, 2004.

[42] D.N. Frey, P. Klotsch, and A. Egli. The automotive free-piston-turbine engine. *SAE Transactions, Society of Automotive Engineers*, 65:628–634, 1957.

[43] S. Goldsborough and P. Van Blarigan. A numerical study of a free piston IC engine operating on homogeneous charge compression ignition combustion. *SAE Paper 990619, Society of Automotive Engineers*, 1999.

[44] S. Goldsborough and P. Van Blarigan. Optimizing the scavenging system for a two-stroke cycle free piston engine for high efficiency and low emissions: A computational approach. *SAE Paper 2003-01-0001, Society of Automotive Engineers*, 2003.

[45] V.I. Golovitchev, M. Bergman, and L. Montorsi. CFD modeling of diesel oil and DME performance in a two-stroke free piston engine. *Combust. Sci. and Tech.*, 179:417–436, 2007.

[46] G.C. Goodwin, S.F. Graebe, and M.E. Salgado. *Control system design.* Prentice Hall, 2001.

[47] R.P. Heintz. Free-piston engine-pump unit. US Patent 4087205, 1978.

[48] R.P. Heintz. Free-piston engine pump. US Patent 4369021, 1983.

[49] R.P. Heintz. Theory of operation of a free piston engine-pump. *Proc. 20th Intersociety Energy Conversion Engineering Conference*, 2:721–728, 1985.

[50] W.P. Hew, J. Jamaludin, M. Tadjuddin, and K.M. Nor. Fabrication and testing of a linear electric generator for use with a free-piston engine. *In: Proceedings of Power and Energy Conference, Kuala Lumpur, Malaysia*, 2003.

[51] J.B. Heywood. *Internal Combustion Engine Fundamentals.* McGraw-Hill, 1988.

[52] A. Hibi and T. Ito. Fundamental test results of a hydraulic free piston internal combustion engine. *Proc. Institution of Mechanical Engineers*, 218:1149–1157, 2004.

[53] A. Hibi and S. Kumagai. Hydraulic free piston internal combustion engine – test result. *Power*, 30:244–249, 1984.

[54] G.F. Hohenberg. Advanced approaches for heat transfer calculations. *Society of Automotive Engineers Special Publications*, SP-449:61–79, 1979.

[55] R. Huber. Present state and future outlook of the free-piston engine. *Transactions of the ASME*, 80(8):1779–1790, 1958.

[56] M.D. Iliev, S.S. Kervanbashiev, S.D. Karamanski, and F.M. Makedonski. Method and apparatus for producing electrical energy from a cyclic combustion process utilizing coupled pistons which reciprocate in unison. US patent 4532431, 1985.

[57] H. Jasak, H.G. Weller, and N. Nordin. In-cylinder CFD simulation using a C++ object-oriented toolkit. *SAE Paper 2004-01-0110, Society of Automotive Engineers*, 2004.

[58] T.A. Johansen. Dept. Engineering Cybernetics, Norwegian University of Science and Technology, Trondheim, Norway, 2005. Personal communication.

[59] T.A. Johansen, O. Egeland, E.Aa. Johannesen, and R. Kvamsdal. Free-piston diesel engine dynamics and control. *In: Proc. American Control Conference*, 2001.

[60] T.A. Johansen, O. Egeland, E.Aa. Johannesen, and R. Kvamsdal. Free-piston diesel engine timing and control — towards electronic cam– and crankshaft. *IEEE Transactions on Control Systems Technology*, 10:177–190, 2002.

[61] G. Flynn Jr. Observations on 25,000 hours of free-piston-engine operation. *SAE Transactions, Society of Automotive Engineers*, 65:508–515, 1957.

[62] K.A. Galitello Jr. Two stroke cycle engine. US Patent 4876991, 1989.

[63] D. Jung and D.N. Assanis. Multi-zone DI Diesel spray combustion model for cycle simulation studies of engine performance and emissions. *SAE Paper 2001-01-1246, Society of Automotive Engineers*, 2001.

[64] A.P. Kleemann, J.C. Dabadie, and S. Henriot. Computational design studies for a high-efficiency and low-emissions free piston engine prototype. *SAE Paper 2004-01-2928, Society of Automotive Engineers*, 2004.

[65] J.F. Kos. Computer optimized hybrid engine. US Patent 5002020, 1990.

[66] M. Larmi, S. Isaksson, S. Tikkanen, and M. Lammila. Performance simulation of a compression ignition free piston engine. *SAE Paper 2001-01-0280, Society of Automotive Engineers*, 2001.

[67] A.L. London and A.K. Oppenheim. The free-piston engine development – present status and design aspects. *Transactions of the American Society of Mechanical Engineers*, 74:1349–1361, 1952.

[68] OpenCFD Ltd. OpenFOAM project web site. `http://www.OpenFOAM.org`, 2007.

[69] Perkins Engines Company Ltd. Company web site. `http://www.perkins.com`, 2007.

[70] T. Lucchini. *Prediction of combustion and pollutant emissions in internal combustion engines*. PhD thesis, Politecnico di Milano, 2006.

[71] J.J. McMullen and W.G. Payne. Performance of free-piston gas generators. *Transactions of the ASME*, 76:1–13, 1954.

[72] J.J. McMullen and R. Ramsey. The free-piston type of gas turbine plant and applications. *Transactions of the ASME*, 76:15–29, 1954.

[73] R. Mikalsen and A.P. Roskilly. A review of free-piston engine history and applications. *Applied Thermal Engineering*, 27:2339–2352, 2007.

[74] R. Mikalsen and A.P. Roskilly. Coupled dynamic–multidimensional modelling of free-piston engine combustion. *Applied Energy*, In press: doi:10.1016/j.apenergy.2008.04.012, 2008.

[75] R. Mikalsen and A.P. Roskilly. The design and simulation of a two-stroke free-piston compression ignition engine for electrical power generation. *Applied Thermal Engineering*, 28:589–600, 2008.

[76] R. Mikalsen and A.P. Roskilly. Performance simulation of a spark ignited free-piston engine generator. *Applied Thermal Engineering*, In press: doi: 10.1016/j.applthermaleng.2007.11.015, 2008.

[77] S.A. Nasar and C. Chen. Optimal design of a tubular permanent magnet linear alternator. *Electric machines and power systems*, 14:249–259, 1988.

[78] N. Nordin. *Complex Chemistry Modeling of Diesel Spray Combustion*. PhD thesis, Chalmers University of Technology, 2001.

[79] O.B. Noren and R.L. Erwin. The future of the free-piston engine in commercial vehicles. *SAE Transactions, Society of Automotive Engineers*, 66:305–314, 1958.

[80] D.Y. Ohm. Analysis of PID and PDF compensators for motion control systems. *In: IEEE Industry Applications Society Annual Meeting*, 3:1923–1929, 1994.

[81] C. Olikara and G.L. Borman. A computer program for calculating properties of equilibrium combustion products with some applications to I.C. engines. *SAE Paper 750468, Society of Automotive Engineers*, 1975.

[82] R.P. Pescara. Motor compressor apparatus. US Patent 1,657,641, 1928.

[83] R.P. Pescara. Motor compressor of the free piston type. US Patent 2,241,957, 1941.

[84] R.M. Phelan. *Automatic control systems*. Cornell University Press, 1977.

[85] J.I. Ramos. *Internal combustion engine modeling*. Hemisphere Publishing Corp., 1989.

[86] R. Redlich. A summary of twenty years experience with linear motors and alternators. *In: Linear Drives for Industry Applications, Nagasaki, Japan*, 1995.

[87] P.A. Rittmaster and J.L. Booth. Hydraulic engine. US Patent 4326380, 1982.

[88] S. Sagov. Energy converter. US Patent 2003/0098587, 2003.

[89] A. Setiawan, L.D. Albright, and R.M. Phelan. Application of pseudo-derivative-feedback algorithm in greenhouse air temperature control. *Computers and Electronics in Agriculture*, 26:283–302, 2000.

[90] J.H.E. Somhorst and P.A.J. Achten. The combustion process in a DI Diesel hydraulic free piston engine. *SAE Paper 960032, Society of Automotive Engineers*, 1996.

[91] D.H. Specht. Evaluation of free piston-gas turbine marine propulsion machinery in GTS William Patterson. *SAE Paper 620280, Society of Automotive Engineers*, 1962.

[92] R. Stone. *Introduction to internal combustion engines*. MacMillian Press Ltd., 1999.

[93] The MathWorks, Inc. Company web site. `http://www.mathworks.com`, 2007.

[94] S. Tikkanen, M. Herranen, M. Lammila, S. Haikio, and M. Vilenius. Free piston engine into work. *In: Eighth Scandinavian International conference on fluid power*, pages 1161–1172, 2003.

[95] S. Tikkanen, M. Herranen, R. Savela, and M. Vilenius. Simulation of a hydraulic free piston engine – a dual piston case. *In: Sixth Scandinavian international conference on fluid power*, pages 339–349, 1999.

[96] S. Tikkanen, M. Lammila, M. Herranen, and M. Vilenius. First cycles of the dual hydraulic free piston engine. *International off-highway and powerplant congress and exposition*, pages 27–36, 2000.

[97] S. Tikkanen and M. Vilenius. Control of a dual hydraulic free piston engine. *Int. J. Vehicle Autonomous Systems*, 4(1):3–23, 2006.

[98] C. Toth-Nagy. *Linear engine development for series hybrid electric vehicles.* PhD thesis, University of West Virginia, 2004.

[99] W.T. Toutant. The Worthington-Junkers free-piston air compressor. *Journal of the American Society of Naval Engineers*, 64(3):583–594, 1952.

[100] A. Uludogan, D.E. Foster, and R.D. Reitz. Modeling the effect of engine speed on the combustion process and emissions in a DI Diesel engine. *SAE Paper 962056, Society of Automotive Engineers*, 1996.

[101] A.F. Underwood. The GMR 4-4 'HYPREX' engine – A concept of the free-piston engine for automotive use. *SAE Transactions, Society of Automotive Engineers*, 65:377–391, 1957.

[102] G. Vael and P.A.J. Achten. The Innas fork lift truck, working under constant pressure. *In: 1. Internationales Fluidtechnisches Kolloquim, Aachen, Germany*, 1998.

[103] R. Vallon. Free-piston electric current generator. US Patent 4403153, 1983.

[104] J. Wang, M. West, D. Howe, H. Zelaya-De La Parra, and W.M. Arshad. Design and experimental verification of a linear permanent magnet generator for a free-piston energy converter. *IEEE Trans. Energy Conversion*, 22(2):299–306, 2007.

[105] H.G. Weller. The development of a new flame area combustion model using conditional averaging. Thermo-Fluids Section Report TF 9307, Imperial College of Science, Technology and Medicine, 1993.

[106] X. Zhang, J. Katzberg, B. Cooke, and J. Kos. Modeling and simulation of a hybrid engine. *Proc. IEEE Communications, Power and Computing Conference*, pages 286–291, 1997.

Appendix A

Chemical reaction mechanism

Listing A.1 shows the settings file for the chemical reaction mechanism used in the multidimensional diesel engine simulations described in Section 5.3.

Listing A.1: Chemical reaction mechanism settings.

```
ELEMENTS
H       O       C       N       AR
END

SPECIE
C7H16   O2      N2      CO      H2O
O       CO2     OH      H       H2
HO2     H2O2    N       NO      C
END

REACTIONS
 C7H16 + 11O2              => 7CO2 + 8H2O        1.00E+8  0.0    15780.0! 1
        FORD    / C7H16 0.25 /
        FORD    / O2 1.5 /
 CO    + O     + M     = CO2   + M           6.170E+14  0.00    3000. ! 96
 CO    + OH            = CO2   + H           3.510E+07  1.30    -758. ! 97
 CO    + O2            = CO2   + O           1.600E+13  0.00   41000. ! 98
 HO2   + CO            = CO2   + OH          5.800E+13  0.00   22930. ! 99
!
 H2    + O2            = OH    + OH          1.700E+13  0.00   47780. !100
 H2    + OH            = H2O   + H           1.170E+09  1.30    3626. !101
 O     + OH            = O2    + H           4.000E+14 -0.50       0. !102
 O     + H2            = OH    + H           5.060E+04  2.67    6290. !103
 H     + HO2           = O     + H2O         3.100E+10  0.00    3590. !104
 O     + OH    + M     = HO2   + M           1.000E+16  0.00       0. !105
       H2O/6.0/  CO2/5.0/  H2/3.3/  CO/2.0/  N2/0.70/
 H     + O2    + M     = HO2   + M           2.800E+18  -.86       0.0!106
 O2/0.00/ H2O/ .00/ CO/0.75/ CO2/1.50/ N2/0.0/
 H     + O2    + O2    = HO2   + O2          2.080E+19 -1.24       0.0!107
 H     + O2    + H2O   = HO2   + H2O         11.26E+18  -.76       0.0!108
 H     + O2    + N2    = HO2   + N2          2.600E+19 -1.24       0.0!109
 OH    + HO2           = H2O   + O2          7.500E+12  0.00       0. !110
 H     + HO2           = OH    + OH          1.700E+14  0.0      875. !111
```

```
O     + HO2          = O2    + OH          1.400E+13  0.00    1073. !112
OH    + OH           = O     + H2O         6.000E+08  1.30       0. !113
H     + H     + M    = H2    + M           1.000E+18 -1.00       0. !114
      H2/0./ H2O/0./ CO2/0./
H     + H     + H2   = H2    + H2          9.200E+16 -0.60       0. !115
H     + H     + H2O  = H2    + H2O         6.000E+19 -1.25       0. !116
H     + H     + CO2  = H2    + CO2         5.490E+20 -2.00       0. !117
H     + OH    + M    = H2O   + M           1.600E+22 -2.00       0. !118
H     + O     + M    = OH    + M           6.200E+16 -0.60       0. !119
O     + O     + M    = O2    + M           1.890E+13  0.00   -1788. !120
H     + HO2          = H2    + O2          1.250E+13  0.00       0. !121
HO2   + HO2          = H2O2  + O2          2.000E+12  0.00       0. !122
OH    + OH    (+M)   = H2O2  (+M)          7.600E+13  -.37       0. !123
    LOW  /  4.300E+18     -.900   -1700.00/
    TROE/    .7346    94.00   1756.00   5182.00 /
      H2/2.00/ H2O/6.00/ CO/1.50/ CO2/2.00/ N2/0.70/
H2O2  + H            = HO2   + H2          1.600E+12  0.00    3800. !124
H2O2  + OH           = H2O   + HO2         1.000E+13  0.00    1800. !125
H2O2  + H            = H2O   + OH          1.000E+13  0.00    3590. !126
H2O2  + O            = H2O   + O2          8.400E+11  0.00    4260. !127
H2O2  + O            = OH    + HO2         2.000E+13  0.00    5900. !128
H2    + HO2          = H2O   + OH          6.500E+11  0.00   18800. !129
!
CO2   + N            = NO    + CO          1.900E+11  0.00    3400. !130
N     + NO           = N2    + O           3.270E+12  0.30       0. !136
N     + O2           = NO    + O           6.400E+09  1.00    6280. !137
N     + OH           = NO    + H           7.333E+13  0.00    1120. !138
!
END
```

Appendix B

Engine dynamic response tests

Figures B.1–B.7 show the dynamic response of the free-piston engine when subjected to step changes in the input variables fuel mass, electric load force, and bounce chamber trapped air mass.

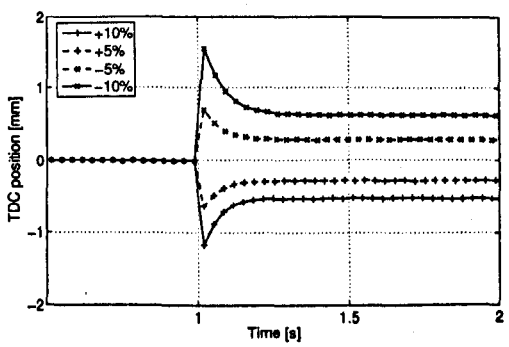

Figure B.1: Engine TDC response to a step change in bounce chamber trapped air mass.

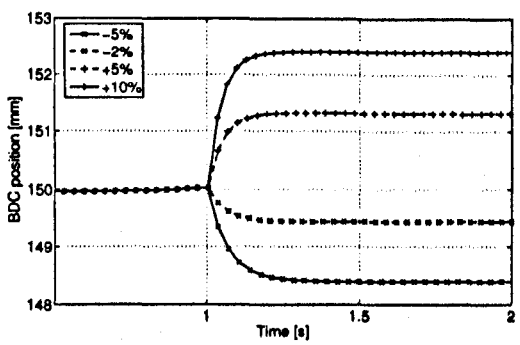

Figure B.2: Engine BDC response to a step change in mass of fuel per injection.

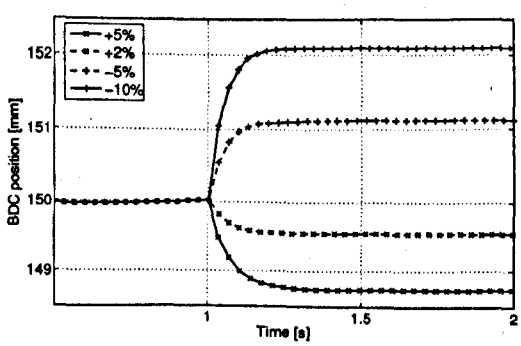

Figure B.3: Engine BDC response to a step change in electric load force.

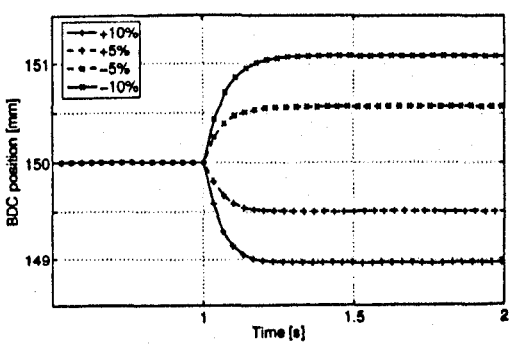

Figure B.4: Engine BDC response to a step change in bounce chamber trapped air mass.

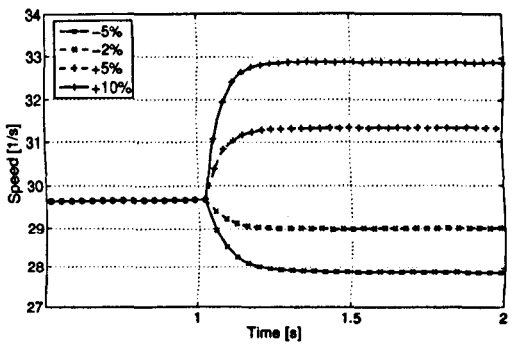

Figure B.5: Engine TDC response to a step change in mass of fuel per injection.

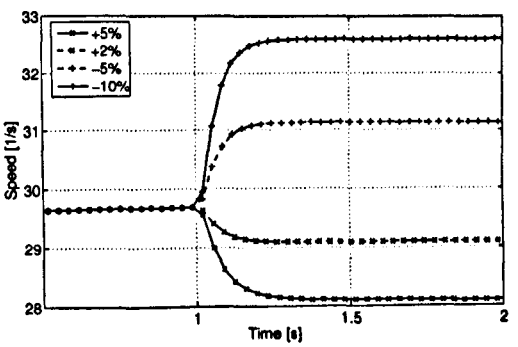

Figure B.6: Engine speed response to a step change in electric load force.

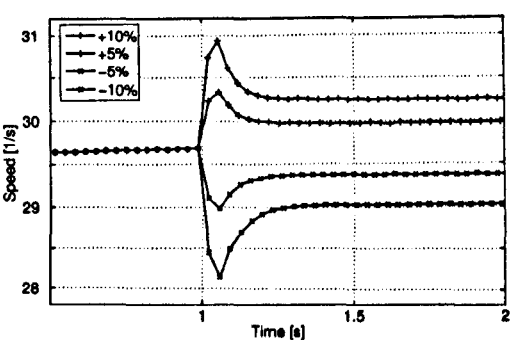

Figure B.7: Engine speed response to a step change in bounce chamber trapped air mass.